Y 3.At7:
36/9-3

POWER REACTOR TECHNOLOGY

A Quarterly Technical Progress Review

Prepared for DIVISION OF TECHNICAL INFORMATION, USAEC, by
ARGONNE NATIONAL LABORATORY

ILLINOIS STATE LIBRARY
FEB 2 - 1967
U. S. Gov. Pub. Depos.

Summer 1966

VOLUME 9

NUMBER 3

How serious are vessel cladding failures? ... see page 101

TECHNICAL PROGRESS REVIEWS

To meet the needs of industry for concise summaries of current atomic developments, the Atomic Energy Commission is publishing this series, Technical Progress Reviews. Issued quarterly, each of the reviews digests and evaluates the latest findings in a specific area of nuclear technology and science.

The journals published in this series are:

Isotopes and Radiation Technology P. S. Baker, A. F. Rupp, and associates
Oak Ridge National Laboratory

Nuclear Safety Wm. B. Cottrell, W. H. Jordan, J. P. Blakely, and associates
Nuclear Safety Information Center, Oak Ridge National Laboratory

Power Reactor Technology
Argonne National Laboratory

Reactor Materials E. M. Simons and associates
Battelle Memorial Institute

See the back cover for availability information.

The views expressed in this publication do not necessarily represent those of the United States Atomic Energy Commission, its divisions or offices, or of any Commission advisory committee or contractor.

Availability of Reports Cited in This Review

Unclassified AEC reports are available for inspection at AEC depository libraries and are sold by the Clearinghouse for Federal Scientific and Technical Information, National Bureau of Standards, U. S. Department of Commerce, 5285 Port Royal Road, Springfield, Va., 22151. Some of the reports cited are not available owing to their preliminary nature; however, the information contained in them will eventually be made available in formal progress or topical reports.

Unclassified reports issued by other Government agencies or private organizations should be requested from the originator.

Unclassified British and Canadian reports may be inspected at AEC depository libraries. British reports are sold by the British Information Service, 45 Rockefeller Plaza, New York, N. Y.; Canadian reports (AECL series) are sold by the Scientific Document Distribution Office, Atomic Energy of Canada, Ltd., Chalk River, Ontario, Canada.

Classified U. S. and foreign reports identified in this journal as Classified may be purchased by properly cleared Access Permit Holders from the Division of Technical Information Extension, U. S. Atomic Energy Commission, P. O. Box 1001, Oak Ridge, Tenn., 37830. Such reports may be inspected at classified AEC depository libraries.

Y 3.AT7:
36/9-3

Contents

Power Reactor Technology

Vol. 9, No. 3

COMPONENTS — How Serious Are Vessel Cladding Failures? 101
Edward A. Wimunc

OPERATING EXPERIENCE — Nuclear Plant Performance—Good and Getting Better 110
George F. Bierman and Walter J. Miller

FLUID AND THERMAL TECHNOLOGY — Applying High-Temperature Instrumentation in Liquid-Metal Experiments 123
Paul A. Lottes

SPECIFIC REACTOR TYPES — Advances in Materials for Organic-Cooled Reactors 137
Edmund S. Sowa

CONTROL AND DYNAMICS — Two Advances in Reactor Neutron-Noise Analysis 142
Charles E. Cohn

PHYSICS — Water-Reactor Lattice Calculations and Measurements 145
Edwin M. Pennington

APPLICATIONS — Nuclear Power To Explore the Ocean Deeps 150
Edward J. Croke

LIMITED COVERAGE OF FUEL PROCESSING

The Technical Progress Review *Reactor Fuel Processing* is being terminated with the Vol. 9, No. 4, issue. Limited coverage of fuel processing will continue in *Power Reactor Technology* beginning with the Winter issue, Vol. 10, No. 1.

Issued quarterly by the U. S. Atomic Energy Commission. Use of funds for printing this publication approved by the Director of the Bureau of the Budget on July 8, 1966.

Power Reactor Technology is a quarterly review of developments in reactor technology—including new concepts and applications as well as research results, analysis, and experience with existing or new components and systems. Prepared by Argonne National Laboratory at the request of the Division of Technical Information of the U. S. Atomic Energy Commission, *Power Reactor Technology* is intended for reactor designers and other technical specialists concerned with the interplay among reactor development, design, construction, operation, and economics. Thus this quarterly journal reports and interprets progress in the power-reactor field in terms of its significance to the reactor designer. Its scope includes research and development in the various technical specialties in the field as well as design and construction practices, reactor concepts, applications, economics, and operating experience.

Some articles summarize and critically evaluate reported developments; others review a topic broadly so that designers can interpret new developments, experience, and trends. All, however, call the reader's attention to reports and publications that merit study. Because any appraisal involves the reviewer's opinion of the significance of the work reported, readers are urged to consult the references for additional information and the judgments of the original authors. If a reader has information that causes his evaluation to reinforce, modify, or contradict the opinions of our reviewers, he is encouraged to write to the Editor.

For reasonably timely coverage, articles often must be based on fragmentary information. Thus, whenever appropriate, continuity will be maintained from one issue to another by use of subject headings that reflect parts of the following scope of the journal:

> CONCEPTS and APPLICATIONS: Progress in evaluating the applicability and economics of various reactor types and systems (including unconventional approaches), as well as of fuel resources and cycles, for utility central-station generation of electricity, auxiliary power, process radiation and heat, desalting, and propulsion—and for terrestrial, undersea, aerospace, and other advanced uses.
>
> ANALYSIS and EXPERIMENTATION: Advancements in the techniques of reactor physics, fluid and thermal technology, power conversion, fuel elements, materials, mechanics, control and dynamics, and reactor safety.
>
> SYSTEMS and COMPONENTS: Experience as reflected in design and construction practice, components, systems technology, and operating performance of various specific types of reactors—including pressurized- and boiling-water reactors, molten-salt, organic-, gas-, and liquid-metal-cooled reactors, as well as generally applicable aspects of research and test reactors.

At Argonne National Laboratory, the Reactor Engineering Division (L. J. Koch, Director) has the principal responsibility for the preparation of *Power Reactor Technology*, with the regular assistance of the Reactor Physics Division (R. A. Avery, Director) and the occasional assistance of other Laboratory divisions (Metallurgy, Chemical Engineering, Chemistry, Reactor Operations, and Idaho). Thus, unless noted otherwise, the reviewers and authors of articles are Laboratory staff members. The editors will welcome interpretive review articles contributed by readers outside the Laboratory.

JAMES J. DUTTON, *Editor*
DAVID H. LENNOX, *Technical Editor;* KARL K. BROWN, *Managing Editor*
EDWARD J. CROKE and RAYMOND GOLD, *Associate Editors*
BARBARA A. SCHMEH, *Assistant Editor*

Argonne National Laboratory

How Serious Are Vessel Cladding Failures?

By Edward A. Wimunc

Defects have been discovered in the thin stainless-steel claddings that line the carbon-steel pressure vessels in three water-reactor systems. Historically, the principal function of reactor-vessel cladding has been to prevent vessel corrosion that would lead to the circulation of radioactive corrosion products through the system; i.e., the principal function of the cladding is to protect the coolant, not the vessel. Although the cladding defects found are not of sufficient area to pose operating problems because of corrosion-product radioactivity, their presence raised questions concerning their cause and their potential for weakening the vessel wall by means of crack propagation or localized corrosion.

In vessel design the thin cladding is not considered to impart any strength to the vessel. Therefore the presence of cracks in the cladding does not impair the vessel strength. However, the possibility of crack propagation into the thick carbon-steel wall led to extensive investigations. The investigations indicate that none of the cracks extend into the carbon steel, that the mechanisms causing the cladding failures are unlikely to cause cracking of the carbon steel, and that the corrosion of the carbon steel is unlikely to jeopardize the integrity of these pressure vessels, all of which are considerably thicker than is dictated by design of boiler and pressure-vessel code requirements.

Careful surveillance programs are being conducted to verify the continuing validity of these conclusions. Their findings will prove invaluable in guiding future design and fabrication practices for reactor vessels. In the meantime it is worthwhile to consider the studies made of the causes and limits of these cladding defects.

The Vessels

The four pressure vessels in which cladding failures have been detected are (1) the Experimental Boiling Water Reactor (EBWR) vessel,[1] (2) the Yankee-Rowe reactor vessel,[2] (3) the Yankee-Rowe reactor-system pressurizer,[3,4] and (4) the Elk River reactor vessel.[5,6] In all but the Yankee reactor vessel, where the cladding was ground down by the friction of loose parts in the bottom of the vessel, the failures were in the form of cracks in the cladding. Although the cracks, porosity, and inclusions in the Elk River reactor cladding that were discovered in 1961 before startup were repaired then, further cracks have been found recently in a section of the weld-overlay cladding known to have a martensitic structure. Thus the Elk River, EBWR, and both Yankee vessels now have cladding defects. About 1 sq ft of the EBWR SA-212B carbon-steel vessel wall is exposed, including areas from which cladding samples were removed for the investigation; only about 2 sq in. of the A-302B carbon-steel reactor-vessel wall is exposed at Yankee.

Because each of these vessels has a different history of construction and operation, it is interesting to consider the cladding methods employed and the locations where the failures occurred.

Cladding Methods

Figure 1 illustrates the principles of the three methods that have been used to line carbon-steel vessel material with stainless steel. The stitch-weld method, which was used to clad the EBWR and Yankee reactor vessels and the Yankee pressurizer vessel, leaves a nonbonded gap between the cladding and base metal. This communicating gap permits a leak in one location to expose much of the carbon steel to reactor water. The stitch-weld technique was discarded several years ago in favor of the weld-overlay cladding method, which, in fact, was also used to clad the nozzle and flange complex areas in all four of these vessels. The roll-bonding process was used to clad the straight shell sections and the heads of the Elk River reactor vessel.

The cracks in the Yankee pressurizer and in the EBWR vessel were in the stitch-welded cladding only (not in the weld-overlay areas, which had been clad

Fig. 1 Three methods for applying stainless-steel cladding to carbon steel for reactor vessels. In the "stitch-weld" method, sheets of stainless steel are resistance-welded to carbon-steel plates in a pattern of spot-welds; after forming, the edges of the panels are butt-welded to each other to form the vessel wall, and the sheets are butt-welded to form a single liner. The weld-overlay technique consists of depositing an overlapping series of arc-melted stainless-steel strips on the carbon steel (and, sometimes, then machining the surface smooth). Roll cladding diffusion-bonds the cladding and base metal by compressing the metals together at suitable temperature.

with a double pass), whereas the porosity, inclusions, and cracks in the Elk River reactor vessel were in the single-pass weld-overlay cladding only (none in the roll-bonded cladding), particularly at the junction of the weld-overlay cladding with the roll-bonded cladding and in certain questionable regions of the weld overlay.

Examining the EBWR

The EBWR operated in the boiling-water-reactor development program from 1956 until 1960 at powers up to 20 Mw(t) and up to 100 Mw(t) in 1961 and 1962 (Refs. 7 and 8). During that time the vessel experienced 15,665 hr (1.8 years) of service when steam was being generated at 489 °F and 600 psig.[9] When plans were made to use the facility in the plutonium-recycle fuel-development program (to learn how isotopic distribution in fuel rods varies as burnup proceeds in a boiling-water reactor), the reactor vessel was examined in 1965 to determine its suitability for further service. However, because the reactor had operated, the core support structure and vessel thermal shield were quite radioactive even after the uranium core was removed. For this reason, thorough inspection was limited to the upper half of the interior walls of the vessel. The visual examination revealed evidence of hairline cracking on the surface of the stitch-weld cladding at locations shown in Fig. 2.

CLADDING PROCESS

The 2.44-in.-thick SA-212B carbon-steel plates for the EBWR vessel shell were clad by spot-welding 0.109-in.-thick 304 stainless-steel sheets to the plates by the intermittent-power pulse (stitch-weld) process while both plate and sheet were submerged in water. The cladding and plate edges were later butt-welded to adjacent similar panels to obtain a continuously clad cylindrical surface. The 4-in.-thick lower headplate was clad in a similar manner before being cut into a circular blank for the head-forming operation. The upper ring forging and upper head were clad by a double pass of the submerged-arc weld-overlay process; no cracks have been found in this cladding.

The fabricator established the integrity of the stitch-weld cladding by introducing 900-psi nitrogen into the annular gap between the cladding and base plate while watching for leakage bubbles in a soap solution applied on the cladding surface. By this means, several cracks were detected in the cladding; these cracks were rewelded before the vessel was shipped to the reactor site. (Further details of EBWR vessel design and construction have been reported.)[10]

Beginning in 1956 the reactor and vessel operated satisfactorily in the boiling-water-reactor development program until no longer needed and was decommissioned in 1962. Before reactor startup again for the plutonium-recycle development program, examination of the vessel indicated that there were fine cracks in the cladding.

INSPECTION AND ANALYSIS

Visual and dye-penetrant inspections of the stitch-clad plates in the upper half of the vessel revealed the cladding cracks, approximately 75% of which were in the steam region (the upper quarter of the vessel). Although the cladding of five of the eight panels contained surface cracks (most of which were near the manually deposited weld overlays that joined abutting

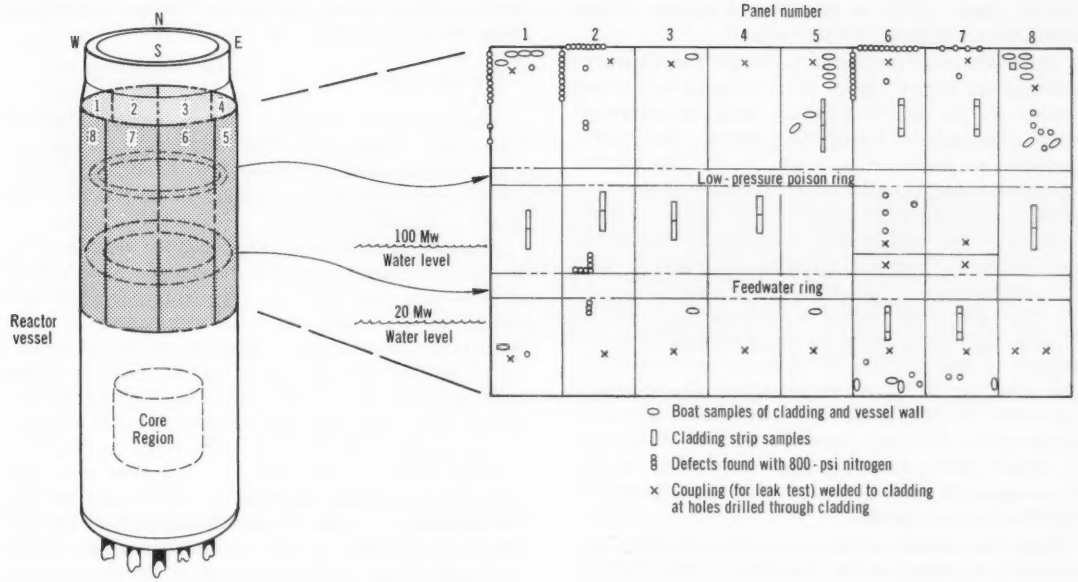

Fig. 2 Cracks were found in the cladding of five of the eight panels that make up the upper half of the EBWR vessel wall. Approximately 75% of the cracks were in the steam region in the top quarter of the vessel; few cracks were found below the waterline.[1]

panels of cladding sheet), few cracks were found below the waterline.

At first it was postulated that the cracks had been caused by service conditions during the most recent years of reactor operation. Fortunately other stitch-clad test plates and vessel-fabrication remnants were available (one of the test remnants had been exposed to the reactor environment for 11,225 hr until it was removed in 1960; a 2-in. plate, fabricated in the same way in 1959 for welding practice prior to a vessel modification,[11–13] had been stored outdoors ever since). Inspection of these plates and remnants negated the postulate. The discovery that the cladding on these plates had cracked (Fig. 3), apparently to an even greater degree than those in the vessel, when exposed not to a reactor environment but only to Illinois weather, was cause for reevaluation. When areas of the test-plate cladding were ground out and repaired by welding to develop methods for repairing the vessel cladding, the cladding cracked severely and extensively.

Initially it was not clear from the visual and dye-check inspections of the vessel whether the crack indications were surface "decorations" or actual cracks. The vessel cladding was leak tested with pressurized nitrogen to check this, as it had been just after fabrication; this test showed that the surface decorations were actually cracks through the cladding. Nearly all the cracks were in the wrought cladding adjacent to the spot-welds, although six cracks either crossed or terminated in the spot-weld

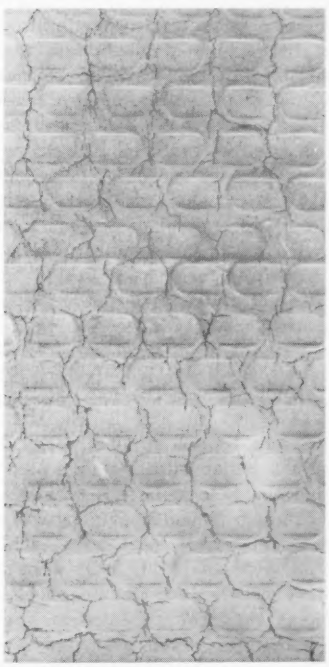

Fig. 3 Fine cracks in surface of 304 stainless-steel cladding on 2-in.-thick practice plate, which became visible after application of dye penetrant, showed that reactor conditions were not necessary to cause cracking.

"thumb print"; none of the through cracks started within the cladding spot-weld nuggets.

The condition of the vessel wall was investigated by grinding out to the carbon steel some of the through cracks in the stainless steel, with dye-penetrant tests interspersed during the process. The cracks appeared to increase in length, width, and number as the cladding was removed, suggesting that they might have originated at the base of the cladding adjacent to the weld areas (at the cladding interface with the gap). However, many cracks started within the cladding — at points remote from either surface (it was recognized that this characteristic of the cracks might have been caused by a changing stress pattern in the cladding as material was removed). The cladding fracture edges were square breaks with little visible ductile flow; many fractures were progressive. Although approximately 40 linear feet of cracks were ground down to and slightly into the base metal, no evidence of crack propagation into the carbon steel was found.

When the surface of the carbon steel between weld nuggets was examined for evidence of corrosive attack, a thin adherent film of black "mill scale" (Fe_3O_4) was found; but there was no evidence of local pitting or of gross generation of red rust (Fe_2O_3). Chloride concentrations detected were low.

Similar tests on the fabrication remnants and on the practice plate showed similar cracking but, again, with no evidence of crack propagation into the base metal. Metallographic examination of these specimens suggested that the cracking originated at the exposed, rather than the cladding-gap, interface. Because at least as much red Fe_2O_3 was found on the carbon steel of these test plates as black Fe_3O_4 on the carbon steel of the vessel itself, and because the test plates were exposed to an entirely different environment (the atmosphere), it was concluded that the reactor environment did not significantly influence corrosion at the interface.

SAMPLING

Numerous "boat" and strip samples were removed from the reactor vessel. The location and extent of sampling are shown in Fig. 2. The boat samples, about 0.5 in. wide and 2.5 in. long, were cut from the vessel with a circular slitting saw so as to include both cladding and base metal; the boat samples were examined metallographically, primarily to determine any cracking in the base metal. The strip samples, about 0.5 in. wide and 8 in. long, were of cladding only and were removed for chemical analysis. Additional samples for chemical analysis were milled from the 4-in.-thick lower headplate remnant and from the 2-in.-thick practice plate. The lower headplate remnant had cladding cracks similar to those found in the vessel. In addition, a crescent-shaped section of the reactor-vessel wall retained from a vessel modification was inspected; no cracks were found in this cladding section or in the vessel panel from which it had been cut.

TEST RESULTS

The chemical analyses showed that the cladding met *ASME Boiler and Pressure Vessel Code* materials requirements,[14] except for a slightly higher sulfur content (0.035 vs. 0.030% in the Code) in the vessel cladding.

Metallographic studies confirmed the results of the grinding explorations inside the reactor vessel. They showed that the cladding, even from one panel believed to be "crack-free" as determined by dye-penetrant examinations, contained numerous unsurfaced cracks. All the cracks in the cladding on the boat samples and the test panels were intergranular, except for a few hot tears inside the weld nuggets. In all cases both the microstructures and Strauss Reagent tests showed that the stainless steel was severely sensitized. Neither the intranugget nor the transgranular cracks in the cladding propagated into the carbon steel. In the bonded region the fusion boundary of the weld kernel stopped all the cracks in the cladding.

Examination of the cladding nuggets (spots where cladding and base metal fused) revealed regions of great complexity (Figs. 4 and 5). In all cases, only the stainless-steel cladding material in the nugget area had been melted by the passage of welding current. Although all the stainless-steel nuggets contained a dendritic kernel that originally was wrought material, the kernels were islands of cast material

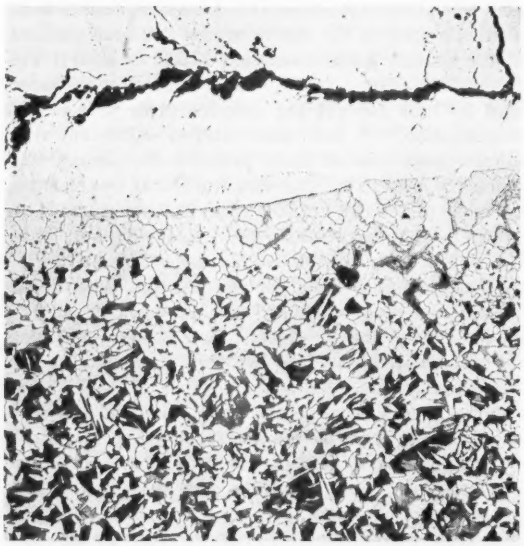

Fig. 4 Lamellar cracks in the EBWR cladding material paralleled the surface.[1]

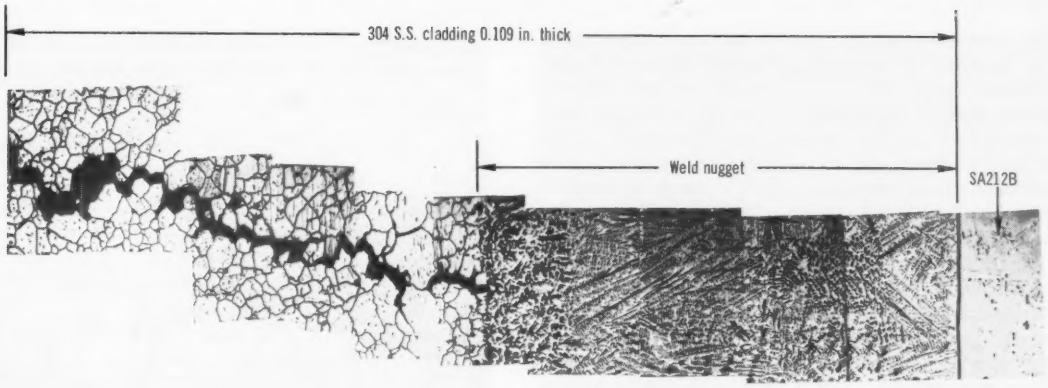

Fig. 5 Cracks in the 304 stainless-steel cladding of EBWR are arrested at the weld nugget by the absence of continuous grain boundaries.[1]

bounded by wrought stainless-steel cladding and the carbon steel. The wrought cladding surrounding the cast kernel contained numerous unsurfaced cracks radiating from the kernel interface as shown in Fig. 6. These cracks, which are usually perpendicular to the surface of the kernel, are primarily due to grain-boundary liquation. No radial cracks were found at the type 304 stainless steel–SA-212B steel interface. However, a thin zone of the cladding, about 0.001 in. thick, was carburized in the bonded zone at the weld nuggets; but this is not considered significant regarding either crack propagation or vessel strength.

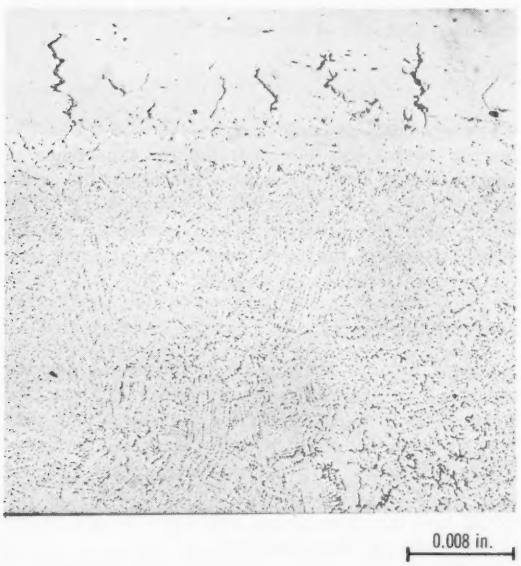

Fig. 6 Unsurfaced cracks in the EBWR wrought cladding radiate from the interface with islands of cast cladding material (weld nuggets).[1]

Although the cracking of the vessel cladding was of great interest, all samples examined were searched primarily for evidence of concurrent cracking of the carbon-steel vessel plate. Several microcracks were found in the carbon steel. As shown in Figs. 7 and 8, a number were filled with intruded stainless steel from the cladding process. Metallographic studies conclusively showed that these microcracks existed before the cladding was applied and were probably formed in the initial fabrication of the plate. Specimens examined showed no evidence of propagation from the surface microcracks.

The hardness survey of the stainless steel and the carbon steel, supporting calculations, and the results of bend tests have been reported.[1] The bend tests on samples of the 2-in. plate attempted to force superficial surface cracks across the cladding and into the carbon steel. For these tests the SA-212B steel was bent back permanently to extend the crack in the 304 stainless-steel cladding. Intermittent incremental bending of a sample that had an intranugget crack only propagated the crack within the cladding to the unbonded interface; continued bending merely opened the crack without propagating it across the interface. Similar results were obtained from the forced development of an embryo crack in the wrought region of the cladding over the cast structure of the weld kernel; the kernel fusion line stopped the crack.

CRACKING MECHANISMS

Chloride stress corrosion, which requires the simultaneous presence of oxygen, stress, and concentrated chloride ions, was considered as a possible cause for the cracking of the austenitic 304 stainless-steel cladding of the EBWR vessel. But it was rejected as the probable primary cause because many unsurfaced and lamellar cracks (Figs. 4 to 6) were found within the stainless steel—and the through cracks in the cladding started at either surface or internally and are intergranular (rather than being

the classical branched "forked lightning" transgranular cracks). Because the evidence indicates a mechanical failure mode, and because a stress analysis shows that the spot-welded cladding might have been stressed beyond the ultimate tensile strength of the stainless steel when the upper and lower vessel courses cooled from the ~1700°F normalizing temperature (at which the courses were rolled vertically to improve concentricity), it was concluded that the cracking within the cladding most probably was caused initially by thermally induced stress ruptures during vessel fabrication and that these unsurfaced cracks propagated by low-cycle fatigue during reactor operation.[15] It also is believed that the mechanism that caused cladding failure would not be different in the inaccessible areas of the vessel. Evaluation of the information available and consideration of the fracture mechanics, radiation effects, temperature, and corrosion phenomena led to the conclusion that the integrity of the vessel has not been significantly impaired by the cracking of the cladding.

Continued operation of the reactor probably will cause more cracks to surface, and efforts to weld the existing cracks or sampled cladding areas would cause more severe cracking. Regardless of the mode of fracture, it is highly improbable that cracks in the stainless steel will propagate into the carbon steel. From the corrosion standpoint, the vessel is believed suitable for further service without the wall being reclad because at its thinnest spot (where boat samples were cut out) the carbon steel is $^{9}/_{16}$ in. thicker than is required by design codes; all SA-212B surfaces that were sampled have been contour-ground to eliminate notches. Nevertheless, a careful surveillance program has been instituted to study the corrosion of the bared steel walls and to verify the continued adequacy of the vessel.[16]

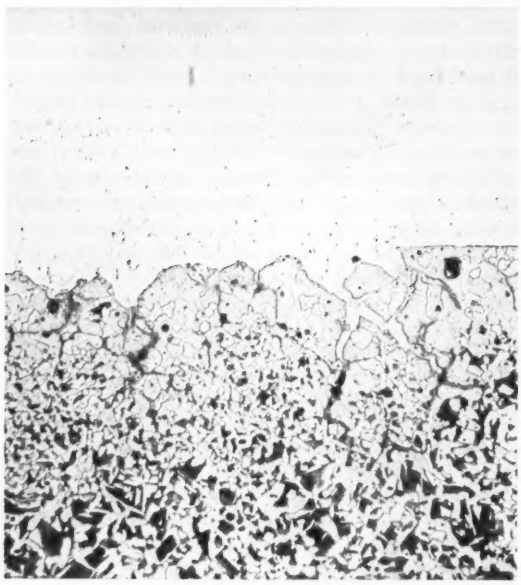

Fig. 7 Microcracks existed in the EBWR vessel SA-212B plate prior to cladding. Some of those under the weld spots became filled with 304 stainless steel in the cladding process.[1]

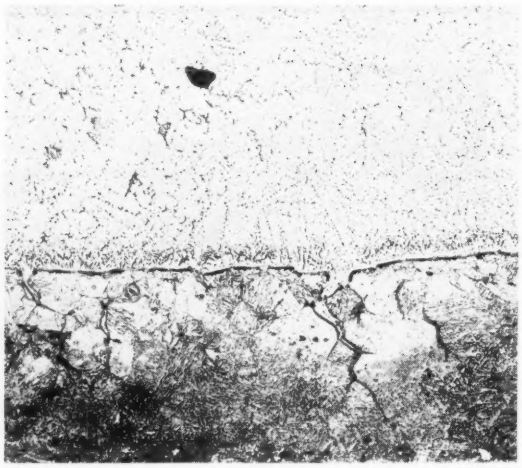

Fig. 8 Microcracks existed in the EBWR vessel SA-212B plate prior to cladding. Some of those under the weld spots became filled with 304 stainless steel in the cladding process.[1]

Yankee Inspections

The foregoing findings and analyses for the EBWR reactor vessel are corroborated by experience at Yankee, where both the reactor vessel and the pressurizer have been inspected and evaluated.[2–4] The major similarity between these two vessels and the EBWR vessel is the method by which cladding was applied—resistance spot welding.

PRESSURIZER VESSEL

Except for the absence of radiation, the service conditions of the Yankee pressurizer approximate those of the EBWR. Exploratory investigations with dye penetrant showed numerous cracks in the pressurizer cladding.[3,4] The checkerboard crack patterns were identical to the EBWR findings, and it is believed that the pressurizer had some cracks in the cladding after it was fabricated.

Explorations in the spot-weld nugget areas showed that the cracks in the cladding do not continue into the carbon-steel vessel material. Analyses of pressurizer operating conditions and all foreseeable effects

of the cracked cladding showed that the pressurizer cracks will not affect operation or present any kind of a safety hazard.

REACTOR VESSEL

Coolant flow within the Yankee reactor vessel caused six holder rods for material irradiation specimens and three locating baskets to break loose. Although four complete irradiation capsules with holders and several locating baskets were recovered in 1963, and four were recovered from within the baffle in 1965, one capsule with its holder rod and two baskets remained in the lower head area until the 1965 refueling.[17,18] At that time it was discovered that several small areas in the lower head cladding had been worn away. As reported by Reed and Tarnuzzer,[19] "When the bottom hemispherical head of the vessel was examined closely, one of the worries of leaving the loose irradiation specimen assemblies (Fig. 9) in the reactor vessel came into view. We

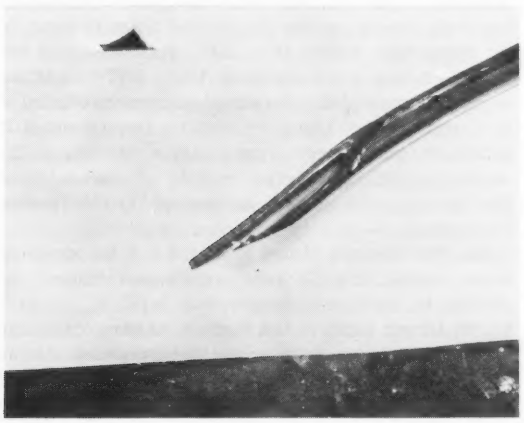

Fig. 9 Irradiation-specimen support rods that broke loose in the Yankee vessel were ground as they whirled around on the vessel bottom. Taper ground on rod shown is radius of bottom section of vessel.[19]

found two small holes (Fig. 10) worn about 0.020 in. through the 0.109-in.-thick cladding. These two holes in the ... cladding resulted in extensive crevice-, galvanic-, and general-corrosion investigations and an extensive evaluation of hydrogen-embrittlement potential. Fortunately all of these investigations turned out favorably and indicated no combination of circumstances that could lead to a potential problem."

Casts of the worn areas in the lower head were made with a curable silicone rubber compound.[2] From these the maximum depth of the penetration from the surface of the cladding measured to be 0.115 in. It was assumed that 0.010 in. of wear had taken place in the 304 stainless-steel cladding in the general area around the penetrations, and there-

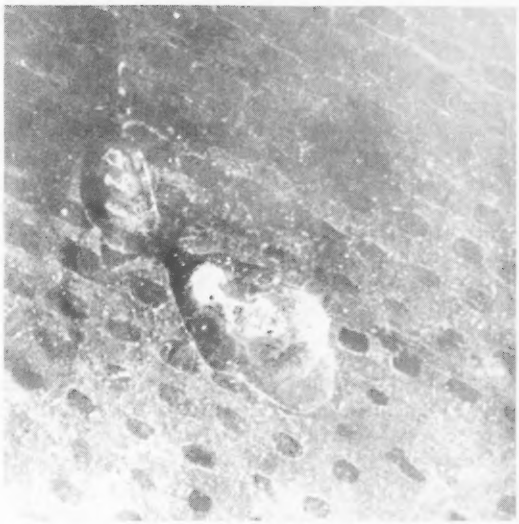

Fig. 10 Carbon steel of Yankee vessel, exposed when debris wore hole in cladding, is seen as light "8"-shape area in this underwater photo.[19]

fore the reduction in the 4.219-in. thickness of the SA-302B carbon-steel vessel wall is approximately 0.016 in.

Repair of these penetrated areas would be difficult because during shutdown, when the pit above the reactor is flooded, the lower head is under about 55 ft of water. Thus the approach was to analyze all possible operational problems that could be foreseen; from this analysis it was concluded that there are no safety problems involved in the continued operation of the vessel with the cladding defects. Details of the analytical methods that led to this conclusion, including mechanical and structural considerations and studies of the sources and effects of hydrogen on the walls of the vessel, various corrosion factors, and effects of the additional radioactive corrosion products, have been reported.[4]

Studies of the effects of the exposed carbon steel in the EBWR vessel and the Yankee vessels corroborate each other.

Elk River Findings

Cracks and other defects were detected in the single-pass weld-overlay cladding in the Elk River reactor vessel after prestartup tests in 1961 during which the system had been heated up nonnuclearly to test piping flexibility.[5,20] The 164 defect areas were ground to the base of the cracks to learn whether the cracks propagated into the carbon steel (they didn't). After the inspection was completed, all the ground areas were filled by a rewelding procedure[5,6] before reactor startup. Since then, the reactor has operated for approximately 1 full-power year,

after which additional cracks were found in the cladding.[21]

VESSEL FABRICATION

Plate material used in the straight shell section and in the heads for the Elk River reactor vessel[22] was clad by a roll-bonding process that complied with ASTM Specification A264 for stainless-steel roll-clad carbon-steel plate; no cracks have been found in this roll-bonded cladding. The 3-in.-thick plate material is A-302B carbon steel, and the cladding is 304 stainless steel. However, the forged material used in the flanges and nozzles is A105-2 carbon steel that was clad with a single-pass weld overlay of 308L stainless steel; the shell flange was overlaid and machined before it was butt-welded to the shell, whereas the head flange was butt-welded to the head before the overlay was applied. Nevertheless, both the shell- and head-flange areas had defects in the overlay cladding.

PRESTARTUP INSPECTION

A systematic inspection program[5] was pursued in 1961 and 1962. All crack or porosity indications were photographed. Because the overlay cladding on the flanges contained defects, 100% of the weld-overlay cladding, including the 10- and 16-in. nozzles, was dye-checked. (Because the reactor had not been operated before the inspection, the vessel was not radioactive and all areas were accessible after most of the vessel internals were removed.) Chemical analyses and hardness measurements were made. On the vessel shell, 109 suspect cladding areas were ground out; another 55 areas were ground out on the reactor-vessel head. A dye check was used in each area after each incremental layer of cladding metal was removed; this procedure was repeated until the carbon steel of the vessel was exposed.

PRESTARTUP TEST RESULTS

It was concluded that the dye-penetrant indications on the vessel shell were caused by porosity or slag inclusions, except for one cladding crack found in one of the 16-in. nozzles and a second crack in a sample adjacent to the first sample. These two cracks apparently resulted from hot shortness (brittle fracture at the high welding temperature) in a local cladding area. Except for these two cracks in this nozzle and one pinhole, all indications had the same appearance and all occurred in the junction of the weld-overlay cladding with the roll-bonded cladding.

When the weld-overlay surfaces of the head flange and head nozzles were examined by dye check, some aligned porosity was seen along the juncture of the Inconel and 308L stainless-steel overlays at the face of the head flange; some random areas of porosity also were seen in the surface of the manual overlay on the ends of all the nozzles. But in none of the ground patches were any unsatisfactory conditions detected in the carbon steel.[20]

The chemical and metallurgical data[20] obtained from the Elk River reactor-vessel patch-grinding program indicated that certain layers of some of the weld overlays contained martensite. No gross cracking was found in the weld overlays. The cracks found in the 16-in. nozzle overlays were hot-short in nature and were confined to the first layer; they did not extend into the base metal.

1966 INSPECTION

After the Elk River reactor had operated for approximately 1 full-power year [27,887 Mwd(t)], all accessible areas of the vessel were inspected again.[21] Inspection of weld-overlay cladding in the shell nozzles (borescopic, visual, and dye penetrant) and the head nozzles and flange (visual and dye penetrant) showed no evidence of cracks. However, although visual inspection of the weld-overlay 20 in. below the shell flange did not show any cracks, dye-penetrant tests uncovered considerable cracking in the weld-overlay within the vessel down to about 10 in. below the flange (Fig. 11). This area was observed during the prestartup 1961–1962 inspection to have a martensitic structure and was predicted at that time to be likely to crack. The martensitic structure was caused by excessive dilution of the austenitic overlay by the melting of carbon steel during the weld-overlay processing at the time of fabrication.

No cracks were found in areas not suspected of being martensitic. Grinding operations showed no cracks to have been deeper than 0.192 in., to have grown larger beneath the surface, to have originated other than at the surface, or to have penetrated as far as the carbon steel. Although the cracks appeared to be intergranular in nature, because they initiated

Fig. 11 Cracks in martensitic stainless-steel weld-overlay cladding just below flange in Elk River reactor vessel were discovered by dye-penetrant inspection in May 1966 (Ref. 21).

at the surface in the martensitic region and not in areas known to have high (0.08%) carbon content, they are believed caused by stress corrosion of martensitic material rather than intergranular corrosion of material with excess carbon content.

It is believed[21] that the reactor can be "operated without removal or repair of the cracks because of the following reasons: (1) No cracks were found which penetrated to the base metal; (2) The cracking observed was confined to an area of relatively low stress; (3) The plant is operated under conditions which prevent brittle fracture propagation; (4) Data available indicate that such defects will not propagate in low cycle fatigue at strain levels present at this location." Continued surveillance is planned during each refueling of the reactor.

Conclusions

Cracks have been found in stainless-steel cladding that was applied to the carbon steel of four reactor vessels by two methods: the stitch-weld process and the weld-overlay process. Although the stitch-weld cladding method has been abandoned for future reactor vessels, weld-overlay claddings apparently can continue to be specified if the deposition conditions and steel constituents are carefully controlled and/or a double pass is employed.

Studies of the four vessels have established that the cladding cracks have not propagated into the base metal, a fact of prime importance for continued safe operation of these vessels. But only continued surveillance of general, pitting, and galvanic corrosion, coupled with water-chemistry evaluations that include frequent analyses of water purity, *p*H, gross activity, and corrosion products, can establish the long-time significance of these vessel-cladding defects. In any case it seems appropriate for reactor-vessel designers and reactor operators to provide for careful inspection of vessel-cladding integrity and to be watchful for new research and performance data on vessel materials.

References

1. N. Balai et al., Inspection, Evaluation, and Operation of the EBWR Reactor Vessel, USAEC Report ANL-7117, Argonne National Laboratory, November 1965.
2. Westinghouse Electric Corp., Atomic Power Division, Evaluation of Yankee Vessel Cladding Penetrations, Report WCAP-2855, Oct. 15, 1965.
3. Westinghouse Electric Corp., Atomic Power Division, Yankee Pressurizer Cladding Evaluation, Report WCAP-2859, Nov. 2, 1965.
4. Westinghouse Electric Corp., Atomic Power Division, Yankee Pressurizer Cladding Evaluation, Report WCAP-2859, Supplement 1, Nov. 23, 1965.
5. K. J. Henry, Investigation of Integrity of Overlay Cladding and Structural Welds of Reactor Vessel and Head, USAEC Report ACNP-62513, Allis-Chalmers Mfg. Co., Mar. 9, 1962.
6. Elk River Reactor Vessel Repaired, Startup Near, *Nucleonics*, 20(7): 68 (July 1962).
7. Reactor File No. 1: EBWR, *Nucleonics*, 15(7): 53 (July 1957).
8. The Experimental Boiling Water Reactor (EBWR), *Power Reactor Technol.*, 1(1): 36-38 (December 1957).
9. N. Balai et al., Summary of the 1965 Partial Inspection of the EBWR Vessel: Cracking of Cladding, *Trans. Am. Nucl. Soc.*, 9(1): 221 (June 1966).
10. Argonne National Laboratory, The Experimental Boiling Water Reactor, USAEC Report ANL-5607, May 1957.
11. J. M. Harrer and T. L. Kettles, Modifying EBWR Vessel for 100-Mw(th) Operation, *Nucleonics*, 19(8): 50-53 (August 1961).
12. Modifications of the EBWR, *Power Reactor Technol.*, 3(3): 62-67 (June 1960).
13. T. L. Kettles and N. Balai, EBWR Reactor Pressure Vessel Revisions for Instrumentation and Increased Steam Output, USAEC Report ANL-6162, Argonne National Laboratory, January 1962.
14. *ASME Boiler and Pressure Vessel Code*, Section II, Material Specifications, 1952 Rev.
15. C. R. Sutton et al., Examination and Evaluation of Experimental Boiling Water Reactor Pressure-Vessel Cladding, *Trans. Am. Nucl. Soc.*, 9(1): 222 (June 1966).
16. R. F. Jones et al., Reactor Vessel Surveillance Program for the Plutonium Recycle Experiment, *Trans. Am. Nucl. Soc.*, 9(1): 222 (June 1966).
17. R. C. Skaardal, Operational Problems and Solutions, *Power Reactor Technol.*, 8(4): 274 (Fall 1965).
18. G. A. Reed, Major Operating and Refueling Problems at Yankee Atomic Electric Company Rowe Power Plant, *Trans. Am. Nucl. Soc.*, 8(Suppl.): 28 (1965).
19. G. Reed and E. Tarnuzzer, Examining Yankee Plant Performance in 1965, *Nucleonics*, 24(3): 42-47 (March 1966).
20. A. L. Schaeffler, Elk River Reactor—Chemical and Metallurgical Aspects of Investigation of Overlay Cladding and Structural Welds of Reactor Vessel, USAEC Report ACNP-62514, Allis-Chalmers Mfg. Co., Mar. 9, 1962.
21. E. B. Norris, The First Inspection of the Elk River Reactor Pressure Vessel After Operation, USAEC Report SWRI 1228-9-8, Southwest Research Institute, June 10, 1966.
22. Allis-Chalmers Mfg. Co., Elk River Reactor Vessel Cladding Defects, USAEC Report TID-13083, May 19, 1961.

Nuclear Plant Performance—Good and Getting Better

By George F. Bierman, Metropolitan Edison Co., and Walter J. Miller, Yankee Atomic Electric Co.

Electric utilities evaluate generating plants on the basis of cost of the power produced and reliability of the plant to produce power when needed. Utilities express the reliability of a plant in terms of its "availability" for operation. Utility-system reserve requirements, plant installation and retirement schedules, and production costs are influenced by plant availability. For nuclear plants, with their lower fuel costs and higher fixed charges (and they are certainly higher, if you remember to include first-core cost), high plant availability is especially desirable. But what availability can we expect, and how can we ensure it?

Study of the operating data for six U. S. utility-operated central-station nuclear power plants that have generated more than 500,000 Mw-hr each (Fig. 1 and Table 1) shows that the availability of a nuclear plant can compare favorably with that of a fossil-fired unit of the same size and degree of maturity. Nuclear plant availability has been adversely affected most by refueling operations, maintenance, and testing. The number and length of outages have decreased as the plants have been debugged and procedures have improved. For example, excluding refueling, the Dresden[1] reactor experienced only one outage — a 4-hr period to test a stuck control rod — during all of 1965, for an availability of greater than 99%. Earlier performance, like that for other plants, was not as spectacular[1–4] (Tables 2 to 4).

From the experience with and performance of these six plants, the following overall judgments can be made:

- Schedules for refueling and plant maintenance outages can be dovetailed with system requirements, as can nuclear plant output.
- Operating, refueling, and maintenance procedures for a water-cooled reactor appear to mature (but not stabilize) after two core lifetimes.
- Refueling can be shortened by design that provides ready access to the core with simple handling equipment.
- Shutdowns caused by malfunctions of fail-safe subsystems should diminish as designs improve.
- Substitution of water type reactors for conventional boilers reduces materials problems for plant operators — because reactor and turbine conditions are much less severe.
- The time it will take future nuclear plants to reach operational maturity will depend on such factors as (1) operating pressure and temperature, (2) quality control during fabrication and construction, and (3) use of components and systems proven by reactor experience or equivalent testing.
- High plant availability for future large plants will come with the modular design approach; more fuel elements, control-rod assemblies, rod drives, coolant loops, etc., can be added, rather than radically changed, to increase capacity.

Although these judgments stem from experience with just six plants, and not from probability mathematics (any sample involving less than 20 plants, nuclear or fossil fired, is regarded[5] as totally unreliable), they seem sound. The growing pains of future plants may be aggravated by their greater power and size, but proper interpretation of the family histories can lead to the best design choices. Then new plants will mature quickly and have high availability.

Evaluating Plant Performance

Plant performance data, summarized in Table 1, can be evaluated in terms of (1) plant capacity factor, which indicates how much power the plant actually generated as compared with how much power it could have generated if it had operated at maximum power

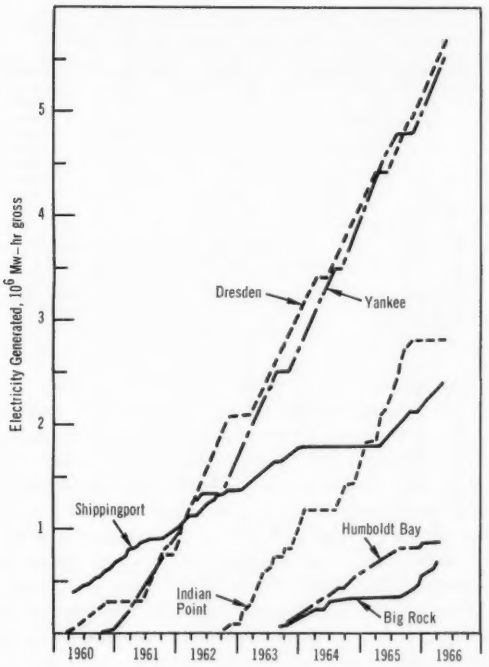

Fig. 1 Electricity generated by these six nuclear central-station power plants totals more than 18 Mw-hr (18×10^9 kw-hr). Refueling operations, maintenance, and testing are the principal drags and cause the flat spots in the curves of power generation.

during all of the period in question (and thus depends on load demand as well as plant reliability); (2) plant availability, which tells the portion of a time period during which a plant was capable of generating electricity; and (3) reactor availability, the portion of a time period during which a reactor was able to make steam. Tables 2 and 3 indicate the major factors affecting plant and reactor availability for five of these stations.

INTERPRETING THE DATA

If the purpose of evaluating the capacity and availability factors is to predict future performance of these or future plants, their operating goals and philosophies must be borne in mind. Specifically, the generation of test information—not electricity—has been the principal goal at Big Rock Point[6–9] and at Shippingport.[10–15] And testing not only reduces capacity factor but also invariably delays system debugging and involves instrument limit settings that cause frequent shutdowns. (Thus evaluation of the operational performance of plants that have dual functions requires careful study.) Dresden, Indian Point, and Shippingport have been load-following plants; as a result, their capacity factors were lower than they might have been, and these plants experienced some shutdowns (e.g., during load swings) that would not have occurred if the plants had been operated to supply the base load demand. On the other hand, Yankee was base-loaded and thus had practically as high a capacity factor as was possible.[16]

Table 1 CAPACITY AND AVAILABILITY FACTORS* FOR SIX MAJOR WATER-REACTOR PLANTS

	Power, Mw(e) net	Date critical	Factors during each year, %							
			1958	1959	1960	1961	1962	1963	1964	1965
Shippingport	60–140 equiv.	12/7/57								
Capacity factor			37	34	45	59	62	66		62†
Plant availability			53	50	50	64	76	81		69†
Reactor availability			68	67	50	64	76	81		71.5†
Dresden	200	10/15/59								
Capacity factor					21.8‡	33	73	53.8	56.2	55.4
Plant availability					32.9‡	38.1	78.6	75.6	80.9	78.7
Reactor availability					58.7‡	40.2	80.6	80.7	82.7	78.3
Yankee	175	8/19/60								
Capacity factor						76‡	55	69	80	65
Plant availability						89‡	64	78	88	73
Reactor availability						90‡	65	78	90	74
Indian Point	255	8/2/62								
Capacity factor							28‡	38	25	47.6
Plant availability										62.2
Reactor availability								67	48	64.0
Big Rock Point	71.5	9/27/62								
Capacity factor								35‡	42	29
Plant availability								39‡	43	30.1
Reactor availability								42‡	56	30.7
Humboldt Bay	50	2/16/63								
Capacity factor								78‡	83	60
Plant availability								81‡	87	77
Reactor availability								82‡	89	79

*Capacity factor = $\frac{\text{Power generated, Mw-hr}}{\text{Max. dependable capacity, Mw} \times \text{period, hr}}$

Plant availability = $\frac{\text{Period, hr} - \text{plant outage, hr}}{\text{Period, hr}}$

Reactor availability = $\frac{\text{Period, hr} - \text{reactor outage, hr}}{\text{Period, hr}}$

†Portion of year after plant modified (5/3/65) to raise power from 60 Mw(e) to 140 Mw(e) equivalent.

‡Portion of year after start of full-power operation.

Table 2 REACTOR-SYSTEM OUTAGES, HOURS (AND NUMBER)

Year	Shippingport			Dresden			Yankee				Big Rock Point			Humboldt Bay		
	Instruments		Other	Instruments	Steam drum	Control-rod drive	Instruments	Valve-stem leaks	Misc. leaks	Other	Instruments	Control-rod drives	Modifications	Instruments	Tests	Other
Forced outages																
1958	14 (3)		26 (2)													
1959	65 (2)		83 (1)													
1960	50 (8)		0	0	23 (2)	1127* (1)										
1961	6 (2)		12 (3)	0	0	3670	5 (2)	105 (3)	36†	6 (1)						
1962	19 (2)		15 (2)	0	18 (1)	0	0	0	0	0						
1963	4 (1)		4 (1)	5 (1)	0	0	7 (2)	0	148 (5)	22 (1)	34 (1)	80 (1)		12 (3)	25‡ (1)	2 (1)
1964	Plant modifications			0	0	0	15 (1)	0	0	22 (1)	30 (1)	0		9 (2)	55 (3)	0
1965	27 (4)		7 (1)	0	0	0	0	0	0	0	0	0	5921 (1)	0	0	4 (1)

Year	Tests	Instruments	Maintenance	Other	Tests	Training and licensing	Maintenance	Tests	Vapor control	Control rods	Other	Instruments	Tests	Inspections	Maintenance	Instruments	Tests	Licensing
Scheduled outages																		
1958	710 (8)	231 (3)	1690 (5)	117 (4)														
1959	831 (5)	0	0	0														
1960	1472 (10)	0	79 (2)	25 (4)	274 (3)	1005 (4)	1283 (1)											
1961	1541 (10)	14 (1)	0	27 (2)	0	67 (1)	1544 (1)	625 (4)	9 (4)	19 (6)	4 (1)							
1962	1465 (6)	20 (1)	0	20 (1)	41 (1)	0	261 (4)	7 (1)	0	0	0							
1963	969 (7)	50 (2)	331 (3)	46 (2)	0	0	0	0	0	0	69 (1)	14 (1)	1420 (6)	0	2274§ (1)	0	79 (1)	0
1964	Plant modifications				104 (1)	0	0	21 (1)	0	0	0	0	1095 (3)	764§	1930§ (0)	0	325¶ (1)	16 (1)
1965	244 (8)	22 (1)	81 (2)	1348 (2)	0	0	4 (1)	68 (1)	9 (4)	0	0	0	0	0	151§ (1)	35 (2)	112 (1)	0

*Shutdown continued into following year.
†Extension of shutdown for other purposes.
‡Includes scheduled outage extensions for testing.
§Includes extension after shutdown for other reason.
¶Includes forced-outage extension.

Table 3 NONREACTOR-SYSTEM OUTAGES, HOURS (AND NUMBER)

Year	Shippingport	Dresden		Yankee			Big Rock Point			Humboldt Bay	
	All causes	Leaks	Other	Control valves	Instruments	Other	Bypass valve	Turbine	Other	Instruments	Other
Forced outages											
1958	122 (2)										
1959	0										
1960	4 (1)	150 (3)	0								
1961	0	0	0	94 (7)	7 (3)	10 (1)					
1962	0	29 (1)	44 (1)	115 (3)	0	0					
1963	0	0	97 (4)	22 (1)	0	7 (2)	26 (2)	0	195* (5)		
1964	Plant modifications	146 (2)	9 (2)	4 (1)	5 (1)	20 (3)	327 (5)	886* (1)	7 (1)		
1965	14 (1)	320 (4)	31 (1)	0	0	15 (1)	0	0	34 (1)	21 (1)	8 (2)

Year	Maintenance	Other	Tests	Inspections	Turbine	Other	All causes	Turbine	Tests	Other
Scheduled outages										
1958	1230 (3)	0								
1959	1421† (2)	44 (1)								
1960	43 (1)	0	35 (4)	7 (1)	78 (2)	132 (2)				
1961	0	0	0	0	59 (1)	79 (1)	0			
1962	0	4 (1)	0	122 (2)	0	0	0			
1963	0	25 (1)	173 (1)	0	97 (2)	119 (2)	1 (1)	0	0	2070‡ (4)
1964	Plant modifications		0	0	0	39 (1)	2 (1)	0	14 (2)	5 (1)
1965	64 (3)		0	0	(2)	60* (1)	8 (1)	18 (1)	0	74 (1)

*Includes extension after shutdown for other reason.
†Shutdown continued in following year.
‡Prior to commercial operation for miscellaneous plant modifications including reactor systems.

Table 4 DAYS REQUIRED FOR REFUELING, OVERHAULING, AND TESTING VARIOUS REACTORS EACH YEAR

Year	Shippingport	Dresden	Yankee	Humboldt Bay
1958	0			
1959	86.3*			
1960	101.5†	0		
1961	54.2	0	0	
1962	36*	54.5*	126.5	
1963	11.1†	68.6†	72	0
1964	‡	57.5	35.6	28.2
1965	0	62.1	93.5	71.8§

*Shutdown continued into following year.
†Includes extension of shutdown from previous year.
‡Plant modifications.
§Length determined by containment-system modifications; refueling was completed in 22 days.

In Tables 2 and 3 we have tried to categorize all outages according to the principal reason for the outage or its extension. However, invariably, scheduled outages have been planned for a combination of reasons; during many of the extended outages, repairs and tests have been made concurrently. Shutdowns frequently have been extended by on-the-spot decisions to perform maintenance work or to run tests. Thus delays not related to the initial cause of an outage are in some cases included as separate outages. Except when noted otherwise, refueling periods are included in determining capacity and availability factors. During outages for reactor tests at zero power and for operator training, the reactor and (therefore) the plant are assumed to be unavailable for generation. Thus time required for testing, inspecting, and training is regarded here as being related to a plant's period of immaturity. Actually, test programs are shrinking as the accuracy of core calculation methods is verified and as experience is gained with cores and system components. But not all test-time eliminated is time saved because maintenance work is often done concurrently with testing; savings vary from 50 to 100% of the test-time eliminated, depending on plant and core age.

MAJOR OUTAGES

Each of the four plants in operation before 1963 has had four or five shutdowns that have had more effect on plant availability factors than have the combined remaining shutdowns. These appear as flat spots in the generation curves in Fig. 1. Although most lengthy shutdowns were for refueling (several were for plant modifications), maintenance usually lengthened the outages.

Except for a 1958 outage to repair a turbine moisture separator and a test and training period at the end of 1962, the major Shippingport outages before 1964 were all during refueling periods.[11,15] The major Dresden outages in 1961 were for control-rod-drive modifications and inspection; however, subsequent major outages were for refueling. Much of Yankee's downtime has occurred at refueling periods; actually, the duration of Yankee's 1962 and 1965 refuelings were extended about 2 months because of maintenance problems and needed modifications.[16,17] The long Indian Point outage in 1964 resulted from a decision to make plant modifications at that time.

MATURITY

Experience shows that reduced maintenance requirements can be expected by the time a plant has operated through two core lifetimes. This is true for maintenance performed during refueling as well as for that performed during shutdowns specifically for maintenance. The eventual refueling time can be estimated fairly accurately after a plant has been refueled twice, by which time procedures will have been established, personnel trained, and equipment debugged. Therefore further improvements can be expected in availability factors for the Humboldt Bay, Big Rock Point, and Indian Point plants. Of course, design improvements will also permit future plants to benefit from this evolution.

Refueling Outages

The major factor limiting availability is scheduled maintenance, which is usually labeled "refueling" but often also includes turbine-generator inspection and overhaul and, with young plants of a new design, extensive modifications. Table 4 summarizes these outages, which greatly reduce overall availability.

IMPACT ON AVAILABILITY

Experience at Dresden 1, which was refueled in 1962, 1964, and 1965 (Fig. 2), is especially significant when examined on a fuel-cycle basis. Although plant availability for a calendar year has not exceeded 80.9%, during Cycle 2 the plant availability was 93.4% and during Cycle 3 it was 96.2%. (During Cycle 2, which extended from Mar. 10, 1963, to Apr. 12, 1964, Dresden generated 1,327,341 Mw-hr of electricity; during Cycle 3, June 7, 1964, to Mar. 28, 1965, the plant generated 983,981 Mw-hr.) But downtime during the first Dresden refueling (after Cycle 1, which lasted 36 months and 23 days) required approximately 123 days; this included turbine inspection and overhaul. The second refueling (96 elements) took only about 57 days, including approximately 1 week for a containment-sphere pressure test.

The third refueling (200 elements) of Dresden 1 began on Mar. 28, 1965. Turbine inspection and overhaul were performed concurrently, and the unit was returned to service on May 29, for a total of approximately 62 days of scheduled-outage time, including another 20-psig pressure test of the plant containment—which illustrates the incentive for devising ways to speed such routine tests. Exclusive of refueling, during 1965 the only outage, either forced or scheduled, involving the reactor was a 4-hr period required to test a stuck control rod. Thus, considering only the reactor, its availability during 1965

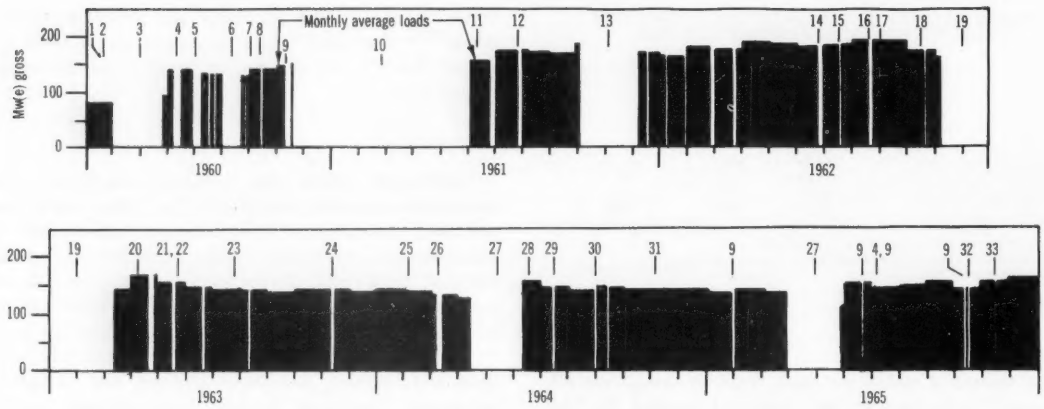

Fig. 2 Dresden Station Unit No. 1, Commonwealth Edison Co., plant outages were for the following reasons:

1. Low drum level and turbine rub
2. Leak in secondary drain
3. Remove test fuel and revise guide tubes
4. Reactor turbine test
5. High drum level and turbine drain
6. Personnel training and miscellaneous repairs
7. Recirculating pump leak (derating)
8. High-pressure turbine drain leak
9. Repair secondary-system leaks
10. Modify control-rod drives
11. Reactor testing (derating)
12. License examinations and turbine maintenance
13. Control rod and drive and inspect reactor internals
14. Scram, friction and temperature-coefficient tests
15. Leak in "D" extraction steam line
16. Motor-generator transient and temperature-coefficient tests
17. Low-drum-level scram
18. Fuel depletion (derating)
19. First refueling and turbine overhaul
20. Condensate demineralizer limitation
21. Scram, pressure-regulator sensing line
22. Turbine vibration and condensate pump leak
23. Repair transformer No. 1 lightning arrester
24. Repair turbine oil system
25. Fuel depletion (derating)
26. Nuclear testing
27. Refueling and sphere test
28. Loss of feedwater pumps
29. Moisture-removal-line leak
30. Extraction and gland line leaks
31. Minimize fuel failures (derating)
32. Control rod stuck
33. Transmission-line storm damage

was 83% including refueling and greater than 99% exclusive of refueling time; overall plant availability was 78.3% including refueling and 94% exclusive of refueling time.

Refueling experience at Dresden,[16] Shippingport,[11,15] and Yankee (Rowe)[17,18] shows that the actual replacement of the fuel need not be a particularly time-consuming operation if the fuel-handling equipment is of reasonably straightforward design for such repetitive operations. But the problems of gaining access to the fuel are another matter, although such difficulties are susceptible to solution by design improvements or evolution of operational procedures. Some steps that can reduce downtime for refueling are:

- Use hydraulic stud tensioners instead of bolt heaters to remove the bolts that fasten the reactor-vessel head.
- Mount control-rod drives on the bottom of the reactor vessel so they will not have to be disconnected from the rods before the vessel head is removed.
- Arrange vessel penetrations for instrumentation connections through the vessel itself or the bottom head, rather than through the vessel head, so that they will not have to be disconnected before the head is removed.
- Minimize and simplify above-core vessel internal structures so that access to the core can be achieved more readily.
- Locate coolant-flow-adjusting orifices in the core grid support structure, rather than on each fuel subassembly, so that it will not be necessary to change orifices when fuel is being "shuffled" during partial refuelings.
- Design and use the simplest and most rugged refueling tools consistent with the precision and handling care needed so that they will function reliably for the repetitive operations required of them.
- Design each fuel subassembly with more and longer fuel rods so as to reduce the number of handling operations per core.

EXPECTATIONS FOR NEW UNITS

Future pressurized-water reactors, with bottom-mounted control-rod drives and instrumentation, few vessel internals above the core, and reasonably straightforward refueling equipment, have been esti-

mated by Yankee Atomic Electric Co. to be refuelable in approximately 16 days. Routine refueling at Yankee (Rowe) now is expected to require about 4 weeks and to be accomplished concurrently with turbine-generator maintenance; the fact that the first four refuelings at Yankee (Rowe) took longer than this (Table 4) is attributable mostly to reactor modification and plant maintenance.

cleanup. In the reactors for the new Dresden 2 and 3 units (Fig. 3), each fuel bundle will produce twice as much power as a Dresden 1 fuel bundle; this will be accomplished by lengthening fuel rods (from 9) to 12 ft and using 49 rods per assembly instead of 36 — and will shorten refueling time by 2 to 4 days.

Table 5 shows our "guesstimates" of scheduled outages for new units using boiling- or pressurized-

Fig. 3 Dresden 2 and 3 will dwarf the present 200-Mw(e) plant (background). Both the new units, scheduled for service in 1969 and 1970, are initially rated at 715 Mw(e) and might stretch to 810.

The second unit at Dresden, which will have an initial capacity of 715 Mw(e) net and an ultimate rating of 793 to 810 Mw(e), is expected to need only 15 to 20 days for refueling, and the forced-outage rate is predicted to be about 1%. The pressure-suppression type containment should halve the down-time for containment leak testing. Thus unit availability should be about 94%.

Unlike Dresden 1, where spent fuel is transferred through canals from the reactor building to a separate storage building, the designs of the new units include spent-fuel storage facilities which are adjacent to the reactors and which eliminate canals and reduce

water reactors. Note that the most extended outage comes in the third year, when the reactivity-holddown neutron absorbers (rods or curtains) are removed and the first partial fuel change is made.

Yankee (Rowe)

Yankee experience shows the advisability of using proven materials and designs where possible and the need for adequate testing where in-pile experience is unavailable.[17–23] Although fretting wear in mechanical joints was not experienced during control-rod-motion proof-tests by the designer, it was discovered during

Table 5 ESTIMATED SCHEDULED OUTAGES FOR LARGE WATER-REACTOR POWER PLANTS*

Plant power and part requiring outage	Days of outage during each year after reactor begins producing power									
	1	2	3	4	5	6	7	8	9	10
600-Mw(e) capacity										
Reactor	0	0	24	18	18	18	18	18	18	18
Turbine†	28 (HP,G)	18 (LP)	18 (LP)	18 (LP)	18 (G)	21 (HP)	18 (LP)	18 (LP)	18 (LP)	18 (G)
800-Mw(e) capacity										
Reactor	0	0	27	20	20	20	20	20	20	20
Turbine†	28 (HP,G)	18 (LP)	18 (LP)	18 (LP)	18 (G)	21 (HP)	18 (LP)	18 (LP)	18 (LP)	18 (G)
1000-Mw(e) capacity										
Reactor	0	0	31	23	23	23	23	23	23	23
Turbine†	28 (HP,G)	28 (HP,G)	24 (2LP)	18 (LP)	18 (LP)	28 (HP,G)	28 (HP,G)	24 (2LP)	18 (LP)	18 (LP)

*Based on three-shift operation with experienced and unlimited manpower.
†HP designates high-pressure turbine; LP is low-pressure turbine; G is generator.

the first refueling, when it caused a 6-week delay.[18] Most of the component failures that caused major delays during refuelings were due to vibration caused by hydraulic forces (Big Rock Point has had similar problems).[24,25] Control-rod rubbing straps, shim-rod surfaces, and in-core instrumentation thimbles fretted and required design modifications. Irradiation specimens became detached in the vessel, and some thermal-shield joint bolts have broken because of vibration caused by hydraulic forces. Activated corrosion products have caused serious delays by contaminating the refueling systems, a delay not anticipated during preirradiation tests. Other delays have been caused by difficulties in debugging the complex fuel-handling equipment. Fortunately, these problems have been recognized and in general have been eliminated.

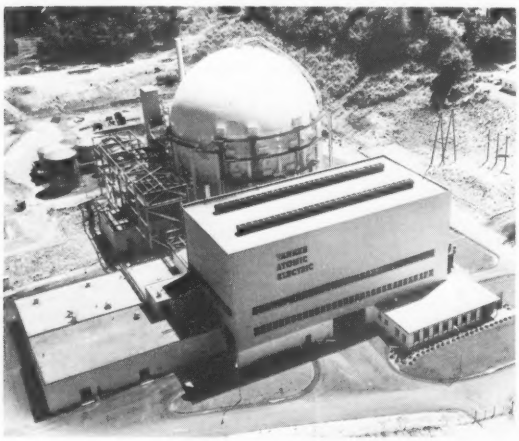

Fig. 4 Yankee (Rowe), with a capacity of 175 Mw(e) net, has generated approximately 5 million Mw-hr since initial criticality Aug. 19, 1960.

During 1961 the Yankee plant experienced various problems that caused relatively short shutdowns (Figs. 4 and 5 and Tables 2 and 3). Downtime for tests to confirm performance calculations reduced plant availability by about 7%. Plant availability was reduced another 3% by all other shutdowns because of such factors as (1) primary-system valve-stem leakage, (2) turbine control-system malfunction, (3) the need to interchange the control rods, or (4) decisions to inspect equipment.

By 1962 many of the causes of the early shutdowns had been eliminated, and the extensive testing required with Core 1 was no longer required. Modifications of the valve-stem packings have prevented

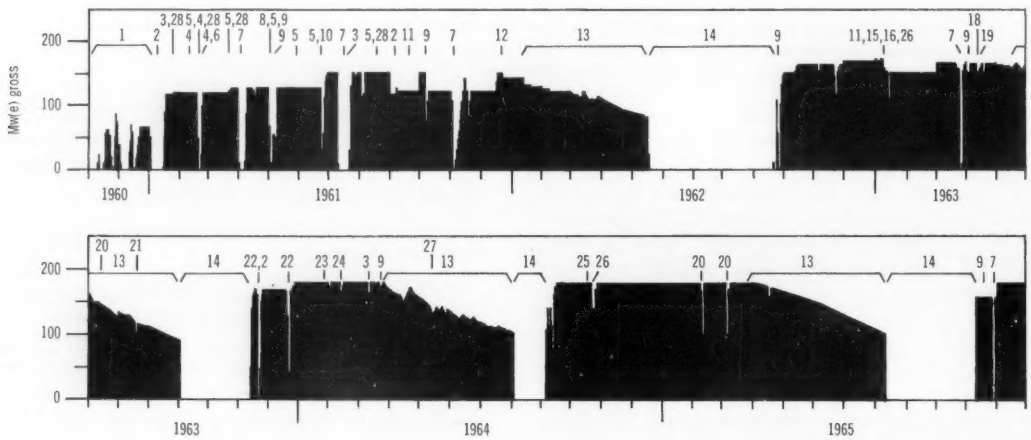

Fig. 5 Yankee (Rowe), Yankee Atomic Electric Co., plant outages had the following principal causes:

1. Initial test operation
2. Turbine vibration
3. Scram by moisture-separator switch
4. Valve stem leak-off
5. Control-rod interchange
6. Scram by instrument noise
7. Scheduled physics testing
8. Modified pressurizer instrumentation
9. Erratic turbine control valves
10. Throttle-valve sticking
11. Boron test
12. Scram by false flow signal
13. Core "stretch-out"
14. Refueling
15. Charging-line relief-valve leak
16. Primary drain-valve leak
17. Primary and secondary maintenance
18. Scram when control rod dropped
19. Flowmeter pipe leak
20. Transmission line fault
21. Scram-detector cable damage
22. Head adapter leak
23. Faulty turbine trip mechanism
24. Control-rod drop tests
25. Condenser baffle
26. Instrument ion scram
27. Low condensate pressure
28. Inspection in vapor container

leakage. The need for shutdown to interchange control rods has been eliminated by operating with soluble boron control and with rods fully withdrawn. There is now no need to shut down for routine inspection of equipment in the vapor container.

For the years in which the plant was refueled, 1962 to 1965, plant availability was 64, 78, 88, and 73%. Except for the effect of core stretch-outs, availability is expected to be comparable with that of fossil-fired plants of like size. The forced-outage rate for these years was 2, 3, 0.8, and 0.2%. Excluding refueling and the effect of stretch-out, reactor availability was 99.8, 97.5, 99+, and 99+% in 1962 to 1965.

REFUELINGS

The major portion of all Yankee maintenance was performed during refuelings (Table 4). At the first refueling the Zircaloy control-rod followers were found to have worn by fretting at the stainless-steel-to-Zircaloy joint where they attach to the control rods. For this reason the followers were replaced with new ones having stainless-steel adapters designed to eliminate wear; but this work delayed operation 6 weeks. Fortunately, the modification proved to be successful. Another week was lost during repair of in-core instrumentation damaged during the refueling. The refueling shutdown extended 2 weeks more because radioactive silver that corroded from the first control rods contaminated the refueling area. These rods have since been replaced by rods that resist corrosion better.[18,25]

At the end of the second refueling shutdown, 14 days were lost to remove the vessel head so that a stuck control rod could be modified to prevent a recurrence; 7 days were used in the inspection of core components and vessel internals. Additional delay was caused by difficulties in attaching the shafts to the control rods. By now, most of these problems appear to have been solved.

The third refueling took 35 days. Three of these 35 days were for unplanned extensions to leak-test neutron sources and to inspect the irradiation specimens. Four days were consumed by difficulties in latching shim rods to their extensions and in coupling drive shafts to control rods. During the fourth refueling, which took 93 days, the core barrel was pulled to provide access to the entire inside of the vessel, the thermal-shield joint was modified, and a secondary core support was installed.[17]

Shippingport

Designed for operation either as a base-loaded or load-following plant, Shippingport (Fig. 6) has been successful in both operating modes. However, tests to determine overall station performance and to evaluate individual systems and components have used large portions of operating time[10–15] (Fig. 7) which have decreased plant capacity factor and caused outages that would not have been experienced had the plant remained base-loaded. For example, the large number of fail-safe protective devices installed for tests often led to spurious shutdowns during power changes and also demanded considerable operator attention because the set points are close to normal operating conditions.

Although the shutdowns resulting from instrument actions or failures were numerous, they were short; the plant may even have profited from these early problems. The 22 forced shutdowns and 7 scheduled shutdowns because of instrument action or need for repairs are more important in considering reliability (to take or hold load) than in calculating capacity factor. Plant forced-outage rates were 3, 4, 1.2, 0.3, 0.5, and 0.1% in the years 1958 to 1963. In 1964 the plant was down for modifications to increase its capacity to 140 Mw(e) net equivalent. For the last 8 months in 1965, the forced-outage rate was 1.2%. (The forced-outage rate of conventional plants is approximately 2%.) Shutdowns decreased as instrumentation systems were debugged and as the design of some components was improved. Improvements made apparent by experience at Shippingport are being made in other plants.

TESTING AND MAINTENANCE

Except when maintenance was clearly related to a test, it was difficult during Seed 1 operation to attribute outages to either maintenance or testing. In most cases they were performed concurrently. However, in Tables 2 and 3 outages are identified with whichever need appeared to be the most pressing. During a very significant percentage of the time Seed 1 was in use, the plant was devoted to testing; station capacity factor was 37%, plant availability was 45%, and reactor availability was 75%. Approximately 12% of Seed 1 operation was spent on maintenance of the moisture separator. Modifications have been made, and similarly modified separators installed at Yankee have had no problems. Another 10% of Seed 1 operation was spent on reactor-systems maintenance; 7% was spent on turbine-plant maintenance. Problems encountered early with governor control valves, steam generators, and main coolant pumps appear to have been solved.

TESTING TAKES TIME

The time spent for testing and training was almost doubled during operation with Seeds 2, 3, and 4 (note item 11, Fig. 7). The outage time attributed to maintenance has become a negligible influence on the plant availability factor. While operating with Seeds 2, 3, and 4, plant capacity factors were 70, 77, and 75% and plant availability was 79, 83, and 82%. Excluding downtime for testing, training, and refueling, reactor availability during each of these periods was 97%. Tables 2 and 3 show that, since the start of operation with Seed 2 early in 1960, the outages for

Fig. 6 Shippingport is a much modified nuclear power station. Initially built for tests and 60 Mw(e), the vessel now has a new head and a core that generates 140 Mw(e) net equivalent. Turbine generators can only use part of the steam; 50 Mw(e) net equivalent is dumped.

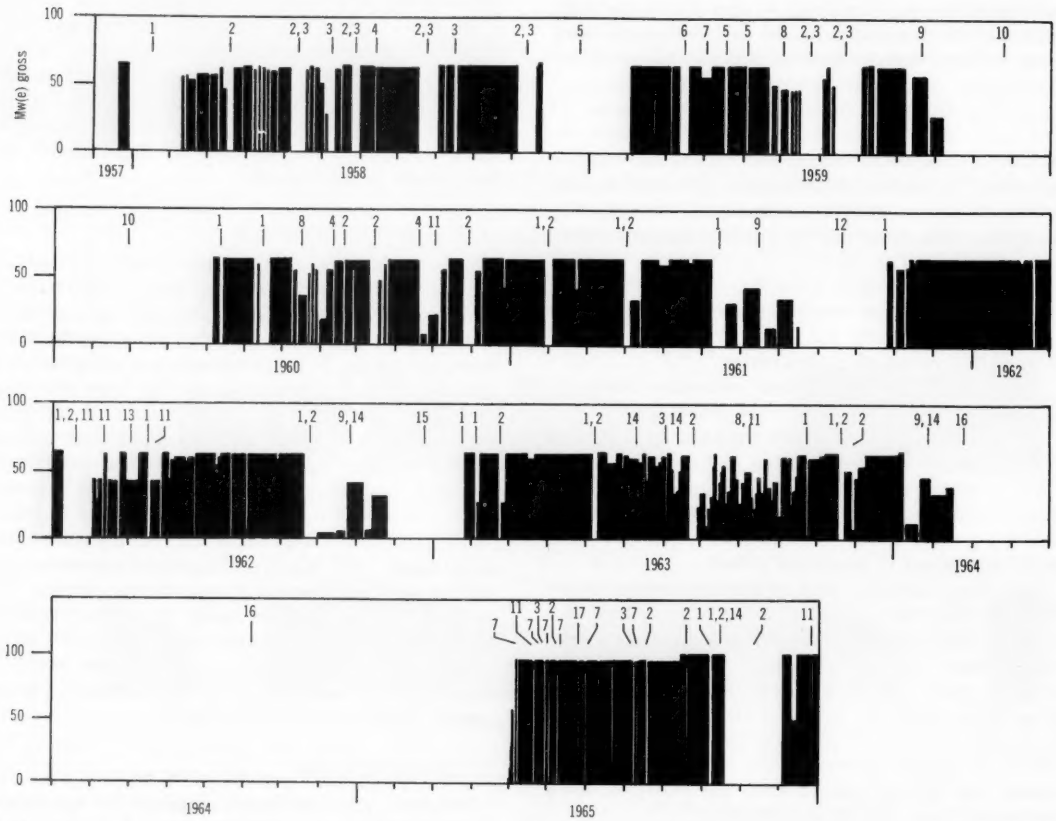

Fig. 7 Shippingport Atomic Power Station, Duquesne Light Co., plant outages were for the following principal reasons:

1. Hot plant and physics testing
2. Plant maintenance
3. Low-power physics testing
4. Returning a reactor coolant loop to service
5. Turbine-blading and moisture-separator repair
6. Turbine governor-valve deficiency
7. Nuclear instrumentation failure
8. System load requirements
9. Extended-life operation at reduced temperature
10. Seed 1 to Seed 2 refueling
11. Training
12. Seed 2 to Seed 3 refueling
13. Xenon oscillation testing
14. Heat-dissipation system testing
15. Seed 3 to Seed 4 refueling
16. Core 1 to Core 2 refueling and plant modifications
17. Control-rod sequence change

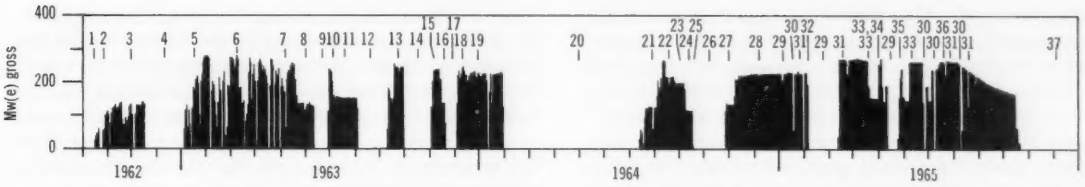

Fig. 8 Indian Point Station, Consolidated Edison Co., plant limits and outages were as follows:

1. First power operation
2. Ascending power tests
3. Limit 50%, single superheater
4. Control-start superheater piping
5. Ascending power tests
6. Load not limited, 89 days
7. Limit 92.5%, coolant pump 122
8. Limit 50%, single superheater
9. Generator hydrogen-seal brackets
10. Limit 85.8%, coolant pumps 122, 131
11. Limit 58%, water pump 12
12. Coolant pumps and circulating-water pumps
13. Limit 92%, primary pump 132
14. Nuclear boiler 14
15. Limit 92%, primary pump 132 (continuous)
16. Limit 50%, single superheater
17. Main-turbine steam-lead crack
18. Limit 92%, primary pump 132 (continuous)
19. Limit 84%, primary pump 132
20. Pool lining, gamma scanning, shim removal
21. Limit 50%, single superheater
22. Load not limited, 10 days
23. Limit 78%, nuclear boiler 11
24. Limit 71%, nuclear boiler 11, primary pump 122
25. Limit 44.5%, nuclear boilers 11 and 14, primary pump 122
26. Nuclear boilers 11 and 14, primary pumps
27. Limit 50%, single superheater, nuclear boiler 11
28. Limit 78%, nuclear boiler 11
29. Rod drive
30. Reactor instrument
31. Plant electrical
32. Weekend and rod drive
33. Control system
34. Deaerator level
35. Condenser leak
36. Superheater
37. Refuel
38. Stretch-out

purposes other than refueling or testing have, with one exception, had an insignificant effect on plant availability factors. The exception was a 10-day shutdown in 1963 for maintenance and test, which influenced availability factors by only 3%. Other maintenance has been performed but was not the primary reason for the outages.

Both plant availability and capacity factor would increase if testings were reduced to a minimum and if the plant were base-loaded, a fact demonstrated when the plant has been base-loaded; a drastic reduction in test operations would result in an increase of around 8% in plant availability. By improving procedures it has been possible to reduce refueling time to 2 months. With the uncomplicated vessel head installed with Core 2 (the older head was complex, designed for test use), it is anticipated that refueling can be accomplished in less than 6 weeks. Quite possibly the plant can continue to operate with no more than two forced shutdowns per year and to have a plant availability of 87%, which compares favorably with experience with fossil plants of this size.

Dresden

In the first two calendar years of Dresden operation (Fig. 2), extensive outages occurred for component modifications and removal of test assemblies (7624.2 hr) and for personnel training (1072 hr). By far the most significant item was the 4797.5 hr required for control-rod-drive mechanism changes. The resulting forced-outage rate for 1960 and 1961 was 38.4%. From 1962 to 1965 the forced-outage rates were 1.3, 1.5, 2.2, and 4.9%, whereas plant availability was 78.6, 75.6, 80.9, and 78.3%.

Practically all outage time in the turbine-condenser portion of the Dresden plant, either scheduled or forced, was precipitated by leaks in piping and flanges; approximately 300 hr were required to repair these leaks and about 60 hr were spent on condenser-tube leaks.[3]

Indian Point

The Indian Point Station (Figs. 8 and 9) had been in operation[26–28] slightly over 3 years when the data

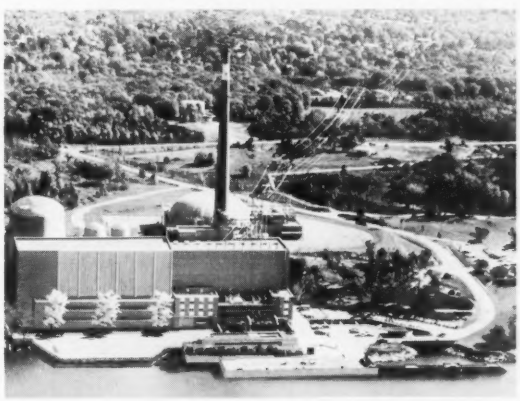

Fig. 9 New Indian Point Station (drawn in at left), 873 Mw(e) net, is to be completed by 1969.

were reviewed. All difficulties appear to be fairly conventional and readily remedied, e.g., by changing gasket materials on pumps. Because few data are available on refueling, estimates of future availability are subject to considerable error. An extended outage to load the reactor with a redesigned core and reactor internals started in October 1965. For 1965, including the 2.5-month shutdown in late 1965, plant availability was 62%.

The 173-day shutdown in 1964, item 20 in Fig. 8, was by far the longest shutdown in over 3 years of operation. It was extended 1 month beyond the time required to remove core shims by a license requirement that the hot fuel be gamma-scanned to confirm core performance calculations. Additional downtime resulted from installation and leak-testing of a stainless-steel pool liner, a step taken to reduce potential radiation and contamination problems. During this outage the oil-fired superheaters were partially retubed.

On completion of the initial 50% power operations in 1962, the plant was down 48 days to modify piping for parallel operation of the oil-fired superheaters. After completion of the ascending power tests to 100% power on Jan. 25, 1963, the plant was not load-limited for 89 days. During this period the plant output was varied considerably, and its performance was satisfactory.

COMPONENTS

Leakage past the thermal barrier of a primary coolant pump on May 6, 1963, caused the load limit to be reduced by 7.5%. This problem has caused six similar reductions for a total of 156 days in 2 years. During a 39-day shutdown starting in September 1964, the thermal barriers in the three pumps were modified and leaks in two nuclear boilers were repaired. In the 2 years of operation, boiler problems caused 22% reduction of load limit during 105 days.

Conventional plant equipment caused an appreciable reduction in plant load factor; superheater problems caused a load limit of 50% for a total of 62 days; circulating-water-pump problems caused a 58% limit for 30 days. The main coolant pumps were repaired during the 38-day shutdown starting in August 1963. A main-turbine steam-lead crack caused a 13-day outage for repairs.

Fail-safe controls caused numerous fast control-rod insertions and scrams that resulted from instrument faults and temporary spurious signals initiated within the systems themselves during operating manipulations. Such outages, which were relatively short, decreased in number as the systems were debugged.

Big Rock Point

This 50-Mw(e) boiling-water-reactor plant (Fig. 10) achieved full power in March 1963. In the research and development program scheduled over the next several years, it is planned to raise the output to 75 Mw(e). In this same period the plant, under AEC contract, is to be available for an extensive irradiation program to test UO_2 fuels that cost less to fabricate, operate to greater burnups, and produce more power per unit volume of core (45 to 60 kw/liter).[6–8] Refinements in fuel-element fabrication made possible by this program will result in improved economics and operation of future cores for this and similar reactors. Operation of Big Rock Point plant also is intended to furnish data on stability, power distribution, fluid flow, and heat transfer.

WIDE DESIGN PARAMETERS

Although the initial rated output for this reactor is 157 Mw(t) at a system pressure of 1050 psia, all components have been designed for operation at 240 Mw(t) and 1470 psia. Obviously, operation over this wide range of conditions can be accomplished only with a highly flexible design. Coupled with provisions for development of high power densities, the result is a reactor that is not optimized for routine power generation; therefore it probably will not achieve the availability expected in a more conventional installation.

VIBRATION

Modifications to the thermal shield and installation of a new thermal-shield seal were completed in August 1965. This outage started in October 1964 when 6 of the 12 thermal-shield holddown studs failed by fatigue; investigation disclosed that coolant flow induced a self-excited vibration of the shield. A new seal design and location of the seal on top of the shield eliminated the problem. Close attention to mechanical design and testing of vessel internals can eliminate a repetition of this experience.[24]

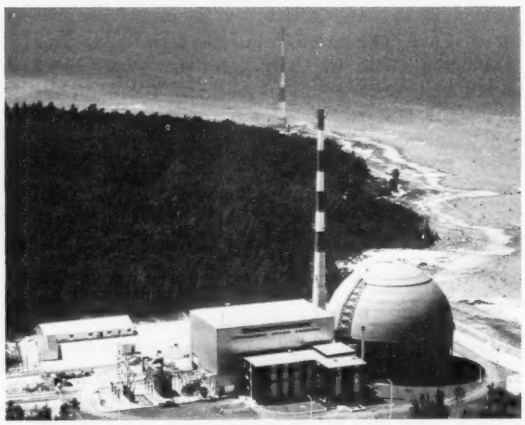

Fig. 10 Big Rock Point plant, following initial criticality in September 1962, has pursued an extensive research and development program designed to uprate core power density with improved fuels.

After the thermal-shield modification was made, one forced outage of 34 hr and two scheduled outages of 169 hr were recorded in 1965. The forced outage was caused by a defective tone relay on a 138-kv transmission line. The scheduled outages were brought about by leaks in the turbine drain manifold, a defective 138-kv circuit breaker, and a need to modify 22 control-rod drives.

Humboldt Bay

Initially licensed to operate at 165 Mw(t) and authorized in May 1965 to increase power to 70 Mw(e) gross [240 Mw(t)], the Humboldt Bay boiling-water reactor began commercial operation Aug. 1, 1963 (Figs. 11 and 12). Routine operation at the uprated power is expected to begin after the 1966 refueling. Experience indicates that a normal refueling operation, not requiring special core work such as removal of poison curtains (large curved plates used to shape flux in new cores), could be completed in 14 to 18 days.

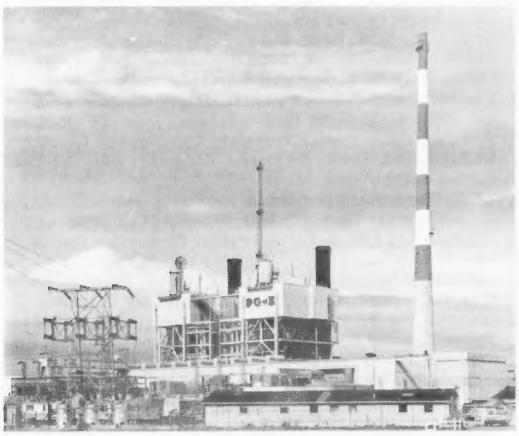

Fig. 11 Humboldt Bay includes two 50-Mw(e) fossil-fired units and the nuclear power plant, Unit No. 3. The 50- to 70-Mw(e) BWR at right uses an underground pressure-suppression containment system.[30]

During the 3672 hr of commercial operation in 1963, plant availability was 81.2%, scheduled-outage time was 660 hr, and the forced outage was 1.2% (Tables 1 to 4).

Scheduled outages in 1964 totaled 1038 hr and included 677.5 hr for the removal of poison curtains, the addition of 14 fuel assemblies, miscellaneous maintenance, operational testing, and the completion of construction work; 1964 included 64 hr of forced outages (for a rate of 0.8%). Plant availability was 87.3%.

In 1965 there were 1945 hr recorded as scheduled outages, including 1724 hr assigned to refueling, containment modification and leakage-rate testing, turbine overhaul, miscellaneous maintenance, and operational testing. Other scheduled outages included scram-system maintenance, testing of turbine trip and reactor protective system, and repair of a turbine-casing joint leak. These required approximately 220 hr, for a total scheduled-outage time of 1945 hr. Forced-outage time for the year was 37 hr. Plant availability, including the time lost for refueling, was 77.4%; excluding refueling, it was 79.5%.

Forced outages in 1965 amounted to 37 hr, but only 6 hr affected reactor availability. Thus, whereas the reactor forced-outage rate was less than 0.1%, the plant forced-outage rate was 0.55%.

Actual availability for the first 38 months of operation, including downtime for refueling, has been 86%. Analysis of experience indicates an availability of greater than 90% can be anticipated over the life of the plant.

Prognosis

The Humboldt Bay plant and the other plants reviewed here are typical in that outages required

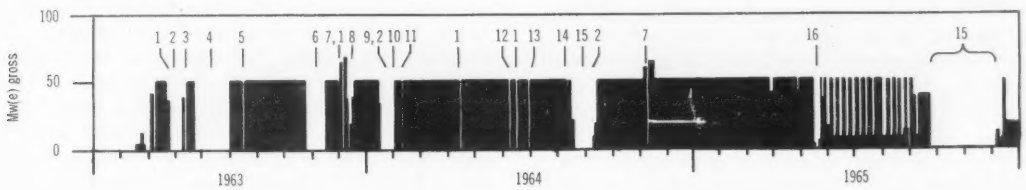

Fig. 12 Humboldt Bay, power plant Unit No. 3 (Units 1 and 2 are fossil-fired), Pacific Gas & Electric Co., plant outages were are foilows:

1. Spurious reactor control system scram
2. Turbine leak
3. Scram-pressure transient
4. Reactor head leak and core changes
5. Turbine steam bypass valve stuck
6. Modify reactor head closure
7. Scram during test, low water level
8. Uprating tests
9. Reactor test and turbine leak
10. Scram during startup, low water level
11. Operator license examination
12. Turbine trip test
13. Scram, turbine control system
14. Turbine test
15. Refueling
16. Drywell vacuum breaker

during the early years of plant life to modify and debug systems should not reappear in future operations. As concluded in a recent report of the Federal Power Commission,[29] future operations of water-reactor stations are expected to demonstrate dependability, flexibility, and availability comparable to modern fossil-fired stations.

* * *

This article is based partly on a paper presented at the Annual Meeting of the American Nuclear Society, June 20–23, 1966. Data in both the paper and this article were obtained primarily by means of questionnaires and with the cooperation of the six utilities operating the plants discussed.

References

1. Operating Experience: Dresden, *Power Reactor Technol.*, 6(2): 60-64 (March 1963).
2. Operating Experience: Dresden, *Power Reactor Technol.*, 5(2): 56-59 (March 1962).
3. Dresden Turbine Inspected and Overhauled, *Nucleonics*, 21(4): 78 (April 1963).
4. The Dresden Nuclear Power Station, *Power Reactor Technol.*, 4(4): 56-58 (September 1961).
5. Report on Equipment Availability for the Five-Year Period 1961–1965, EEI Publication No. 65-35, Edison Electric Institute, New York, May 1965.
6. R. L. Haueter et al., Operating Big Rock Point, *Nucleonics*, 22(11): 41 (November 1964).
7. R. N. Duncan et al., Advances in High-Power Density BWR's — Part I, Toward Low-Cost High Performance BWR Fuel, *Nucleonics*, 23(4): 50 (April 1965).
8. N. H. Barth and R. K. Haling, Advances in High-Power-Density BWR's — Part II, Power Flattening Techniques Boost BWR Core Capabilities, *Nucleonics*, 23(5): 72 (May 1965).
9. Walter Mitchell III, Humboldt Bay and Big Rock Point, *Power Reactor Technol.*, 7(1): 70-84 (Winter 1963–1964).
10. Operating Experience: Shippingport, *Power Reactor Technol.*, 7(2): 193-196 (Spring 1964).
11. R. E. Barclay and W. J. O'Brien, Third Shippingport Refueling Still Faster, *Nucleonics*, 21(9): 70 (September 1963).
12. Operating Experience: Shippingport, *Power Reactor Technol.*, 6(3): 49-56 (June 1963).
13. Operating Experience: Shippingport, *Power Reactor Technol.*, 6(2): 64-67 (March 1963).
14. Operating Experience: Shippingport, *Power Reactor Technol.*, 5(4): 61-72 (September 1962).
15. J. J. Dutton, Two Shippingport Refuelings, *Nucleonics*, 20(4): 66-70 (April 1962).
16. Operating History of U. S. Nuclear Power Reactors, USAEC Report TID-8214, 1964.
17. G. A. Reed and E. Tarnuzzer, Examining Yankee Plant Performance in 1965, *Nucleonics*, 24(3): 42 (March 1966).
18. K. K. Brown, Three Yankee Refuelings Point Toward Minimum Downtime, *Nucleonics*, 23(1): 64-70 (January 1965).
19. Operating Experience: Yankee, *Power Reactor Technol.*, 6(4): 82-91 (Fall 1963).
20. W. D. Craig, Inspecting Water Reactors, *Nucleonics*, 20(4): 57-60 (April 1962).
21. Yankee Operators Discover Reactivity Anomalies, Prepare to Refuel, Hope to Raise Power, *Nucleonics*, 20(3): 84, 86 (March 1962).
22. R. J. Coe, G. A. Reed, and D. E. Vandenburgh, Yankee Reactor Operates on Schedule, Below Budget, *Nucleonics*, 19(3): 53-55 (March 1961).
23. Yankee Nuclear Power Station, *Power Reactor Technol.*, 4(3): 47-55 (June 1961).
24. F. H. Martens, Design Foresight Can Simplify Reactor Modifications, *Power Reactor Technol.*, 9(2): 74-79 (Spring 1966).
25. R. C. Skaardal, Operational Problems and Solutions, *Power Reactor Technol.*, 8(4): 271-279 (Fall 1965).
26. Consolidated Edison Nuclear Steam-Generating Station, *Power Reactor Technol.*, 7(3): 313 (Summer 1964).
27. Nucleonics Reactor File No. 14, Indian Point on the Line, *Nucleonics*, 21(4): (April 1963).
28. Consolidated Edison Nuclear Steam Generating Station, *Power Reactor Technol.*, 6(3): 28-48 (June 1963).
29. National Power Survey, Federal Power Commission, Washington. October 1964.
30. J. C. Carroll and J. O. Schuyler, Humboldt Bay Reactor Operating Experience, *Nucl. Safety*, 6(4): 441-451 (Summer 1965).

Applying High-Temperature Instrumentation in Liquid-Metal Experiments

By Paul A. Lottes

Liquid-metal technology stands today where water technology stood about 15 years ago. Rapid evolution is needed because liquid metals at high temperatures are of great importance for fast breeder reactors (at ~1200°F) and also for space power systems (at ~2000°F). Only in the past few years have data in significant quantities been reported, notably at the more recent of a series of conferences on high-temperature liquid-metal heat-transfer technology.[1,2] The earlier conferences[3,4] formulated many of the plans and ideas from which the recent data have grown. The latest conference emphasized instrumentation but also included many experimental results. Topics discussed included thermodynamic and heat-transfer measurements, vapor-quality and volume-fraction measurements, bearing-film measurements, and liquid-level and impurity measurements.

Instrumentation

Because liquid metals are difficult to handle and temperatures are high, exotic loops and heaters[5,6] are required, as are unusual pressure-measuring devices.[7,8] Void-fraction measurements[9] are made with gamma,[10,11] electromagnetic,[12,13] and X-ray[11] methods and calorimeters.[14] Bearing-film measurements, of special interest for aerospace application,[15] rely heavily on eddy-current methods,[16,17] although magnetic inductance[13] underlies some instruments. Unique equipment is being used for liquid-level and impurity measurements[18–22] and for cavitation damage studies.[23]

HEATERS

Experimental techniques for delivering large heat fluxes to flowing liquid metals include a thermal-radiation heater and an electron-bombardment heater.[5] The thermal-radiation heater is a d-c-heated tantalum sheet capable of delivering heat fluxes up to 62,000 Btu/(hr)(sq ft) for coolant temperatures up to 1400°F. The electron-bombardment heater uses a 20,000-volt 10-amp power supply and directs a uniform stream of high-velocity electrons against the inside wall of an evacuated tube to achieve heat fluxes up to 20,000 Btu/(hr)(sq ft) in a sodium-cooled system; since the conference, the heater has achieved 350,000 Btu/(hr)(sq ft) and is expected to generate 10^6 Btu/(hr)(sq ft).

A conduction type electric heater capable of delivering 5 Mw to flowing lithium at temperatures near 2000°F has also been developed.[6] The design was based on high-temperature electrical-breakdown data for fired ceramics and requires heat generated in the current element to be transferred by conduction across an electrical insulator and metal sheath to the liquid-metal stream.

Breakdown strength and insulator leakage currents for swaged ceramics were reported for a small test heater[6] that had a 0.125-in.-diameter tantalum center, 0.070 in. of swaged alumina insulation, and a 0.38-in.-diameter niobium–1% zirconium sheath. Resistivity measurements of the alumina after 500 hr of testing at 2540°F centerline temperature with a surface flux of 130 watts/sq in. [37,800 Btu/(hr)(sq ft)] showed a linear relation between leakage current and applied potential up to approximately 3 volts/mil. The average resistivity was 0.25×10^5 ohm-cm at approximately 2270°F, whereas the value in the literature for fired alumina at this temperature is 10^5 ohm-cm. The author concludes that swaged conduction heaters can be used at elevated temperatures with field strengths up to 3 volts/mil across the ceramic.

PRESSURE-MEASURING DEVICES

A device for measuring pressures before and after blade rows in a potassium-vapor turbine has been

developed.[7] Used to measure total and static pressure in a two-stage 200-hp potassium turbine at the inlet and outlet, the static pressures between all blade rows, and the total flow rate of potassium vapor to the turbine, the device is based on flowing a metered amount of inert gas through a 0.005-in.-diameter orifice in the sensor lines to pressure taps. The flow of inert gas prevents the diffusion of potassium vapor into the sensor lines. In this way the potassium vapor is contained within the experimental facility, and the pressure transducers operate in an inert-gas environment at moderate temperature.

In another pressure transducer for liquid-metal systems, a thermionic diode sensor converts the motion of a pressure-actuated refractory-alloy capsule into a suitable electric output.[8] It was developed to be capable of operating in liquid potassium up to 1800°F. Main problem areas include the high-temperature diaphragm-deflection characteristics, diaphragm compatibility with liquid metals, and the accuracy and sensitivity of the thermionic diode sensor. Figure 1 shows the transducer design, and Fig. 2 shows typical diode characteristics. The alloys selected for investigation as diaphragm materials were C-129 (Nb–10 W–10 Hf–0.1 Y), FS-85 (Nb–28 Ta–10 W–1 Zr), T-222 (Ta–10 W–2.5 Hf), and W–25 Re. Test results on compatibility, accuracy, and sensitivity are detailed.[8]

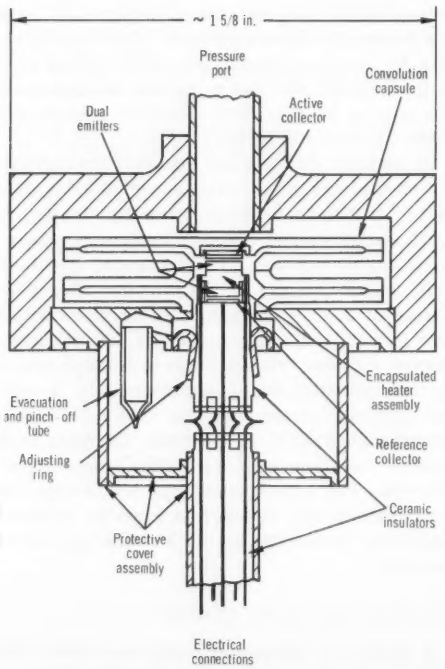

Fig. 1 Pressure transducer incorporates a double-convolution pressure capsule and a thermionic diode sensor.[8]

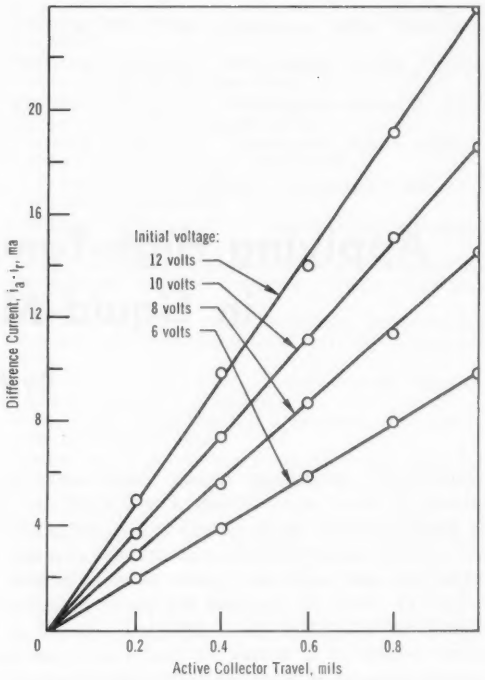

Fig. 2 Calibration data for a thermionic diode sensor show that it is suitable for use in a pressure transducer.[8]

VOLUME-FRACTION MEASUREMENTS

Numerous techniques have been described for volume-fraction measurements. These include gamma attenuation,[10,11] electromagnetic flowmeters,[12,13] X-ray methods,[12] and calorimeters.[14]

Gamma-Attenuation Methods. Volume fractions have been measured in a two-phase boiling sodium system both by gamma attenuation and with electromagnetic flowmeters. These methods and the accuracy involved under various conditions have been examined.[9,10]

One-shot gamma-attenuation methods (in which all the cross section of a flow channel is studied at once) are simple and easy to use, although they are less accurate than the traversing-beam methods. As a result of recent efforts to improve the accuracy of these techniques, design criteria have been developed that will reduce errors[11] to less than or equal to 5%. The shape of the collimator used in one-shot techniques is reported to greatly affect the dependence of the void-fraction measurement on the void distribution in a flow channel.

Electromagnetic Methods. In addition to the volume-fraction application mentioned above,[10] electromagnetic flowmeters have been used in the SNAP-10A flight system.[13] The NaK flow rates were mea-

sured electromagnetically by utilizing a secondary set of electrodes located approximately 0.25 in. from the main electrodes on a thermoelectric-powered d-c conduction pump. Pressure was indirectly monitored during the SNAP-10A flight by measuring the position of the bellows in two expansion compensators. Temperatures were measured with resistance type detectors and with chromel–constantan thermocouples. Data on bellows position (pressure indication) and system temperatures were given as a function of flight time (up to 1000 hr).

Observation of thermoelectric effect associated with the use of an electromagnetic flowmeter in a condensing alkali-metal test loop was reported but not explained.[24] A flowmeter output of approximately 10 μv was observed for zero-flow conditions. Also reported was the time required for the flowmeters and a-c conduction pumps to reach steady-state performance. Less than half an hour was required with a type 316 stainless-steel loop operating at 300°F, but an 8-hr soak at 800 to 1000°F was required with a refractory-metal loop (Nb–1% Zr).

X-Ray Methods. These techniques for determining void fractions in water systems can be extended for use in liquid-metal systems.[12] Estimates of attainable accuracy and space and time resolution are given for a measurement system used with a liquid-potassium laboratory experiment. In this feasibility experiment, liquid potassium was boiled in an induction-heated stainless-steel test section (0.218 in. in inside diameter by 0.016 in. in wall thickness). More than 10^8 X-ray quanta/sec (roughly equivalent to a radioactive source of 1000-curie strength) were detected with a beam area of 0.02 sq in., X-ray mean energy of approximately 47 kev, and energy width at half maximum of approximately 5 kev. The X-ray intensity in 1 msec was measured to within 0.2% accuracy, corresponding to an accuracy of better than

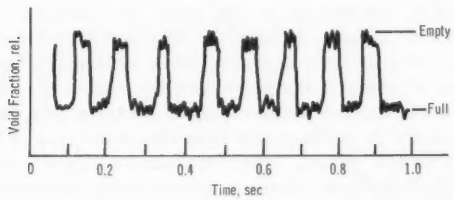

Fig. 3 X-ray measurements demonstrate periodic voiding of liquid potassium;[12] test was at atmospheric pressure, 50,000 Btu/(hr)(sq ft).

1% in the void fraction. Figure 3 demonstrates the void-measurement response.

Pressure and Void Fraction. Instrumentation for these measurements, and also data on two-phase friction factors and volume fractions for two-phase liquid-metal coolants, are given in Ref. 9. Gamma attenuation of ^{170}Tm is used to measure void fraction. Pressure drops were measured with a Taylor transmitter connected to a stainless-steel diaphragm assembly that contained a pressure-transmitting eutectic NaK.

Flow-Rate Calorimeter. Of more interest to liquid-metal turbine designers than to reactor designers, a flow-rate calorimeter has been described in which a known amount of heat is added to a flowing stream of wet liquid-metal vapor.[14] The device determines vapor dryness (or percent moisture by weight in vapor) and is quite useful for measuring "quality" in the region from 80 to 100%. Moisture content is deduced from a heat balance (accurate physical properties and accurate temperature measurements are required). The preliminary tests discussed were performed with steam as the working fluid. Scheduled future tests will use 1500°F potassium, and more advanced tests are proposed at 2000°F.

BEARING-FILM MEASUREMENTS

Although reactor designers may not have a direct interest in liquid-metal turbine bearings, techniques described in some of these measurements should be of use in other applications. The status of bearing problems related to high-speed applications has been comprehensively reviewed;[15] the review includes an excellent discussion of the fundamentals of bearing design as well as an up-to-date evaluation of problems remaining to be solved.

Eddy Currents. An eddy-current technique was developed to measure potassium film thickness and to detect film discontinuities.[16] The transducer configuration was that of a small flat coil of wire buried in an electrically nonconducting bearing sleeve near the inner surface. Electric currents are induced in the adjacent liquid potassium and bearing journal. Then the effect of this induced current upon the apparent impedance of the transducer coil is used to determine the film thickness.

Reference 17 reports the development of a film-thickness transducer of the eddy-current type that is capable of measuring the radial motion of a potassium turbine shaft rotating at up to 24,000 rpm. The measuring system is accurate to ±0.00005 in. and will operate at 650°F. Shaft motion is detected by sensing the thickness variation of a 0.015-in. nominal thickness film of potassium located between the transducer and the shaft. Design features and curves along with some actual turbine performance data were included.

Magnetic Inductance. A magnetic-inductance transducer has been developed which consists of a coil of wire surrounding a core of ferromagnetic material specially chosen to exhibit a large Villari effect (strain dependence of permeability).[16] In operation, potassium film pressure deflects a thin diaphragm

in the bearing sleeve, thus straining the Villari-effect core that restrains the back side of the diaphragm. When properly calibrated, the transducer measures film pressure.

LIQUID-LEVEL MEASUREMENTS

A system capable of sensing and tracking the level of liquid metals (Fig. 4) uses a scanning eddy-current probe to sense level and a servo to position the device on the level.[18] The probe position is transmitted electrically to a remote indicator which can be calibrated (in percent or inches). The eddy-current probe is capable of sensing through vessel walls up to 0.2 in. thick. With the use of a stainless-steel tube to contain the liquid metal, and with air cooling, the system is capable of continuous operation at 1800°F and is accurate to 0.1 in. of liquid level.

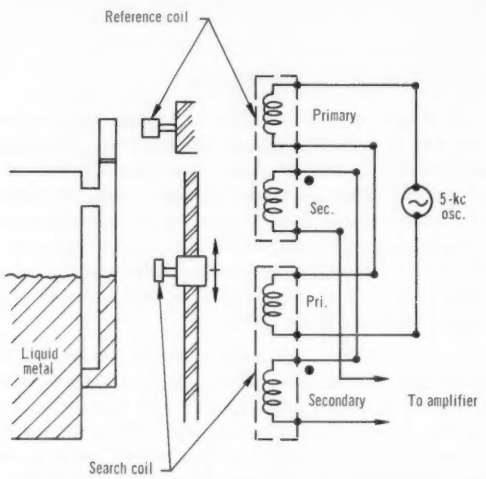

Fig. 4 Level detector for liquid metals uses two electrically identical coils, each containing primary and secondary, and is wired so that eddy currents indicate level.[18]

A similar probe developed as a level-seeking device (operating as an eddy-current unit that is motor driven to follow the liquid level) has been used in an experimental facility.[20] Advantages of the probe are that it requires a minimum of headroom, has a continuous linear response with level, operates automatically over the entire range (no switching, no manual manipulation), and operates in a thimble so that complete removal is simple. The probe is not exposed to sodium vapor and is easy to lubricate. Disadvantages are that the probe may require temperature compensation, is sensitive to sodium impurities, and is exceedingly slow.

Portable Unit. A battery-operated portable system with a hand-held probe for determining the liquid level in shipping containers, locating freeze or oxide plugs, etc., was described.[18] The probe has been used for detecting liquid levels in a 1600°F potassium system. Eddy-current sensor output is approximately 250 μv for a 2-in. travel (combined sensor travel of 1 in. above and 1 in. below the liquid level).

Pressure Transducers. Problems related to both instrumentation and control are emphasized in Ref. 19, which discusses experience with industrial pressure transducers in a potassium system. Temperature variations along condenser tubes (in a radiation-cooled condenser simulating a space power plant condenser) were detected qualitatively by taking photographs of the condenser with 9000 A Polaroid infrared-sensitive film. Results indicated that substantial temperature differences (of the order of 100°F) are easily detected (see Fig. 5). No indication was given regarding the smallest possible variation that could be detected. The object, however, was to detect large temperature imbalances in the parallel tube bank of the condenser, and hence the method proved to be quite useful.

Liquid-level devices of various types—resistance, inductive, and ultrasonic—were discussed. Figure 6, which indicates the sensitivity achieved in liquid-level determinations with an I-tube in one of the test systems, is typical for these devices.

IMPURITY MEASUREMENTS

Sodium oxide determinations were made by the technique of using a plugging valve.[20] The particular valve used differed from other designs in that the bellows sealed the sodium vapor from all parts having relative motion. The valve was also fabricated with relaxed tolerances which eliminated binding at high temperatures.

Dissolved-Oxygen Monitor. An on-line instrument for continuously measuring the effective oxygen content in liquid metals is capable of detecting concentration changes of a few parts per million.[21] The sensor of the instrument is installed directly in an operating system and provides a continuous indication of changes in oxygen activity without the necessity for sampling and chemical analysis. The sensor consists of an electrode assembly made from a solid electrolyte (thoria–yttria tube) and a copper–copper oxide reference electrode located inside the bottom of the assembly tube. Figure 7 shows the relative size and location of the assembly parts. In practice the meter must be calibrated if it is to be used for measuring absolute values of oxygen concentration.

The author states that the meter measures the thermodynamic activity of dissolved oxygen (effective oxidizing potential of the liquid metal) in liquid metals. Since oxygen activity, rather than total oxygen, effectively determines corrosion rates, the usefulness of the meter is evident for monitoring oxygen activity in liquid-metal systems in which low corrosion rates must be maintained.

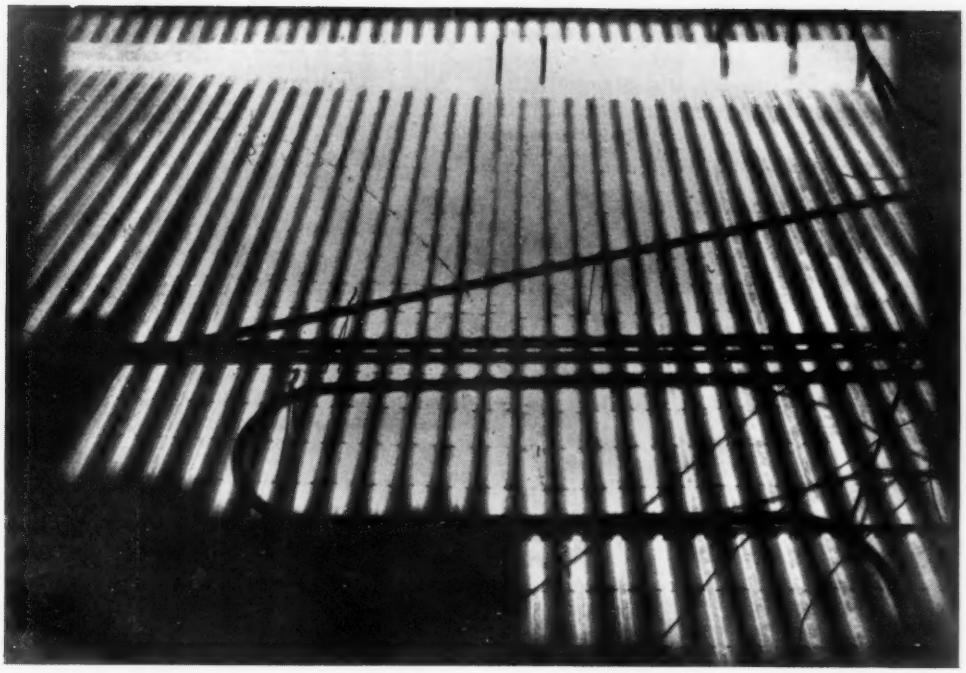

Fig. 5 Nonuniform loading of radiator tube banks is recorded in photograph taken with 9000 A Polaroid infrared film.[19]

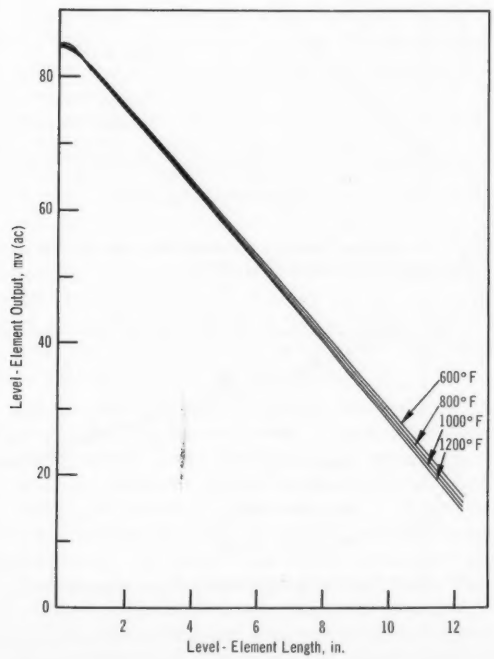

Fig. 6 Results for a resistance type liquid-level manometer, showing instrument sensitivity.[19]

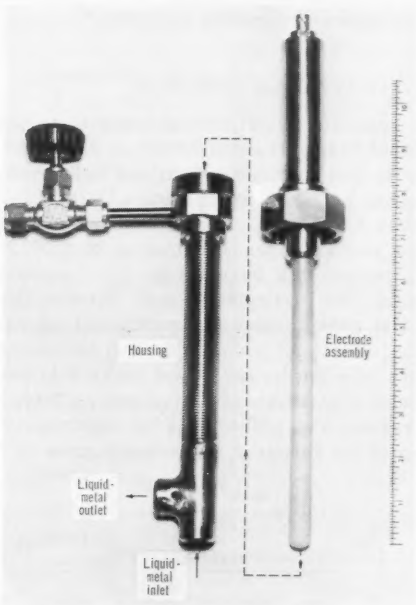

Fig. 7 Sensor for a liquid-metal oxygen meter. Key elements in the electrode assembly are a solid-electrolyte thoria–yttria tube and a copper–copper oxide reference electrode.[21]

Monitoring Inert Gases. Reference 22 describes an inert-gas purity meter that is particularly useful in glove boxes used to handle alkali metals. Sensor in the device is a hot titanium wire filament. Lifetime of the filament, which is consumed by oxidizing impurities in the gas, is a measure of the total concentration of such impurities. Figure 8 shows a typical calibration chart for the meter.

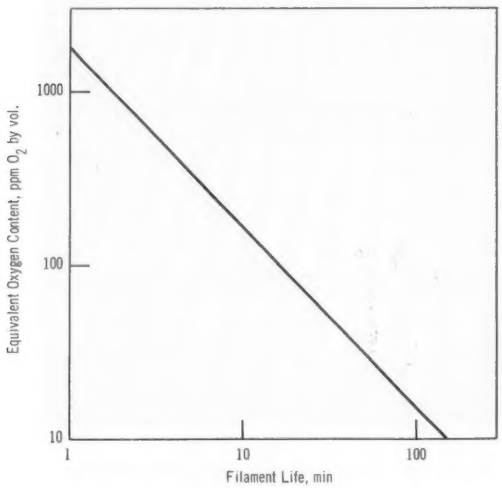

Fig. 8 Calibration chart for a gas-purity tester that measures equivalent oxygen content with a hot-wire filament that is consumed by oxidizing impurities.[22]

CAVITATION DAMAGE STUDIES

A complete description is given of an apparatus designed to impart small-amplitude sinusoidal vibrations to test specimens of various metals submerged in pools of liquid alkali metals.[23] The facility described is capable of maintaining a test retort of liquid sodium at temperatures up to 1500°F for an 8-hr period with an oxide purity of approximately 35 ppm. The particular mode of vibration chosen for the test rods allowed an experimental determination of the velocity of sound in the test pieces. From the values thus determined, it was possible to deduce the modulus of elasticity of the test pieces. Table 1 shows the results; Fig. 9 illustrates the apparatus used, and some of the results of the tests are given in Figs. 10 and 11.

Table 1 TEST PARAMETERS OF HIGH-FREQUENCY FATIGUE SPECIMENS

Metal	Temp., °F	Wavelength, in.	Modulus of elasticity, 10^6 psi	Specimen length, in.	Resonant frequency, cps
316 stainless steel	1000	12.2	21.8	5.500	14,140
	1500	11.3	18.5	5.125	14,080
TZM alloy	1000	15.0	42.0	7.000	13,990
	1500	14.5	39.0	6.750	14,080

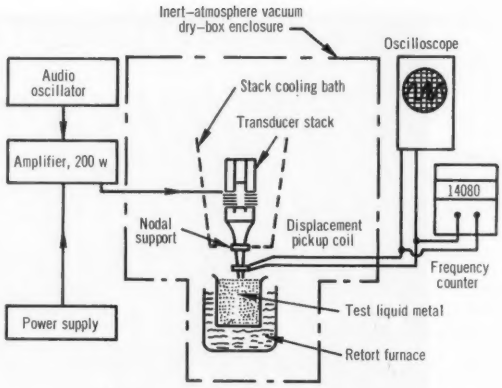

Fig. 9 Magnetostriction apparatus used for cavitation damage tests and for high-frequency fatigue tests.[23]

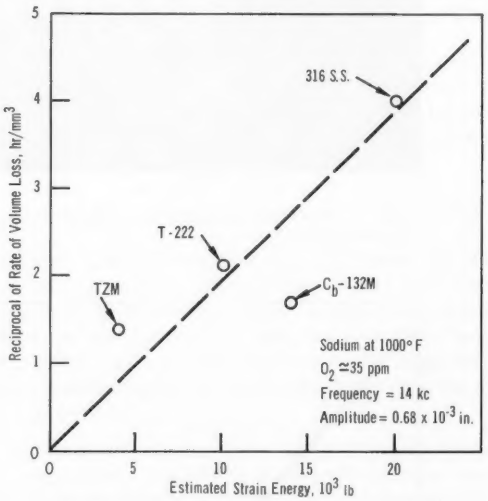

Fig. 10 Relation between cavitation damage resistance and estimated strain energy[23] at 1000°F.

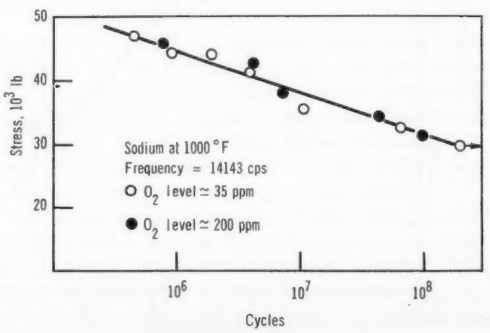

Fig. 11 High-frequency fatigue curve for type 316 stainless steel in 1000°F liquid sodium.[23]

Theory and Experiment

Although emphasizing instrumentation, the Conference included many papers that focused on theoretical and experimental heat transfer and fluid flow.

LOCAL HEAT FLUX

A new method has been developed for determining local heat flux and fully developed local overall heat-transfer coefficients in liquid metals for laminar-flow double-pipe heat exchangers.[25] The method is based on the application of basic physical principles rather than on the use of the customary heat-transfer coefficient. The mathematical solution uses expressions for the fluid temperature distribution which involve infinite series of exponential functions of the heat-exchanger axial position multiplied by an "eigenvalue." As a result, when the logarithm of a suitably expressed outer-wall temperature difference is plotted vs. axial position, the graph exhibits a linear portion that corresponds to the fully developed region of the heat exchanger—if such a region exists. From this slope it is possible to deduce the local overall heat-transfer coefficient. Methods are outlined for application to both cocurrent- and countercurrent-flow double-pipe heat exchangers, as well as to an idealized version of a liquid-metal-cooled or -heated condenser or boiler.

INVERSE TEMPERATURE PROFILES

Nonequilibrium inverse temperature profiles have been observed in boiling two-phase flow of potassium.[26] For certain tests the fluid centerline temperature at a given axial position was higher than the wall temperature at the same axial position. Test conditions where this phenomenon was noticed covered the following ranges: mass velocity, 3 to 10×10^5 lb/(hr)(sq ft); potassium temperature, 1510 to 1650°F; boiling pressure, 28 to 42 psia; vapor quality, 0.7 to 17.0%; boiling heat flux, 10,200 to 81,700 Btu/(hr)(sq ft). Measured differences between the inner-wall temperature and the fluid centerline temperature ranged from +4 to −9°F. Errors in instrumentation were eliminated by checking single-phase flow conditions which gave positive temperature differences up to approximately 30°F as expected.

Cause. The observed negative temperature differences are suggested to result when nonequilibrium exists between liquid and vapor and there is a decrease in pressure (and corresponding saturation temperature) along the flow channel, i.e., the observed phenomenon merely reflects the state of nonequilibrium. The vapor essentially does not have sufficient time to transfer its heat back to the liquid (at lower saturation temperature downstream). A very steep temperature gradient in the fluid direction is needed for this phenomenon to exist. Figure 12 shows some of the data that exhibit nonequilibrium conditions.

SUPERHEAT IN BOILING SYSTEMS

Very high liquid superheats are possible in boiling liquid-metal systems.[27] For potassium boiling on an as-received (commercially smooth) surface, the superheat measured ranged from 500°F at a saturation temperature of 1500°F down to 230°F at a saturation temperature of 1770°F. Wall-temperature oscil-

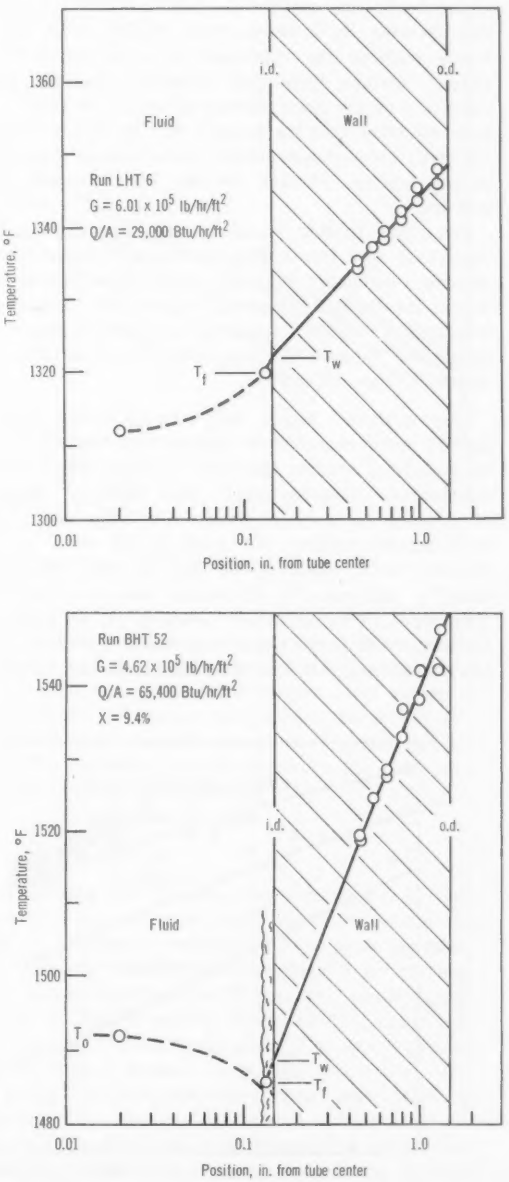

Fig. 12 Boiling-temperature profiles. These experimental data, for both liquid (left) and two-phase flow, show the inverse profile (right) in the fluid during two-phase flow.[26]

lations, which occurred in the presence of these large superheats, were 170 to 300°F at a frequency of 1.5 cycles/min. Owing to maximum-temperature limitations, sodium could not be boiled on this as-received surface.

Surface Effects. Significant reductions in both the magnitude of the superheat and the amplitude of the wall-temperature fluctuations were achieved by modifying the boiling surface. A surface containing 0.006-in.-diameter by 0.040-in.-deep drilled holes effectively reduced the superheat by a factor of 40. A porous surface formed by sintering stainless-steel particles on the inner surface of one of the tubes was less effective than the surface with the drilled holes, but still showed appreciable reduction in superheat during boiling. Similar results were obtained with sodium.

Over the limited range of the experiments, the superheat data (for both potassium and sodium) correlated reasonably well with predictions based on a model involving a spherical vapor bubble in thermal equilibrium within a liquid pool of uniform temperature. The theory was presented;[27] typical data are shown in Figs. 13 and 14.

Vaporization. Large wall superheats (150 to 200°F) were required to initiate vaporization in sodium boiling studies that used a single tube-in-shell counterflow heat-exchanger test section.[28] Boiling took place in a $\frac{1}{2}$-in.-ID by 4-ft-long inner tube; pressurized sodium was used in the shell as the heating fluid. Tests up to 2000°F were conducted using a niobium–1% zirconium loop in a vacuum. Two types of vaporization resulted: (1) an apparent flashing, with large liquid superheats and (2) a more normal boiling with low wall superheats and qualities up to 80%. Liquid-phase convective heat-transfer data and pressure-drop results were also obtained.

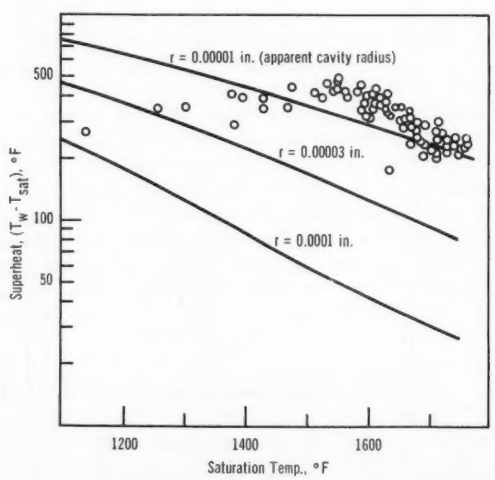

Fig. 13 Liquid superheat with potassium boiling on as-received (commercially smooth) surfaces.[27]

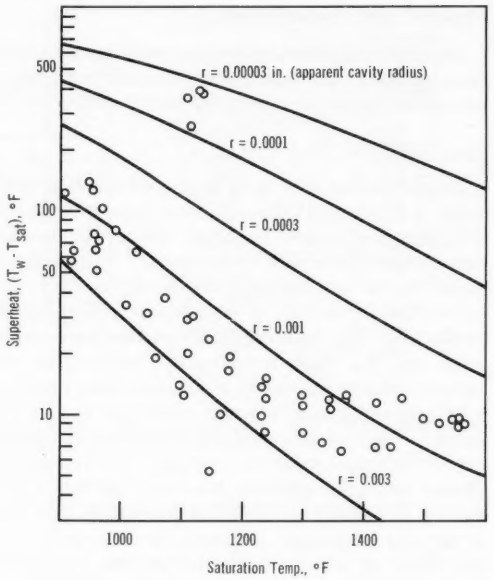

Fig. 14 Liquid superheat with potassium boiling on a pitted surface that was formed by drilling 0.006-in.-diameter holes 40 mils deep on 2-in. centers.[27]

The protective vacuum environment for the refractory-metal components was noteworthy. Despite large outgassing sources, pressures of 10^{-7} torr were obtained at loop operating conditions.

RESULTS FOR POTASSIUM

Two-phase pressure-drop data were reported[29] for boiling potassium in forced-convection flow through a vertical circular tube. The data from a single series of measurements on a 6-ft-long tube with pressure taps at 1-ft intervals over the last 4 ft of length were compared with existing correlations from the literature for nonmetallic fluids. Calculated exit pressures from these correlations compared favorably with the measured values.

Figure 15 compares potassium data with Martinelli type correlations.[9] Figure 16 compares the various liquid-fraction correlations available in the literature. Slip ratio is shown in Fig. 17 as a function of void fraction and quality. Of interest is the fact that the authors report much higher slips for the metallic systems than those ordinarily experienced with nonmetallic flows. No explanation was offered other than the possible effects of wetting.[11]

Boiling potassium heat-transfer and pressure-drop data have been obtained in a radiant-heated niobium-alloy facility at temperatures up to 2100°F and in a two-loop sodium-heated Haynes 25 facility up to 1750°F (Ref. 30). Tests were reported for exit vapor

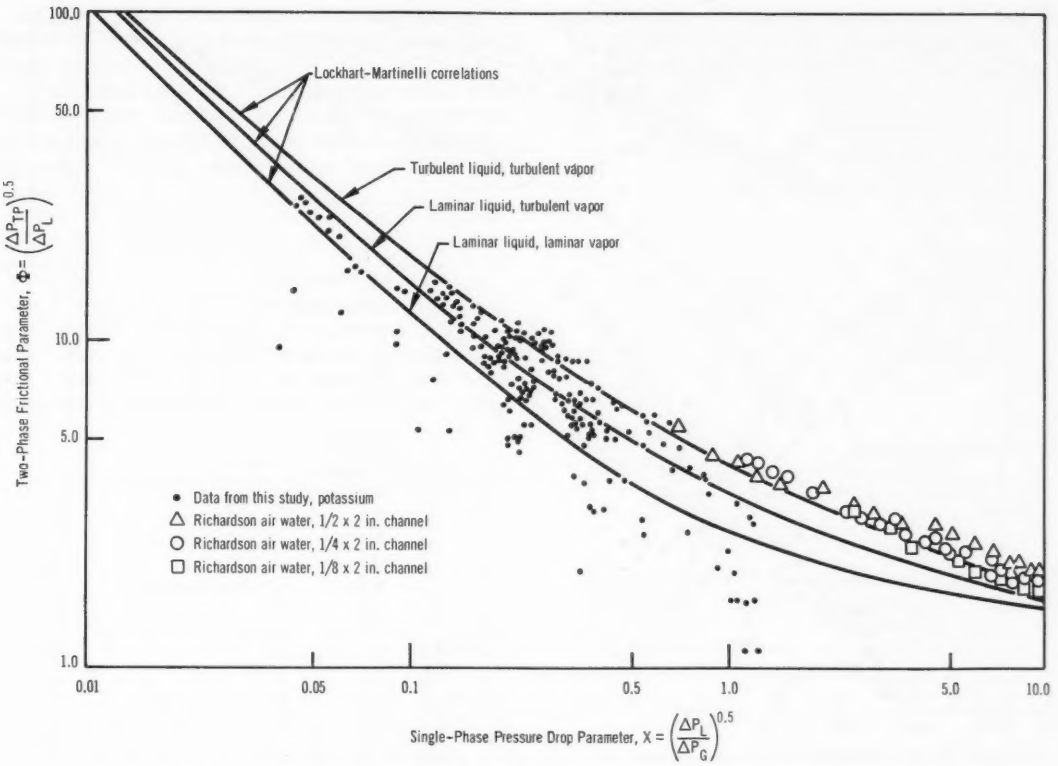

Fig. 15 Martinelli type plot of potassium two-phase frictional pressure-drop data.[9]

conditions up to about 200°F superheat. Various diameters of tubing were used with and without instrumented vortex-generator inserts. The single-tube test section in the Haynes 25 facility was a tube-in-shell heat exchanger instrumented so that both local and average heat-transfer and pressure-drop data could be obtained. Test conditions were chosen to simulate those encountered by a large space power system.

Although instrumentation and measurement techniques were described, greater emphasis was placed on the data collected. Heat-transfer data in the nucleate, transition, and film-boiling regions, and some measurements of critical heat flux were presented. Typical pressure-drop data are shown in Fig. 18, potassium transition boiling data in Fig. 19, and critical-heat-flux data in Fig. 20. The value of a_R in Figs. 19 and 20 represents the radial acceleration of the fluid at the tube wall developed by the helical inserts used in the experiments. The method of calculating a_R and the quality and limitations of the data are treated in detail.[30]

Condensing potassium experiments have used both nickel[31] and HS-25 condensers.[28] Potassium studies that have emphasized the experimental techniques used to obtain local condensing heat-transfer data in thick-wall high-purity nickel condenser tubes, and in which the radial temperature profile was measured at two axial locations, have yielded local values of heat flux and tube inner-wall temperature. A $\frac{1}{4}$-in.-ID instrumented tubular insert was centered in the $\frac{5}{8}$-in.-ID condenser tube to measure the potassium axial temperature distribution.

RESULTS FOR SODIUM

Recent Argonne National Laboratory work on two-phase flow of boiling sodium[19] covers the following range of variables: pressure, 2 to 17 psia; temperature, 1300 to 1650°F; inlet velocity, 1 to 5 ft/sec; boiler power density, 0 to 200 kw/liter; liquid superheat, 10 to 100°F; quality, 0.0005 to 0.01; vapor volume fraction, 0 to 0.87; slip ratio, 5 to 100; frictional pressure loss, 0 to 40 in. H_2O; boiling operation, 1000 hr. In this system, flowing sodium was heated by electrical resistance heaters within the coolant. Volume fractions were measured with gamma-attenuation techniques and electromagnetic flowmeters. Typical measured liquid superheats (Fig. 21) are substantially lower than those reported in Ref. 27. However, as Fig. 22 shows, the systems are quite different. Sodium experiments both with pool boiling and forced

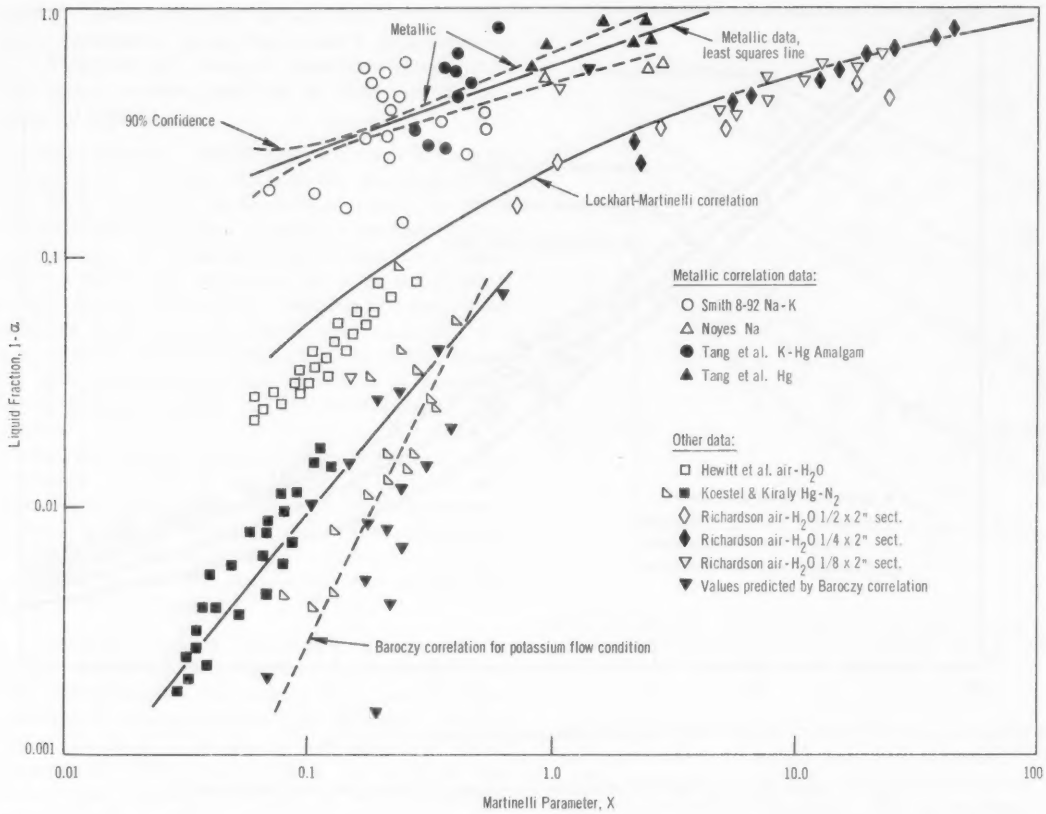

Fig. 16 Metallic liquid-fraction correlations compared with other data and correlations. Although the data scatter appreciably, they consistently yield lower void fractions than nonmetallic fluids.[9]

convection were summarized.[32] The test section for the pool-boiling experiments was a ¼-in.-diameter horizontal cylinder, whereas the forced-flow apparatus utilized an annular vertical test section formed with ¼- and ½-in.-diameter tubes 27 in. long. Other forced-convection heat-transfer data for NaK are reported[5] for the Peclet-number range from 9 to 200, which covers the laminar, transition, and turbulent regions.

Pool-boiling data for sodium and potassium at up to 10^6 Btu/(hr)(sq ft) have been reported.[28] Similar data up to 1.6×10^6 Btu/(hr)(sq ft) were also reported for a forced-convection system for inlet velocities between 0.5 and 6.0 ft/sec, pressures of 1.5 to 10 psia, average subcoolings to 116°F, and qualities up to 14% (Ref. 28). Pressure drop and void fraction were measured in an unheated vertical section of the loop over approximately the same range of conditions. Most of the data, summarized in seven figures, are compared to other reported results (pressure-drop data to Martinelli type correlations). Generally speaking, trends are similar to those for nonmetallic liquids; however, slip ratios proved much higher than for nonmetallic fluids (as in other findings).[9]

RESULTS FOR MERCURY

The mercury boiler for the SNAP-8 system (Rankine-cycle) has been extensively described;[33] summary findings are:

- The initial boiler performance characteristics (thermal load) depend on the condition of the internal-wall surfaces of the mercury flow passages and on the thermal and dynamic conditions imposed by the flow-passage geometry.
- High-velocity liquid-phase vortex flow at the preheat section end point, combined with similar dynamic conditions in the low-vapor-quality section, demonstrate excellent boiler-conditioning effects when the mercury flow passage is cleaned by established methods prior to mercury injection.
- The boiling heat-transfer results obtained from a fully conditioned boiler are in close agreement with the predictions established by the dropwise dry-wall boiling heat-transfer correlations.

• The two-phase flow pressure-drop data are correlated by means of a technique similar to the Martinelli method.

• The introduction of a tight preheat-section plug insert to obtain annular flow and high liquid velocity also improved the boiler performance stability significantly. (The plug insert caused liquid to flow in annular flow.)

• Mercury inventory variations (variation in liquid holdup) were minimized with the tight plug-insert geometry.

An X-ray movie has been filmed that presents a visual insight into two-phase flow patterns in a NaK-heated mercury boiler.[34] The prototype boiler had four tubes, each one with an internal swirl wire turbulator throughout the boiling section and a plug insert in the low-quality boiling section. The significant observation of the deconditioned state (when poorer heat transfer is obtained) was the existence of slug flow.

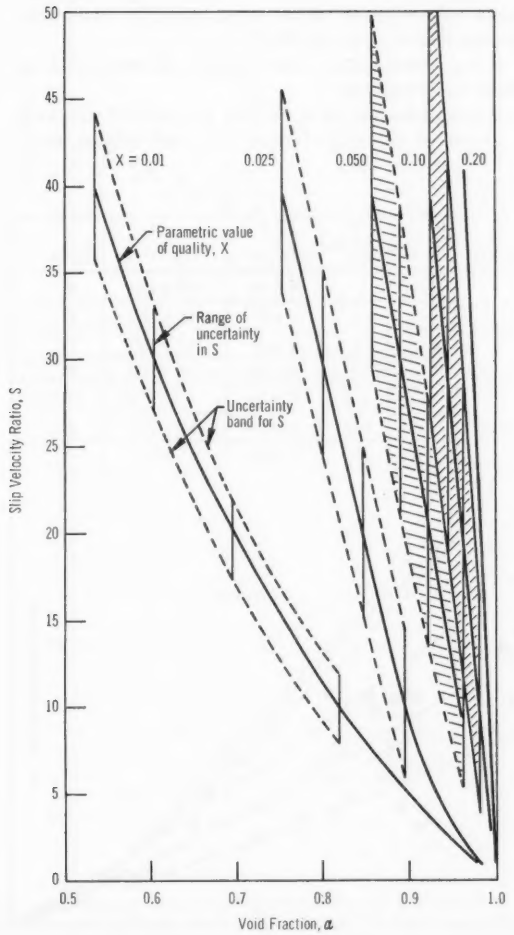

Fig. 17 Uncertainty in slip ratios increases with void fraction and quality (X). These data, obtained with radiation-attenuation techniques, are of value for qualities below approximately 0.15 (Ref. 9).

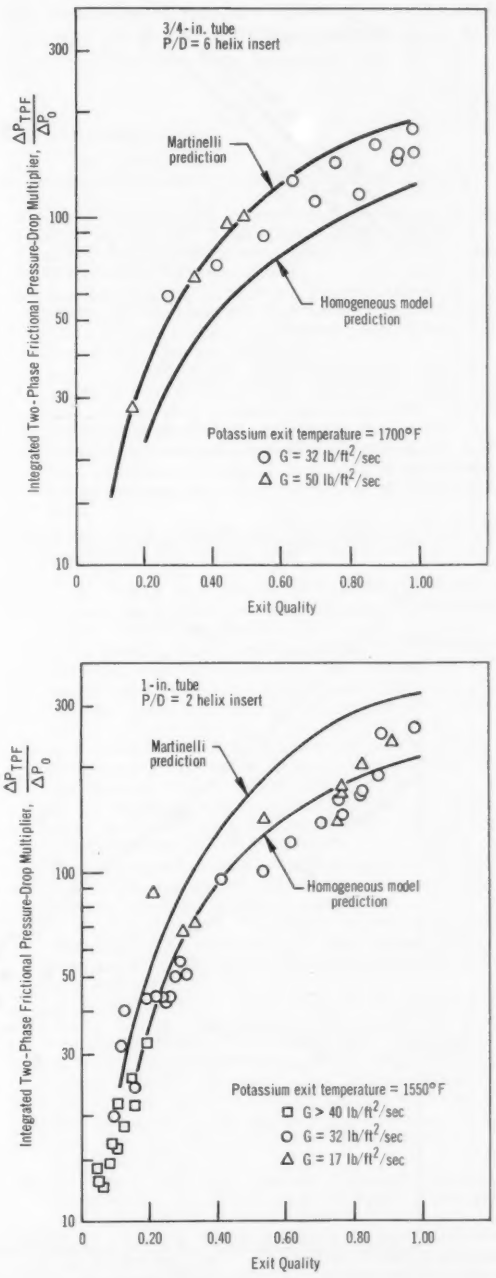

Fig. 18 Typical two-phase potassium frictional pressure-drop multipliers calculated from experimental data are compared to curves of predictions from models.[30]

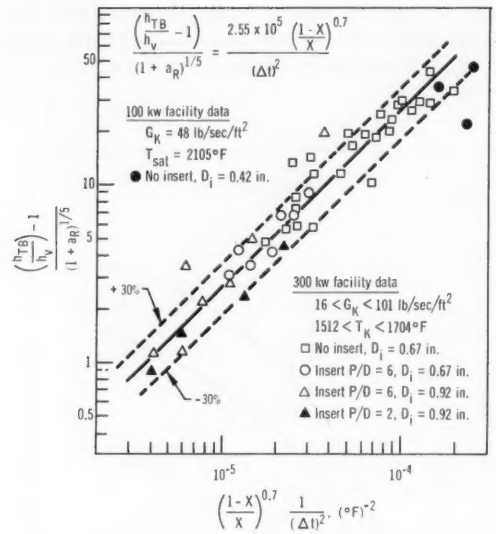
$\frac{\left(\frac{h_{TB}}{h_v}-1\right)}{(1+a_R)^{1/5}} = \frac{2.55 \times 10^5 \left(\frac{1-X}{X}\right)^{0.7}}{(\Delta t)^2}$
100 kw facility data
G_K = 48 lb/sec/ft²
T_{sat} = 2105°F
● No insert, D_i = 0.42 in.
300 kw facility data
16 < G_K < 101 lb/sec/ft²
1512 < T_K < 1704°F
□ No insert, D_i = 0.67 in.
○ Insert P/D = 6, D_i = 0.67 in.
△ Insert P/D = 6, D_i = 0.92 in.
▲ Insert P/D = 2, D_i = 0.92 in.
+30%
-30%
$\frac{\left(\frac{h_{TB}}{h_v}\right)-1}{(1+a_R)^{1/5}}$
$\left(\frac{1-X}{X}\right)^{0.7} \frac{1}{(\Delta t)^2}$, (°F)⁻²

Fig. 19 Potassium transition boiling data obtained for various test geometries and plotted in terms of the empirical equation given.[30]

An activation method of determining vapor quality with trace amounts of ^{203}Hg (half-life of 48 days) has been studied[13] and is estimated to be accurate within 1% at a vapor quality of 95%.

Haynes 25 Surfaces. Performance of Haynes 25 surfaces with mercury has been studied in a series of boiler conditioning experiments.[13] Conclusions are:

- Exposure of clean Haynes 25 surface at 1200°F to air for a few hours had no deleterious effect on pool-boiling heat transfer at a mercury saturation temperature of 950°F for heat fluxes to at least 200,000 Btu/(hr)(sq ft).
- Pool-boiling heat transfer for a descaled-and-pickled Haynes 25 surface is essentially the same as for a degreased and cleaned surface except for an initial period of lower performance for the descaled-and-pickled surface.
- Degreased-and-cleaned and descaled-and-pickled surfaces remained wetted when cooled to room temperature after being at 950°F.
- The wetting of a clean Haynes 25 surface is not likely to be uniform.
- Contamination of a Haynes 25 surface with even a trace of oil will reduce the pool-boiling heat-

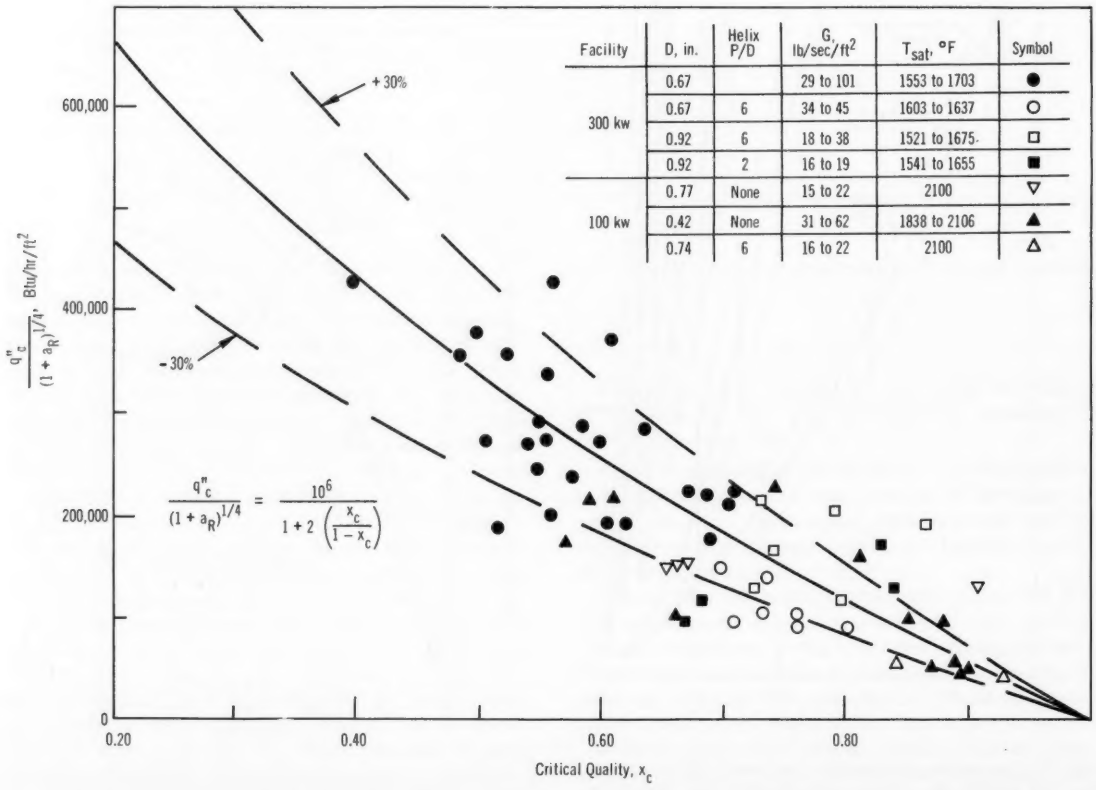

Fig. 20 Potassium critical heat-flux data show a trend toward decreasing heat flux with increasing vapor quality.[30]

transfer performance of the surface. However, the reduction is fairly small, and restoration to the performance of a clean surface may be possible with operating time.

- Gross contamination of a Haynes 25 surface with oil effects a drastic reduction in pool-boiling heat-transfer performance at mercury saturation temperatures greater than 650°F, a moderate reduction below approximately 650°F.
- A clean Haynes 25 heat-transfer surface will not remain clean in an oil-contaminated mercury system even when kept completely submerged in the liquid mercury.
- Degree of wetting and pool-boiling heat-transfer performance are directly related.

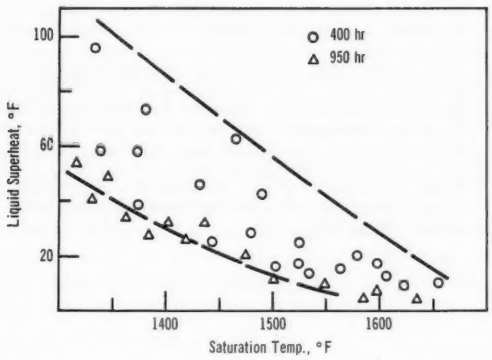

Fig. 21 Liquid superheat measurements indicate a decrease (with time) in the amount of superheat required to initiate boiling.[10]

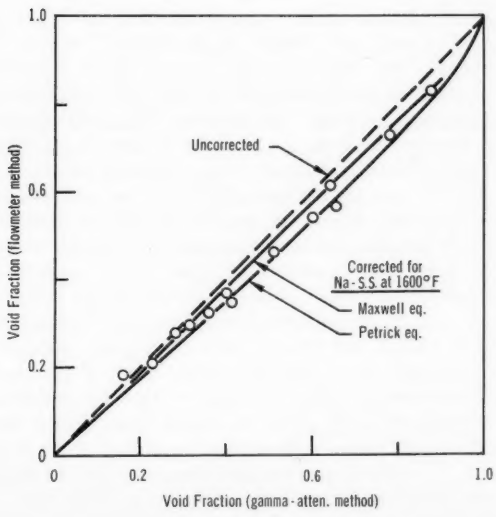

Fig. 22 Void-fraction data. Results indicate that the electromagnetic flowmeter is adequate for vertical upflow of two-phase liquid metals.[10]

RUBIDIUM AND CESIUM

Some preliminary data were presented[24] for condensing rubidium and cesium in horizontal and vertical flow for heat fluxes up to 140,000 Btu/(hr)(sq ft) and temperatures in the range of 1000 to 1400°F. The maximum temperature difference for condensing under any set of test conditions was found to be 13°F, but most of the data were less than 5°F.

References

References 5 through 34 are papers published in Ref. 2

1. Oak Ridge National Laboratory, Proceedings of 1963 High-Temperature Liquid-Metal Heat Transfer Technology Meeting, September 4–6, 1963, USAEC Report ORNL-3605. November 1964.
2. Argonne National Laboratory, Proceedings of the Conference on Application of High Temperature Instrumentation to Liquid-Metal Experiments, September 28–29, 1965, USAEC Report ANL-7100.
3. Argonne National Laboratory, Meeting on High Temperature Liquid Metal Heat Transfer Technology, June 14–15, 1961, USAEC Report ANL-6507, February 1962. (Classified)
4. Brookhaven National Laboratory, Proceedings of 1962 High-Temperature Liquid-Metal Heat Transfer Technology Meeting, May 17–18, 1962, USAEC Report BNL-756.
5. R. E. Holtz (Argonne National Laboratory), Heating Techniques for Liquid Metal Loops, USAEC Report ANL-7100, p. 9.
6. L. G. Hayes (Jet Propulsion Laboratory), Electrical Heater for Liquid Metals at Elevated Temperatures, USAEC Report ANL-7100, p. 23.
7. G. C. Wesling, R. J. Rossbach, and W. M. Shaffernocker (General Electric Company), Development of Efflux Measuring Device for Performance Evaluation of Potassium Vapor Turbine, USAEC Report ANL-7100, p. 127.
8. A. J. Cassano and R. E. Engdahl (Consolidated Controls Corporation), Pressure Transducer for Liquid Metal Applications, USAEC Report ANL-7100, p. 165.
9. R. E. Balzhiser and L. R. Smith (University of Michigan), Instrumentation for Two Phase Metallic Flows, USAEC Report ANL-7100, p. 217.
10. J. B. Heineman (Argonne National Laboratory), Forced Convection Boiling Sodium Studies at Low Pressure, USAEC Report ANL-7100, p. 189.
11. J. K. Ferrell and J. W. McGee (North Carolina State University), An Accurate One-Shot Gamma Attenuation Technique for Measuring Void Fractions, USAEC Report ANL-7100, p. 247.
12. L. B. Wentz, L. G. Neal, and R. W. Wright (TRW Systems), X-Ray Measurement of Void Dynamics in Boiling Liquid Metals, USAEC Report ANL-7100, p. 195.
13. H. H. Hanlin (Atomics International), High Temperature Liquid Metal Instrumentation at Atomics International for: (1) The SNAP 10A Flight System, (2) Boiler Conditioning Experiments and Mercury Vapor Quality Measurement for Mercury Rankine Systems, USAEC Report ANL-7100, p. 641.
14. P. Tauson and R. L. Ammon (Westinghouse Electric Corporation), Development of Alkali Metal Quality Meter, USAEC Report ANL-7100, p. 271.
15. E. B. Arwas, F. K. Orcutt, and B. Sternlicht (Mechanical Technology Inc.), Approaches to the Measurement of the Steady State and Dynamic Performance Characteristics of Liquid-Metal Lubricated Bearings, USAEC Report ANL-7100, p. 331.
16. D. R. Grieser (Battelle Memorial Institute) and J. L. Morris (Air Force Aero Propulsion Laboratory),

Liquid-Metal Lubricated Bearing Instrumentation, USAEC Report ANL-7100, p. 291.
17. L. W. Stillwell and R. Herman (AiResearch Manufacturing Co.), Development of Performance-Measuring Instrumentation for a Liquid-Metal Turbine-Driven Bearing Test Rig, USAEC Report ANL-7100, p. 307.
18. L. W. Stillwell (AiResearch Manufacturing Co.), Liquid-Metal Level Detector and Indicator, USAEC Report ANL-7100, p. 367.
19. H. J. Metz and M. M. Yarosh (Oak Ridge National Laboratory), Experiences and Developments in Instrumentation for Liquid Metal Experiments, USAEC Report ANL-7100, p. 379.
20. A. G. Hosler (Chicago Operations Office) and F. A. Smith (Argonne National Laboratory), Impurity and Liquid Level Measurements for the Faret Loop, USAEC Report ANL-7100, p. 413.
21. B. Minushkin (United Nuclear Corp.), The Liquid Metal Oxygen Meter, USAEC Report ANL-7100, p. 427.
22. J. McKee (United Nuclear Corp.), An Inert Gas Purity Tester, USAEC Report ANL-7100, p. 443.
23. H. S. Preiser and A. Thiruvengadam (Hydronautics, Inc.), Instrumentation for Evaluating Cavitation Damage Resistance and High Frequency Fatigue of Refractory Alloys in High Temperature Liquid Alkali Metals, USAEC Report ANL-7100, p. 455.
24. C. R. Fisher and J. H. Moskowitz, Jr. (Aerojet-General Nucleonics), Flow Instrumentation and Operating Experience in a Condensing Alkali Metals Test Loop, USAEC Report ANL-7100, p. 45.
25. R. P. Stein (Argonne National Laboratory), A Method for the Determination of Local Heat Fluxes in Liquid Metal Heat Exchangers, USAEC Report ANL-7100, p. 483.
26. J. C. Chen (Brookhaven National Laboratory), Existence of Non-Equilibrium Inverse Temperature Profile in Boiling Two-Phase Flow, USAEC Report ANL-7100, p. 499.
27. J. A. Edwards and H. W. Hoffman (Oak Ridge National Laboratory), Superheat with Boiling Alkali Metals, USAEC Report ANL-7100, p. 515.
28. J. P. Lewis (National Aeronautics and Space Administration), Experimental Studies of Boiling of Sodium and Condensing of Potassium, USAEC Report ANL-7100, p. 513.
29. R. P. Wichner and H. W. Hoffman (Oak Ridge National Laboratory), Pressure Drop with Forced-Convection Boiling of Potassium, USAEC Report ANL-7100, p. 535.
30. J. A. Bond, J. R. Peterson, and F. E. Tippets (General Electric Company), Heat Transfer and Pressure Drop Measurements for High Temperature Boiling Potassium in Forced Convection, USAEC Report ANL-7100, p. 53.
31. S. G. Sawochka (General Electric Company), Measurements of Forced Convection Condensing Potassium Heat Transfer, USAEC Report ANL-7100, p. 97.
32. H. Lurie (Atomics International), Sodium Boiling Heat Transfer and Hydrodynamics, USAEC Report ANL-7100, p. 549.
33. A. J. Sellers and M. K. Wong (Aerojet-General Corporation) and G. M. Thur (National Aeronautics and Space Administration), Recent Developments in Heat Transfer and Development of the Mercury Boiler for the SNAP-8 System, USAEC Report ANL-7100, p. 573.
34. R. J. Ziobro (TRW Equipment Laboratories), X-Ray Movie Film Report of Flow Patterns in a Once-Through Forced Circulation NaK Heated Mercury Boiler, USAEC Report ANL-7100, p. 633.

Advances in Materials for Organic-Cooled Reactors

By Edmund S. Sowa

Although organic coolants themselves cause no major corrosion problems in reactor systems, the successful development of organic-cooled reactors depends on understanding and solving problems related to (1) the most economically performing fuel elements and fuel-cladding and "pressure"-tube materials, (2) control of coolant impurities that cause fouling of heat-transfer surfaces, and (3) irradiation decomposition of the coolant. Recent engineering studies that indicate good progress toward the solution of these problems will be discussed in this article.

Background

Early efforts to capitalize on the advantages of organic coolants led to construction of reactors that used the organic as both coolant and moderator: the 6-Mw(t) Organic Moderated Reactor Experiment,[1-3] the 11.4-Mw(e) Piqua plant,[4] and the Russian 750-kw(e) ARBUS plant.[5] Numerous other organic-reactor designs have been reported—24 are listed in Ref. 6—and interest remains active in the United States, Europe,[7-9] and Canada.[10] However, the interest now is in reactors that are cooled by organics but moderated by heavy water. Such heavy-water organic-cooled reactors (HWOCR) combine the heat-transfer-system design advantages of organic coolants (low vapor pressure at high temperature) with the nuclear merits of heavy-water moderation.[11] The first such reactor is the 40- to 60-Mw(t) WR-1 at Whiteshell, Manitoba;[12] its principal functions are to test fuel, coolant, and other components for future power reactors.[13] Data from the WR-1 are expected to contribute greatly to the U. S. HWOCR program,[14,15] for which consideration is being given to construction of a prototype in the size range 350- to 750-Mw(e) to begin operation in the mid-1970s.

The prime interest in organic-cooled power reactors in the United States nowadays is for large advanced converters that can conserve fuel resources while producing power competitively; large dual-purpose power and desalting plants are one segment of this interest. In Europe and Canada the interest stems from a desire to operate power reactors with natural uranium, which, of course, is possible with a D_2O moderator. In either situation the incentive is economy. As compared with either H_2O-cooled and -moderated reactors or with reactors that are both cooled and moderated by an organic, heavy-water moderation gives better neutron economy, which leads to higher burnups for equivalent enrichments, and lower fuel costs. The organic coolant permits use of some higher density fuels (such as uranium carbide) that are not suitable for water-cooled reactors, and lower fuel costs help to compensate for the higher capital costs of the D_2O-moderated reactors.[16]

ADVANTAGES OF ORGANIC COOLANT

In a heavy-water reactor, replacement of D_2O coolant by organic coolant reduces the D_2O inventory by 5 to 20% (D_2O costs ~$20/lb, and the organics cost 12 to 40 cents/lb).[3,17,18] Organic coolants are compatible with mild-steel piping and vessels, an advantage that has promoted their use in the chemical industry. Other engineering advantages (Table 1) follow from the fact that the high temperature (600 to 800°F) achievable with low pressure (15 to 300 psi) in organic coolants simplifies reactor-vessel, piping-system design, and materials considerations.

Table 1 COMPARISON OF ORGANIC- AND D_2O-COOLED D_2O-MODERATED REACTORS[17]

Coolant	Coolant outlet temp., °F	Net overall efficiency, %	Design pressure, psi	Coolant-contained energy, rel.
D_2O	570	30.7	1560	8
Organic	760	34.2	300	1

As compared with water-cooled reactors, several advantages accrue from the favorable temperature–pressure relation in organic-cooled reactors: (1) the high temperature permits the generating plant to operate at a high thermal efficiency and (2) the moderate pressure permits savings in reactor-vessel and -system cost—and also allows construction of larger reactor vessels, including those of the modular pressure-tube type—as well as a reduction in D_2O leakage. Because organic coolants are compatible with sintered aluminum powder (SAP), which has a higher thermal conductivity than the zirconium used for cladding fuel in water reactors, finned SAP can be used to clad the fuel in organic reactors. The resulting higher power that can be obtained from each fuel channel means that reactor capital cost can be reduced.

Fuel Testing

Fuels of interest for organic reactors, UO_2 and UC, have been irradiated recently in the WR-1, NRX, and NRU. Uranium carbide is of major interest as a power-reactor fuel for the HWOCR concept because it offers higher power densities than UO_2; for the same reason, metallic uranium fuel also is of prospective interest.[16]

Uranium carbide fuels clad with SAP have been irradiated to burnups to a maximum of 11,100 Mwd per metric ton of uranium.[19] In elements fitted with internal thermocouples, the center temperature in one element was measured as 2948°F during the initial phase of the irradiation but fell to 1832°F at the end of the 3-month test period as fuel swelling improved the thermal contact between fuel and cladding. The density decreases for the two high-burnup cases are shown in Table 2, whose data are for

Table 2 IRRADIATION EFFECTS ON SAP-CLAD UC ELEMENTS[19]

Carbon content, wt.%	Average burnup, Mwd/metric ton of U	Density decrease, %
4.61	11,100	4.2–5.9
4.69–4.72	10,200	3.1–4.3

hypostoichiometric UC. The improvement in swelling characteristics with increasing carbon content is illustrated by these results. More recent experiments in an organic-cooled loop in the NRU reactor using hyperstoichiometric UC (~5 wt.% carbon), which is the fuel composition proposed for HWOCR, exhibit a density decrease as low as 2% per 10,000 Mwd per metric ton of uranium burnup.[20]

Uranium dioxide fuel clad with zirconium–2.5% niobium has been operated as the first fuel charge in the WR-1 (Ref. 12). Table 3 compares calculated and experimental data from fuel operated in organic coolant. The target burnups for these fuels are 7500 Mwd per metric ton of uranium.

Table 3 COMPARISON OF CALCULATED AND EXPERIMENTAL DATA FOR FUEL IRRADIATED UNDER WR-1 CONDITIONS[12]

Parameter	Calculated	Experimental
Cladding temperature	808°F	813–824°F
UO_2 maximum temperature	≈3270°F	≈3270°F
Fission-gas release in one experiment	18.8%	≈9%
Pressure drop across fuel rod	4.7 kg/cm^2	4.4 kg/cm^2

A multibundle fuel assembly is under irradiation in an NRU reactor organic loop to establish fuel characteristics for the HWOCR.[20,21] The fuel elements for the first irradiation were composed of SAP-clad UC and Zircaloy-clad UO_2 bundles. The peak fuel-centerline temperatures were 2000°F for the UC and 3000°F for the UO_2. Corresponding peak cladding temperatures were 850 and 860°F. The coolant used is Santowax OM at 570 to 650°F. By April 1966 some of the test fuel had reached peak burnups of 10,000 Mwd per metric ton of uranium for the UC and 8400 Mwd per metric ton of uranium for the UO_2, and the bundles were removed for hot-cell examination. The loop position now contains a multibundle assembly similar to the one removed and is being used to determine gross effects of coolant composition and purity on film formation.

Cladding and Pressure-Tube Materials

Two types of alloys that appear satisfactory for use in organic-reactor cores are SAP and the zirconium alloys.

SINTERED ALUMINUM POWDER

Sintered aluminum powder is the reference material selected for the fuel cladding and for pressure tubes.[3] Sintered aluminum powder exhibits low ductility at elevated temperature and low strain rate. Because the in-core behavior of fuel cladding is affected primarily by long-term effects such as creep, this property influences the design. Although zirconium alloys have greater ductility, this ductility can be lost if the alloy becomes hydrided at the approximately 800°F temperatures in the HWOCR.

The Al_2O_3 content in SAP adds high-temperature strength to the basic aluminum matrix. The fact that SAP has a much higher thermal conductivity than the zirconium alloys gives it excellent prospects; power densities achievable with UC fuel clad in finned SAP cladding can make this the most promising fuel for the HWOCR when manufacturing processes are developed for reliably producing high-quality SAP.[16] Although some irradiations of SAP-clad UO_2 at high linear heat rates (>15 kw/ft) have exhibited ratchetting effects, no chemical or mechanical incompatibility has been noted between UC and SAP.[23]

ZIRCONIUM ALLOYS

The zirconium alloys are generally satisfactory but are affected by hydriding, which causes embrittle-

ment. Chlorine impurities in the coolant disastrously increase hydriding of the zirconium alloys; tests in 752°F Santowax OM with 5 to 10 ppm chlorine resulted in hydriding rates up to 100 times greater than the normal 4×10^{-2} $\mu g/(cm^2)(hr)$ (which is 570 ppm/year for the cladding thickness in WR-1) found in clean (<2 ppm chlorine) coolant at 867°F (Ref. 22).

Two promising alloys that have shown hydriding rates (at 752°F) a half to a third of that of zirconium–2.5% niobium are zirconium–0.7% copper–0.2% iron and a Russian alloy called Ozhennite (zirconium–0.2% tin–0.1% iron–0.1% nickel–0.1% niobium). Because hydriding of pressure tubes may limit the life of zirconium–2.5% niobium, the performance of these alloys is very significant. Estimated operating times for pressure tubes of several alloys show the superiority of Ozhennite (Table 4). However, the creep behavior of these alloys is not known as yet. Nevertheless, pressure-tube life depends strongly on the design criteria and operating conditions. It might be possible to design for any tube life with any of these alloys by thickening the tube wall, although this involves a cost penalty because of increased parasitic absorption of neutrons.

Table 4 RELATIVE PERFORMANCE OF ZIRCONIUM ALLOYS IN ORGANIC* COOLANT[22]

Alloy	Operational life, years
Zircaloy-2	1–3
Zr–2.5% Nb	5
Ozhennite	~15

*Santowax OM or HB-40 at 687 to 752°F.

Coolant Performance

A summary of the chemical behavior of organic coolants was presented in a previous issue of *Power Reactor Technology*.[23] From the summary it can be seen that corrosion effects produced by high-purity coolant can be expected to be relatively small. However, breakdown of the coolant into lighter molecular-weight components and polymerization into high-boiling compositions can produce significant changes in coolant properties, and these, in turn, must be investigated to determine possible interference with reactor operation (although AECL calculations of fuel performance in a variety of coolant compositions, including up to 40% high-boiling compounds, indicate very little difference in heat-transfer behavior for any of the coolants).[16] The cost of organic-coolant makeup (12 to 40 cents/lb) to compensate for decomposition adds slightly to the cost of running a reactor. In a HWOCR system these costs amount to an additional 0.1 to 0.2 mill/kw-hr in operating costs and do not seriously affect the economic potential of these plants. Organic makeup costs can be reduced by up to an order of magnitude if the high-boiling compounds are reconstituted for reuse as coolant by hydrocracking. Such systems are being developed and are expected to reduce HWOCR operating costs by approximately 0.1 mill/kw-hr.[3]

Some proponents of organic reactors believe that changes in the coolant during use are not necessarily deleterious.[24] They emphasize the viewpoints that: (1) the coolant is not the feed material that one starts with but is the mixture obtained during steady operation of the reactor system; (2) the properties of the mixture generally are superior to those of the feed material; and (3) a range of properties is available from a given material, and reactor operating conditions will be chosen to take maximum advantage of these properties.

IN-REACTOR TESTS

Loop irradiations, important because organics decompose and polymerize when irradiated, have been performed under reactor conditions, and the physicochemical behavior of the coolants has been determined.[25] Major interest has centered on Santowax OM and HB-40 (Table 5).[26] The HB-40 coolant, a mixture of terphenyls reacted catalytically with hydrogen to form a 40%-saturated hydrocarbon, has the advantage of remaining liquid at room temperature, and thus offers greater handling convenience under operational conditions. Its major disadvantage lies in a lower autoignition temperature than that of Santowax OM (706 vs. 1072°F). However, the autoignition temperature is increased by irradiation, and so this disadvantage lessens during operation.

The NRX loop irradiations and WR-1 experience have shown that the performance of HB-40 is similar to Santowax OM.[25] Coolant decomposition results in a consumption rate of approximately 50 g/kw-hr absorbed, approximately equal for both compositions.

Table 5 PHYSICAL PROPERTIES OF TWO MAIN ORGANIC COOLANTS[26]

Temperature, °F	Density, g/cm³		Specific heat, Btu/(lb)(°F)		Viscosity, centipoise		Thermal conductivity, Btu/(hr)(ft)(°F)	
	Santowax OM	HB-40	Santowax OM	HB-40	Santowax OM	HB-40	Santowax OM	HB-40
400	0.950	0.866	0.492	0.45	0.85	0.82	0.071	0.065
500	0.904	0.828	0.531	0.49	0.47	0.53	0.069	0.065
600	0.859	0.788	0.568	0.53	0.31	0.36	0.066	0.065
700	0.813	0.737	0.604	0.57	0.23	0.26	0.064	0.065
800	0.765	0.682	0.640		0.17	0.16		

Decomposition of coolant from both pyrolytic and radiolytic processes produces high-boiling compounds and volatile products. In HB-40 at high temperatures, thermal degradation of high-boiling compounds partly offsets radiolytic production. The production of volatiles during HB-40 irradiation produced increased vapor pressure, which can be reduced by stripping out the volatiles (e.g., by helium purge) at the expense of a slight increase in coolant consumption. The increase in high-boiling compounds also increases the viscosity of the fluid (~0.4 raised to 0.5 centistokes at 662°F and 30% high boilers).[3] In these loop irradiations, composition was maintained by distillation purification and recovery, the technique to be employed also in a reactor system.

IMPURITY CONTROL

The most economical solution to the fouling and hydriding problems involves the control of impurities in the coolant, especially such impurities as chlorine and oxygen.[27] A fouling mass-transfer mechanism has been described in which an iron compound is formed and subsequently decomposes at the fuel-element surface to produce fouling.[23] Generally, fouling potentials are considered adequate if the chlorine-impurity content is kept at approximately 1 or 2 ppm and the water content is approximately 50 to 200 ppm[3,16,18] (water is added to the organic to impede polymerization). These conditions can be achieved with careful quality control—degassing and exclusion of air—in the initial charge of coolant followed by continuing control in subsequent makeup additions. Continuous side-stream purification through an absorbent such as Attapulgus clay is helpful in maintaining a low fouling potential.[16]

COKING

Another phenomenon that has been observed in organic reactors is coke formation caused by local overheating and irradiation of stagnant organic fluid. Such overheating has occurred in the Piqua reactor,[28] where a large mass of coke formed in the nearly stagnant organic fluid in the moderator region between fuel channels, not in the fuel channel itself. The stagnation caused continuous irradiation of a large quantity of organic material for an extended time. After the coke mass is removed from the Piqua reactor and the core is renovated, the core will be modified to prevent stagnation and excessive irradiation of the organic fluid.

Unlike the Piqua reactor, in an HWOCR the moderator would be heavy water and would not coke. The organic coolant would flow past the fuel at approximately 30 ft/sec, at which velocity there have been no instances of coking on heat-transfer surfaces[16] because the organic would be (1) irradiated for very short times and (2) continuously stripped of polymerized products by distillation during circulation through the primary coolant system.

* * *

I want particularly to acknowledge the contributions and comments extended by R. G. Hart (of Atomic Energy of Canada Ltd.) and B. L. Hoffman (of Atomics International) and their associates.

References

1. C. J. Raseman and L. Green, Commercial Power Reactors Cooled with Sodium, Heavy Water, or Organic Liquids, in *Reactor Technology, Selected Reviews — 1964*, L. E. Link (Ed.), USAEC Report TID-8540, pp. 111-129, 1964.
2. Reactor Table, *Nucleonics*, 19(11): 134-135 (November 1961).
3. B. L. Hoffman, Atomics International, personal communication.
4. Organic-Moderated Reactors: Piqua Auxiliary Systems, *Power Reactor Technol.*, 4(2): 82-88 (March 1961).
5. K. K. Polushkin et al., The ARBUS Organic Cooled and Moderated Nuclear Power Station, in *Proceedings of the Third United Nations International Conference on the Peaceful Uses of Atomic Energy, Geneva, 1964*, Vol. 5, pp. 487-495, United Nations, New York, 1965.
6. *Organic Coolants and Moderators*, Bibliographical Series No. 17, pp. 2-3, International Atomic Energy Agency, Vienna, 1965 (STI/PUB/21/17).
7. J. C. Leny, Towards an ORGEL Prototype, *Euratom*, 4(4): 122-126 (December 1965).
8. J. C. Leny and S. Orlowsk, The ORGEL Project, *Nucl. Eng.*, 10(106): 96-100 (March 1965).
9. H. W. Schleicher, Corrosion Studies in Organic Coolants for Nuclear Reactors, Report EUR-379 (CONF-28-6), European Atomic Energy Community, 1963.
10. WR-1: Unique Among Research Reactors, *Can. Nucl. Technol.*, 4(4): 30 (Fall 1965).
11. W. M. Campbell, A Current Assessment of the Organic-Cooled Heavy Water Moderated Reactor, in Papers Presented by AECL to the International Conference of the Canadian Nuclear Association, Ottawa, Ontario, May 28–30, 1962, Canadian Report AECL-1692, February 1963.
12. R. G. Hart et al., (AECL, Whiteshell), UO_2 Fuels in Organic Cooled Reactors, *Trans. Am. Nucl. Soc.*, 9(1): 47-48 (June 1966).
13. Canada and the Organic Reactor, *Can. Nucl. Technol.*, 5(4): 26-27 (July–August 1966).
14. *Nucleonics Week*, 7(25): 5 (June 23, 1966).
15. F. M. Stern, R. P. Varnes, and J. R. Hume, Design of the HWOCR Demonstration Plant, *Trans. Am. Nucl. Soc.*, 9(1): 213 (June 1966).
16. R. G. Hart, Atomic Energy of Canada Ltd., personal communication, Aug. 2, 1966.
17. K. H. Campbell, Evolution and Promises of Organic-Cooled Reactors, *Nucl. Eng.*, 11(117): 102-105 (February 1966).
18. A. N. Tardiff, U. S. Atomic Energy Commission, personal communication.
19. W. G. Mathers et al., UC Fuels in Organic Reactors, *Trans. Am. Nucl. Soc.*, 9(1): 46-47 (June 1966).
20. S. O. Arneson, R. H. Young, and W. P. Chernock, HWOCR Fuel-Irradiation Tests, *Trans. Am. Nucl. Soc.*, 9(1): 48-49 (June 1966).
21. Heavy Water Organic Cooled Reactor, Quarterly Technical Progress Report, July–September 1966, USAEC Report AI-CE-54, Atomics International and Combustion Engineering, Inc., Oct. 15, 1966.
22. J. Boulton, S. R. Hatcher, and R. E. Hollies (AECL, Whiteshell), The Use of Zirconium Alloys in Organic Coolants, *Trans. Am. Nucl. Soc.*, 9(1): 45-46 (June 1966).

23. J. E. Sawyers, Advancements in Organic Coolants, *Power Reactor Technol.*, 8(4): 290-295 (Winter 1965–1966).
24. M. Tomlinson, Atomic Energy of Canada Ltd., personal communication, Aug. 9, 1966.
25. M. C. Arneson et al., Some Characteristics of Irradiated HB-40, An Organic Liquid Coolant for Reactors, *Trans. Am. Nucl. Soc.*, 9(1): 44-45 (June 1966).
26. H. Mandel, Heavy Water Organic Cooled Reactor, USAEC Report AI-CE-15, p. 13, Atomics International and Combustion Engineering, Inc., Apr. 15, 1966.
27. B. A. Finlay, J. L. Smee, and S. R. Halcher (AECL, Whiteshell), Organic Coolant Performance in Reactor Loops, *Trans. Am. Nucl. Soc.*, 9(1): 44 (June 1966).
28. Piqua Nuclear Power Facility, Monthly Operating Report No. 37, USAEC Report COO-652-27, May 1966.

Two Advances in Reactor Neutron-Noise Analysis

By Charles E. Cohn

Measurement of the fluctuations in the neutron flux in chain-reacting systems and interpretation in terms of reactor kinetics and safety characteristics have been particularly useful for subcritical and critical assemblies and for training or research reactors. Although transfer functions, stabilities, and the ratio of delayed-neutron fraction to neutron lifetime have been measured in preoperational tests with a number of power reactors[1] (N.S. *Savannah,* Yankee, and Dresden, for instance), the numerous sources of noise in power reactors during operation have limited the usefulness of the technique. However, two relatively new developments, which permit faster measurements or lower detector efficiencies, have extended the usefulness of noise analysis and hold great promise for routine measurements on power reactors. These developments were described at the second symposium on Neutron Noise, Waves, and Pulse Propagation, which was held at the University of Florida.[2–4] The first symposium has been reported previously.[1,5]

Although the second symposium covered a broad field of work, both fundamental[6–24] and applied,[25–32] this article is restricted primarily to the experimental techniques of special interest to readers concerned with power reactors.

Pseudorandom Binary Inputs

The experimental technique of greatest interest for power-reactor applications, such as reliable and accurate measurements of shutdown reactivity, is the use of pseudorandom binary-input signals for measuring system transfer functions. Because the technique is compatible with typical reactor hardware (the control rod can be made to jump between two-position solenoids nearly instantaneously), and, although the statistical characteristics make the signal appear to be a random variable, the prescribed sequence of the binary signal means that the mathematical characteristics are known exactly. Thus techniques of random theory can be applied to yield measurements of increased precision.

The binary signal has an autocorrelation function (a measure of the degree of correlation in successive values of some signal, e.g., neutron level, coolant temperature, or fuel temperature) which approaches a delta function. Thus it contains components of all frequencies. The system transfer function is obtained by correlating this input signal and the resulting system output.

The two-valued nature of the input signal makes it easy to generate and also simplifies cross-correlation by eliminating the need for multipliers. The pseudorandom nature and small amplitude of the input signal assure minimum disturbance to the normal operation of the system being measured. Moreover, the technique frequently yields the same precision from measurements taken in 5 to 500% less time than with previous methods.

The method has been used for measuring transfer functions on critical reactors of the NERVA[33] and Phoebus[34] rocket types and others,[35] as well as on subcritical systems.[36] For the rocket reactors the input signals were superimposed on the reactor power demand (by oscillating the control drum) and in other cases on the hydrogen-turbopump speed demand, which varied between 21,000 and 23,000 rpm. For the subcritical reactor systems, the neutron source strength was varied in binary fashion by deflecting an accelerator beam on and off the target.

Two-Detector Cross-Correlation

Because it suppresses the effect of the unwanted background noise originating in the detector itself, the two-detector cross-correlation method allows measurement of reactor neutron noise with detector

efficiencies a hundred times lower than the 10^{-4} efficiency practicable with the conventional single-detector method. This gives the user more freedom in selecting detector location, size, and geometry. For instance, this is important for power reactors because the neutron detectors can be moved from the reactor vessel to shielded regions where the gamma background is lower.

The method was used originally in a pool type reactor in Japan[37] and in an Argonaut type reactor in Germany.[38] Stegemann[38] reports that the technique gives reliable measurements of prompt-neutron decay, absolute reactor power, and shutdown reactivity when the outputs from cross-correlated detectors have a ratio of correlated-to-uncorrelated noise of 0.1; in an equivalent single-detector experiment, this ratio would be approximately 2.

Lower detector efficiencies suffice because the correlation between the detection noise from two separate detectors has an expectation value of zero; thus only the correlated or reactor-noise component is seen. However, the detection-noise components introduce random error into the results. So a decrease in detection efficiency calls for longer measuring time to get statistical data for acceptable precision.

General Applications

Some power-reactor applications of more familiar noise-analysis techniques were also discussed at the meeting. These included measurements on the Molten Salt Reactor Experiment (MSRE) circulating-fuel reactor[39] which clearly showed the significant change in the transfer function produced by fuel circulation; rapid fuel flow reduces the effective delayed-neutron fraction in the core. Experiments have been made to detect the onset of nucleate boiling by analysis of neutron-flux noise[40] and of acoustical noise.[41] Low-frequency resonances have also been observed (Fig. 1) in a swimming-pool reactor with forced circulation and are believed to be caused by coolant-flow fluctuations that excite vibration of a control rod.[42]

MSRE DELAYED-NEUTRON FRACTIONS

Neutron fluctuation measurements were made at zero power to determine the difference in the effective delayed-neutron fraction β_e when fuel is, and is not, circulating in the primary loop.[39] When fuel is circulating, some precursors decay outside the core and lower β_e. Figure 2 shows power-density spectra that were analyzed with a point-reactor model assuming one average delayed group of neutrons. For a least-squares fit, β_e increased by a factor of 1.56 ± 0.21 when circulation ceased. For the same conditions, control-rod calibration measurements showed an increase by a factor of 1.47.

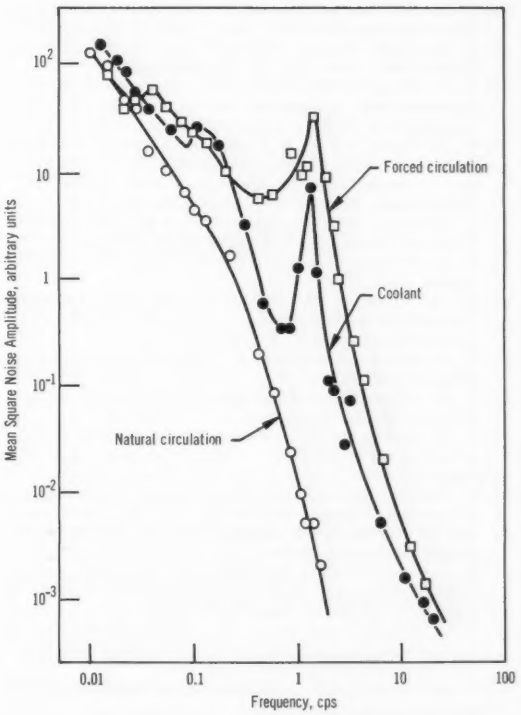

Fig. 1 Low-frequency resonances are induced by control-rod vibrations generated when coolant flow fluctuates in Hitachi Test Reactor at 80 kw (Ref. 42).

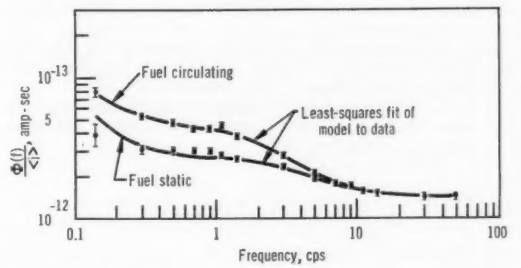

Fig. 2 Analysis of power-density spectra for the MSRE shows that the delayed-neutron fraction β_e decreases when fuel is circulated.[39]

References

Except for Refs. 1 and 3 to 5, all references are papers in Ref. 2.

1. M. F. Valerino, Conference on Noise Analysis in Nuclear Systems, *Power Reactor Technol.*, 7(3): 248-264 (Summer 1964).
2. Proceedings of the Symposium on Neutron Noise, Waves, and Pulse Propagation, held at University of Florida, Gainesville, Fla., February 14–16, 1966, USAEC Report CONF-660206, 1966.

3. D. N. Fry, Symposium on Neutron Noise, Waves, and Pulse Propagation, *Nucl. Safety*, 8(1): 37-40 (Fall 1966).
4. R. E. Uhrig, Neutron Noise, Waves, and Pulse Propagation, *Nucl. News*, 9(5): 32-33 (May 1966).
5. R. E. Uhrig (Coordinator), *Noise Analysis in Nuclear Systems*, AEC Symposium Series, No. 4 (TID-7679), University of Florida, Gainesville, Fla., June 1964.
6. R. B. Perez and R. E. Uhrig, Development of Neutron Waves and Pulse Propagation Techniques, Paper 1-1.
7. M. N. Moore, On the General Theory of Excitation Experiments in Space Dependent Kinetics, Paper 1-2.
8. A. Travelli, The Complex Relaxation Length of Neutron Waves in Multigroup Transport Theory, Paper 1-3.
9. R. L. Brehm, Analysis of Neutron Wave-Type Experiments, Paper 1-4.
10. M. J. Ohanian, R. B. Perez, and R. G. Cockrell, Propagation of Monochromatic Neutron Waves in Fast Nonmultiplying Media, Paper 1-5.
11. H. H. Kunaish, Consistent P-3 Theory of Neutron Wave Propagation, Paper 1-6.
12. G. H. Miley, Pulse Propagation Experiments Using a Reactor Source, Paper 2-1.
13. J. H. Dunlap and R. B. Perez, The Dispersion Law for a Natural Uranium, Heavy Water, Subcritical Assembly, Paper 2-2.
14. K. Sumita and A. Takahashi, A Simple Pulsed Neutron Source for Thermal Neutron Propagation Experiments and Its Application in Homogeneous and Heterogeneous Graphite Systems, Paper 2-3.
15. R. S. Booth and W. A. Frankhauser, Theoretical Justification for Neutron Pulse Propagation Experiments in Fast Nonmoderating Assemblies, Paper 2-4.
16. R. J. Johnson and R. N. Macdonald, Calculation of Space-Dependent Effects in Pile Oscillator and Reactor Noise Measurements, Paper 2-5.
17. J. R. Sheff, Space Dependent Cross-Spectral Density in a Bare Cube, Paper 2-6.
18. J. B. Dragt, Analysis of Reactor Noise Measured in a Zero Power Reactor and Calculations on Its Accuracy, Paper 3-3.
19. L. G. Kemeny, Fundamental Aspects of Stochastic Processes and Fluctuation Phenomena in Fission Reactors, Paper 5-1.
20. M. Natelson, R. K. Osborn, and F. Shure, Recent Developments in the Analysis of Neutron Noise Experiments, Paper 5-2.
21. R. J. Gelinas and R. K. Osborn, Reactor Noise Analysis from Observations on the High Energy Gamma Radiation from the Reactor Core, Paper 5-3.
22. R. J. Hooper and E. P. Gyftopoulos, On the Measurement of Characteristic Kernels of a Class of Nonlinear Systems, Paper 5-4.
23. A. Z. Akcasu, Angular Correlations in Neutron Density Fluctuations, Paper 5-5.
24. H. Borgwaldt and D. Sanitz, The Modal Synthesis of Rossi-Alpha Data for Moderator-Reflected Fast Assemblies, Paper 5-6.
25. M. A. Schultz, Measurement of Shutdown Reactivity in Large Gamma Fields, Paper 3-4.
26. E. S. Kenney, Noise Analysis of Nuclear Reactors Using Gamma Radiation, Paper 3-5.
27. H. Kataoka and M. Kubo, Identification of Transfer Function of Reactor Control System by Noise Analysis, Paper 3-6.
28. R. W. Albrecht and E. J. McGrath, Bias in Nuclear Reactor Power Spectral Density Estimates with Finite Record Lengths, Paper 3-7.
29. P. Meyer and E. Garelis, Impulse Response Measurements Using a Pseudorandom Source Input, Paper 4-3.
30. R. L. Randall and P. J. Pekrul, Applications of Analog Time and Frequency-Correlation Computers to Reactor System Analysis, Paper 6-3.
31. R. W. Albrecht and G. M. Hess, Reactor Noise Experiments in Reflected Plutonium Assemblies, Paper 6-4.
32. D. Babala et al., A Review of "NORA" Project Noise Experiments, Paper 6-7.
33. A. A. Wasserman et al., NERVA Reactor Transfer Function Measurements Using Cross-Correlation Techniques, Paper 4-2.
34. J. A. Johnson, Measurement of Pressure-to-Pressure Transfer Functions Through the Phoebus-1A Nuclear Reactor, Paper 6-5.
35. M. Hara and N. Suda, Some Investigations in the Application of Pseudorandom Binary Signals to Reactor Dynamics Measurements, Paper 4-1.
36. R. E. Uhrig and M. J. Ohanian, Pseudorandom Pulsing of Subcritical Systems, Paper 4-4.
37. T. Nomura, S. Gotoh, and K. Yamaki, Reactivity Measurements by Neutron Noise Analysis Using Two-Detector Correlation Method and Supercritical Reactor Noise Analysis, Paper 3-2.
38. W. Seifritz, D. Stegemann, and W. Vath, Two-Detector Cross-Correlation Experiments in the Fast-Thermal Argonaut Reactor "STARK" at Karlsruhe, Paper 3-1.
39. D. N. Fry et al., Neutron Fluctuation Measurements at Oak Ridge National Laboratory, Paper 6-1.
40. V. Rajagopal, Some Applications of Noise Measurements in Pressurized Water Reactors, Paper 6-2.
41. R. F. Saxe, Noise Analysis of the Oak Ridge Research Reactor, Paper 3-8.
42. S. Yamada and H. Kage, Reactor Noise Caused by Coolant Flow Fluctuations, Paper 6-6.

Water-Reactor Lattice Calculations and Measurements

By Edwin M. Pennington

Critical experiments—performed both to provide data that are used in power-reactor design and to test calculational methods—are the basis for many advances in water-reactor technology. Recent work encompasses heavy-water-moderated critical assemblies at Chalk River (where, for the first time, UC has been used with heavy water) and several light-water-moderated assemblies. The work with light-water lattices extends and interprets the data over a broader range of mixed-oxide fuel compositions.

Heavy-Water Lattices

Because not enough UC fuel was available to build critical lattices without a UO_2 driver zone, clusters of UC fuel were substituted into the central region of lattices containing UO_2 fuel. The validity of lattice parameters and analytical methods for these substitution experiments was studied in detail; the conclusion is that such substitution methods generally give results of adequate accuracy.

BUCKLING MEASUREMENTS FOR UC

Experiments have been carried out using seven-rod clusters of natural UC fuel in D_2O-moderated lattices in the ZED-2 critical facility at Chalk River.[1] The rods were of 2.52-cm-diameter UC clad in 1-mm-thick aluminum. The cluster arrangement was a central rod plus six rods on a 5.90-cm-diameter circle. Each cluster was contained in an aluminum pressure tube 9.1 cm in inside diameter with a 2-mm-thick wall and a calandria tube 10.1 cm in inside diameter with a 1.5-mm-thick wall.

Bucklings were determined by the substitution method in which up to 25 UC clusters successively replaced reference fuel at the core center. Nineteen-rod CANDU type bundles of UO_2 fuel were used as the reference. The difference in buckling between test and reference regions was derived from the changes in critical moderator level.

Measurements were made in square lattices at several pitches from 20 to 32 cm, with the UC clusters having four different coolants: D_2O, air, HB-40 ($C_{18}H_{22}$), and Dowtherm A. The reference fuel always had D_2O coolant.

Four methods were used in the analysis of the critical-height measurements. All methods gave reasonably good results except for the case of air-cooled clusters, where a problem with diffusion coefficients arose. To test the methods, substitution experiments were performed using fuel assemblies for which bucklings had been determined by flux-mapping experiments. The best agreement was given by a heterogeneous source-sink method, programmed under the name MICRETE.[2] It is believed that the bucklings for the seven-rod UC clusters determined by MICRETE, which range from about 1.9 m^{-2} to 5.0 m^{-2}, are accurate to less than or equal to 0.10 m^{-2}.

FINE STRUCTURE AND SPECTRUM PARAMETERS

Neutron-density fine structure and spectrum parameters were measured for the seven-rod UC clusters.[3] As is typical for D_2O-moderated lattices, the neutron-density fine structure is quite pronounced. The ratio of average neutron density in one of the six outer rods to that in the center rod varies from about 1.27 in a 20-cm-pitch lattice with air coolant to 1.61 in a 28-cm-pitch lattice with HB-40 coolant. Corresponding ratios of the moderator average neutron density to the average in the seven fuel rods are 2.063 and 3.257. These two values have since[27] been revised to 2.151 and 3.275.

The Westcott epithermal index r and the effective neutron temperature T_n were measured in the fuel, on the surface of the calandria tube, and at the cell boundary. These values were derived from the activity

ratios of indium to manganese and ^{177}Lu to manganese with a modification of the technique of Chidley et al.[4] The largest value of r was 0.0935 for the fuel of the 20-cm-pitch lattice with air coolant. The highest effective neutron temperature was about 100°C above the physical moderator temperature and occurred in the fuel of the 20-cm-pitch lattice with HB-40 coolant. For the loosest lattices the effective temperatures at the cell boundary differed little from the physical temperature.

VALIDITY

A study was made to determine whether lattice parameters can be obtained by using as few as seven test fuel rods at the center of a driver lattice.[5] Measurements were made both in the ZEEP reactor at 18- and 22-cm triangular lattice spacings and in the ZED-2 reactor at a 22-cm triangular lattice spacing. The ZEEP rods, which are 3.25-cm-diameter natural-uranium-metal rods, served as the driver fuel in the ZEEP reactor, and CANDU type 19-element natural-UO_2 fuel assemblies were the driver fuel in ZED-2. The natural-uranium test assemblies were 7-element UO_2, 19-element UO_2, and 19-element uranium-metal clusters, as well as ZEEP rods. The moderator was D_2O in all cases, and D_2O and HB-40 coolants were used.

If the neutron spectrum at the boundary of the center cell of the seven-element test region matches that in a full lattice of test fuel, then reaction-rate measurements in the central assembly of the test region should give the full-lattice values. Therefore Westcott's index r and the neutron temperature excess over the moderator temperature ΔT were measured at a central-cell boundary position midway between the central assembly and an assembly in the first ring of the test region. Comparisons with earlier values obtained using full lattices of test rods show that, for the 22-cm spacing, r and ΔT reached their equilibrium values at the central-cell boundary — whereas for the 18-cm spacing, ΔT but not r reached equilibrium.

Measurements of various lattice parameters were made in the fuel of the central 19-element UO_2 assembly containing D_2O coolant in the 18-cm ZEEP lattices. The results obtained agreed well with full-lattice results and indicate that, for natural-uranium D_2O-moderated lattices, lattice parameters can be measured using only seven test rods, even with the large mismatch of rod sizes in these experiments.

BUCKLINGS FROM SUBSTITUTION EXPERIMENTS

The MICRETE program,[2] which performs a two-group heterogeneous reactor calculation, has been used to determine the bucklings of natural-uranium D_2O-moderated lattices from measured changes in critical moderator height when 1 to 25 fuel assemblies are substituted into a reference core. In addition to the critical D_2O levels, the analysis requires calculated two-group parameters. However, the derived bucklings are insensitive to these, and they may be calculated by standard methods. First, a MICRETE calculation is performed for the reflected reference core using the observed height and calculated parameters. Then values of the resonance escape probability p and the effective outer radius of the D_2O reflector are adjusted until the reactor is critical and has a buckling, determined by the calculated flux shape near the core center, in agreement with the flux-mapping value. One or more test assemblies are then substituted in the calculation for reference assemblies, and their p value is adjusted until criticality is calculated to occur at the measured critical height. Then a MICRETE calculation is performed for a full lattice of test assemblies using the derived value of p and the other calculated parameters for the test lattice. After the dimensions of this core are altered until the system is critical, the buckling is determined from the flux shape near the center.

Application of MICRETE calculations to substitution experiments performed in the ZEEP and ZED-2 assemblies showed that values from MICRETE analysis with seven or more test rods and D_2O coolant are generally in good agreement with flux-mapping values. The largest buckling error for seven rods and D_2O coolant was 0.20 m^{-2}. Agreement is not as good for lattices with seven test rods and HB-40 or helium coolant, where the errors in bucklings were as large as 0.5 m^{-2} with the organic coolant and 0.7 m^{-2} with the helium.

Light-Water Lattices

Recent experiments have been performed with light-water lattices at Battelle–Northwest and at Argonne. At Battelle–Northwest the experiments used 2 wt.% PuO_2-UO_2 fuel with three different isotopic compositions of plutonium. These experiments supplemented previous ones at Battelle–Northwest performed with 1.5 wt.% PuO_2-UO_2 fuel. The Argonne experiments utilized 3.04% enriched UO_2 fuel and were done to extend the range of investigation of light-water lattices to highly undermoderated assemblies. Agreement between theory and experiment is usually satisfactory, although there are exceptions. Reference 6 comments on the state of the art of light-water criticals.

In connection with the analysis of light-water lattices, considerable work has been done in recent years on the behavior of the thermal disadvantage factor in tightly packed lattices and on the determination of bucklings by variable loading techniques. The main features of this work are also outlined here.

$PuO_2-UO_2-H_2O$ LATTICES

Subcritical experiments and analytical correlations were performed for $PuO_2-UO_2-H_2O$ lattices at Battelle–Northwest.[7] The fuel was 2 wt.% PuO_2-UO_2 (vibratory compacted) contained in 0.030-in.-thick

Zircaloy tubes 0.508 in. in inside diameter. The uranium in the UO_2 was of natural enrichment, whereas three compositions of plutonium were, by weight, (1) 91.62% ^{239}Pu, 7.65% ^{240}Pu, 0.70% ^{241}Pu, and 0.03% ^{242}Pu; (2) 81.11% ^{239}Pu, 16.54% ^{240}Pu, 2.15% ^{241}Pu, and 0.20% ^{242}Pu; and (3) 71.76% ^{239}Pu, 23.50% ^{240}Pu, 4.08% ^{241}Pu, and 0.66% ^{242}Pu. The rods were loaded in hexagonal lattices at spacings yielding moderator-to-PuO_2-UO_2 volume ratios of 0.61 to 9.7. All lattices were completely reflected with H_2O. The experimental procedures were the same as those used in determining critical masses and bucklings of 1.5 wt.% $PuO_2-UO_2-H_2O$ lattices.[8]

The calculations were performed using one-dimensional four-energy-group diffusion theory for a homogeneous core and H_2O reflector. Axial leakage effects were accounted for with transverse bucklings. Cross sections for the homogenized lattice were obtained using the HRG (Hanford-Revised GAM) code[9] for nonthermal events and the THERMOS code[10] with the Nelkin kernel for hydrogen in the thermal-energy range. Microscopic cross sections were taken from the Battelle–Northwest master library.[11]

The calculated multiplications, k_{eff}, for most of the lattices are somewhat low. Use of the more recently evaluated value of 2.115 for the thermal η of ^{239}Pu, rather than the older value of 2.093 which was used in the calculations, would increase the multiplications by about 1% and yield better agreement with experiment.

There are two main factors that make calculations for thermal plutonium lattices difficult. One is the fact that the plutonium cross sections are not, in general, as accurately known as those for uranium. The other is the presence of large low-lying resonances in ^{239}Pu, ^{240}Pu, and ^{241}Pu, which makes an accurate treatment of near-thermal events important. Uncertainties in resonance cross sections lead to larger uncertainties in multiplication values than do the uncertainties in thermal cross sections.[28]

UO_2-H_2O LATTICES

The High Conversion Critical Experiment (Hi-C) was initiated at Argonne to extend the range of investigation with light-water-moderated slightly enriched UO_2 cores to lower water-to-fuel ratios. Lattices were assembled with hydrogen-to-^{238}U atom ratios of from 4.16 to 0.50, which correspond to water-to-UO_2 volume ratios of from 1.37 to 0.17. The fuel consisted of 0.935-cm-diameter 3.04% enriched UO_2 pellets loaded in cladding tubes of either 0.048-cm-thick aluminum or 0.0496-cm-thick stainless steel. Both square and triangular lattice arrays were used.

Various cell parameters were measured in the full range of lattices; critical bucklings and reflector savings were measured in the looser assemblies. Calculations of critical bucklings and cell parameters were carried out in the framework of four-group diffusion theory. Cross sections for three fast groups were obtained using the GAM-I code,[12] whereas those for the thermal group were found using THERMOS[10] with the Nelkin kernel for hydrogen.

The critical bucklings, obtained by using the four-group constants in fundamental mode calculations, are in good agreement with experimental values.[13] Values of k_{eff} averaged about 0.5% too high when the P_1 approximation was used in GAM-I and about 1% too high when the B_1 approximation was used. Preliminary calculations yielded values much higher than experiment. The improvement resulted from replacing ^{238}U and ^{235}U cross sections in the original GAM-I library by values obtained from Hanford. Agreement between theory and experiment was reasonably good for reflector savings and various cell parameters, except for the case of the ^{238}U-to-^{235}U fission ratio δ^{28}, for which experimental values were much higher than calculated ones.

Improvements could be made in the theoretical methods used in the Hi-C program, although those used should be reasonably accurate. However, the extreme undermoderation of the lattices makes nonthermal events very important; thus inaccuracies in nonthermal cross sections can produce large uncertainties in the calculations. Figure 1 illustrates the large contribution of nonthermal events to criticality. The parameters plotted against the hydrogen-to-^{238}U atom ratio are p_1, λ_f, and τ of the two-group criticality equation used in the study of light-water lattices at Brookhaven.[14] This equation is

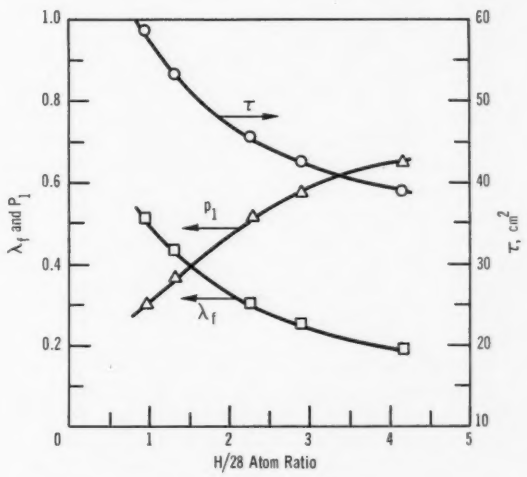

Fig. 1 Two-group parameters for Hi-C aluminum-clad lattices. The ordinate for p_1 and λ_f is dimensionless.[13]

$$\frac{(1-p_1)(\eta f)_1}{1+\tau B^2} + \frac{p_1(\eta f)_2}{(1+\tau B^2)(1+L^2B^2)} = 1 \qquad (1)$$

where the two terms on the left side are denoted by λ_f and λ_t and represent contributions from nonthermal and thermal neutrons, respectively.

DISADVANTAGE FACTORS IN TIGHTLY PACKED LATTICES

A problem that has received considerable attention in the last 2 or 3 years is that of disadvantage factors in tightly packed lattices of cylindrical fuel rods. Experimental evidence has been presented[15] that the cell disadvantage factor is not necessarily a monotonically decreasing function as the pitch decreases, although large error bars are associated with the results.

In Ref. 16, solutions of the P_3 approximation to the one-velocity Boltzmann equation for a two-region two-dimensional cell of cylindrical fuel rods in a moderator are obtained. It is found that the disadvantage factor δ has a minimum as the lattice pitch is decreased with the moderator cross section remaining constant. The breakdown of monotonic behavior of δ increases for cores where the optical thickness of the fuel is larger. Monte Carlo results for a few cases where the fuel rod has unit optical thickness show the same trend as the P_3 results. The two-dimensional P_1 approximation also yielded a minimum in the δ curve.

It has been shown that δ has a minimum as the moderator cross section is decreased at constant lattice pitch.[17] Both Brissenden's approximate collision-probability method[18] for a square cell and a cylindrical-cell approximation with the isotropic (white) boundary condition suggested by Honeck[19] were used.

Calculations corresponding to the experimental Hi-C lattices[15] using the THERMOS code[10] with 27 groups and the isotropic boundary condition, as well as in a cylindrical-cell collision-probability code with isotropic return and one-group cross sections from THERMOS, did not yield a minimum in δ. However, this lack of a minimum was the result of the progressive hardening of the cross sections as the pitch was decreased. When the one-group cylindrical-cell collision-probability calculations were repeated using constant cross sections, a minimum in δ was obtained.

Many of the results obtained for disadvantage factors in tightly packed lattices have been summarized.[20] Table 1, which is adapted from Ref. 20, presents trends of the disadvantage factor calculated by various methods. In the table an A-series lattice is one for which the moderator cross section is held constant and the moderator thickness decreased, whereas a B-series lattice has fixed-cell dimensions and the moderator cross section is decreased. The quantities Σ_1, a, and V are the moderator cross section, fuel radius, and moderator-to-fuel volume ratio, respectively.

Table 1 DISADVANTAGE-FACTOR TRENDS

Method	A-series lattice $\Sigma_1 a = 1$ (constant)	B-series lattice $V = 1$ (constant)
P_1 approximation, cylindrical	Monotonic decrease	Monotonic decrease
P_1 Cohen,[24] square	Increases below $V = 0.681$	Monotonic decrease
P_3 Clendenin,[25] cylindrical		
(*a*) Boundary condition $\psi_{33} = 0$	Increases below a certain V	Monotonic decrease
(*b*) Boundary condition $\psi_{31} = 0$	Monotonic decrease	Monotonic decrease
Amouyal[26]	Monotonic decrease	Increases below a certain $\Sigma_1 a$
Collision probability, flat-flux approximation[20]		
(*a*) Cylindricized	Increases below a certain V	Increases below a certain $\Sigma_1 a$
(*b*) Exact square or hexagonal cell	Increases below a certain V	Increases below a certain $\Sigma_1 a$

Reference 20 also points out that the cylindrical-cell approximation with isotropic boundary condition breaks down somewhat for very tightly packed lattices — in that the disadvantage factor does not increase rapidly enough with decreasing pitch. Thus it is expected that, if an exact multigroup thermal calculation were carried out for the Hi-C lattices, rather than one using the isotropic boundary condition as in THERMOS, the disadvantage factor would show a minimum in spite of the tendency of the hardening of the cross sections to counteract the effect. This is in qualitative agreement with the results of 36-group Monte Carlo calculations[21] which treat the cell geometry exactly.

A significant effect has been discovered[22] in connection with the interpretation of thermal disadvantage-factor measurements. Three-dimensional Monte Carlo calculations explicitly including foils indicate that the flux in a foil is often considerably different from the flux in the medium in which it is placed, even for optically thin foils. The flux peaking or dipping depends strongly on the medium surrounding the foil.

Calculations were carried out using a 32-group thermal Monte Carlo code, DRAM, both for some lattices at Bettis Atomic Power Laboratory and for the Argonne Hi-C lattices. Thermal disadvantage factors were calculated both for the foil regions and for unperturbed regions in the rod and moderator. For all lattices the disadvantage factors for the unperturbed region were higher than those for the foil regions; disadvantage factors for the foil regions were in agreement with the experimental values. These results explain why calculated disadvantage factors tend to be larger than measured ones.

BUCKLINGS BY VARIABLE LOADING TECHNIQUES

In determining experimental bucklings from "variable-loading" techniques, to obtain accurate results it is necessary to allow for the variation in radial-reflector savings. The equation

$$\lambda r = \frac{\lambda_0}{(1 + M^2 B_z^2)^{1/2}} \frac{K_0\{[(1/M^2) + B_z^2]^{1/2} r\}}{K_1\{[(1/M^2) + B_z^2]^{1/2} r\}} + \Delta\lambda \qquad (2)$$

has been proposed[23] for the radial-reflector savings. In Eq. 2, B_z^2 is the axial buckling, λ_0 and M^2 are constants to be determined from the fit to a series of loadings, K_0 and K_1 are Bessel functions, and $\Delta\lambda$ is a correction for having assumed a linear extrapolation of the flux from its value at the core boundary to the radius at which it is zero.

Equation 2 was tested by using it in a variable-loading analysis of a series of theoretical four-group two-region cores. The variable-loading bucklings agreed with the infinite lattice values within 0.1 m^{-2}. Also both variable-loading and "flux-shape" techniques were applied to 32 experimental cores. The results were in good agreement for lattices where the radial buckling was less than 50 m^{-2}. For lattices with larger radial bucklings, the flux-shape values were systematically high. This illustrates the breakdown of the flux-shape technique for cores of small radius where radial energy transients are significant. For such cores the variable-loading method with variable-reflector savings is more suitable.

References

1. R. E. Green et al., Experimental Bucklings for Seven-Rod Clusters of Natural UC in Heavy Water Moderator, *Trans. Am. Nucl. Soc.*, 9(1): 123 (June 1966).
2. D. S. Craig et al., Bucklings from Substituion Experiments by Use of Source-Sink Calculation, *Trans. Am. Nucl. Soc.*, 9(1): 126 (June 1966).
3. R. E. Kay and R. E. Green, Experimental Neutron-Density Fine Structures and Spectrum Parameters for Natural-UC Clusters in Heavy-Water-Moderated Lattices with Air, Heavy Water, and Organic Coolants, *Trans. Am. Nucl. Soc.*, 9(1): 124 (June 1966).
4. B. G. Chidley et al., Neutron Temperatures in a CANDU-Type Power Reactor, *Nucl. Sci. Eng.*, 16(1): 39 (May 1963).
5. A. Okazaki and D. S. Craig, Measurement of Lattice Parameters in Natural-Uranium/Heavy-Water Lattices Using a Few Rods, *Trans. Am. Nucl. Soc.*, 9(1): 125 (June 1966).
6. C. N. Kelber, Water-Reactor Data Generally Verify Theory, *Power Reactor Technol.*, 8(4): 214-215 (Fall 1965).
7. R. C. Liikala and W. P. Stinson, Experimental and Analytical Results for $PuO_2-UO_2-H_2O$ Lattices, *Trans. Am. Nucl. Soc.*, 9(1): 127 (June 1966).
8. L. C. Schmid et al., Critical Masses and Bucklings of $PuO_2-UO_2-H_2O$ Systems, *Trans. Am. Nucl. Soc.*, 7(2): 216 (November 1964).
9. J. L. Carter, Jr., HRG-Hanford Revised GAM, Battelle–Northwest, unpublished.
10. H. C. Honeck, THERMOS, A Thermalization Transport Theory Code for Reactor Lattice Calculations, USAEC Report BNL-5826, Brookhaven National Laboratory, September 1961.
11. K. B. Stewart, BNW Master Library, USAEC Report BNWL-CC-325, Vols. I, II, and III, Battelle – Northwest, Sept. 1, 1965.
12. G. D. Joanou and J. S. Dudek, GAM-I: A Consistent P-1 Multigroup Code for the Calculation of Fast Neutron Spectra and Multigroup Constants, USAEC Report GA-1850, General Atomic Division, General Dynamics Corp., June 28, 1961.
13. A. R. Boynton and E. M. Pennington, Critical Experiments and Calculations in Some Very Undermoderated, Slightly Enriched, Uranium Oxide/Water Lattices, *Trans. Am. Nucl. Soc.*, 9(1): 129 (June 1966).
14. R. L. Hellens and H. C. Honeck, A Summary and Preliminary Analysis of the BNL Slightly Enriched Uranium, Water Moderated Lattice Measurements, in *Light Water Lattices*, pp. 27-71, Technical Report Series, No. 12, International Atomic Energy Agency, Vienna, 1962 (STI/DOC/10/12).
15. A. R. Boynton, Thermal Disadvantage Factors in Very Undermoderated Water–Uranium Oxide Lattices, *Nucl. Sci. Eng.*, 23(4): 393 (December 1965).
16. T. E. Dudley, Disadvantage Factors in Close-Packed Lattices, *Trans. Am. Nucl. Soc.*, 9(1): 130 (June 1966).
17. Z. Weiss and R. J. J. Stamm'ler, Calculation of Disadvantage Factors in Small Cells, *Nucl. Sci. Eng.*, 19(3): 374 (July 1964).
18. R. J. Brissenden, A Formula for the Escape Probability of a Rod in a Uniform Lattice, British Report AEEW-R-282, April 1963.
19. H. C. Honeck, Some Methods for Improving the Cylindrical Reflecting Boundary Condition in Cell Calculations of the Thermal Neutron Flux, *Trans. Am. Nucl. Soc.*, 5(2): 350 (November 1962).
20. Y. Fukai, On the Disadvantage Factor in a Closely Packed Cylindrical Lattice, *J. Nucl. Sci. Technol. (Tokyo)*, 3(4): 165 (April 1966).
21. J. Hardy et al., Thermal Neutron Spectral and Spatial Distributions in Light Water Moderated Uranium Lattices, USAEC Report WAPD-T-1594, Westinghouse Electric Corp., Bettis Atomic Power Laboratory, April 1963; also in *Exponential and Critical Experiments*, Symposium Proceedings, Amsterdam, 1963, Vol. II, pp. 339-359, International Atomic Energy Agency, Vienna, 1964 (STI/PUB/79).
22. F. E. Dunn, Flux Dipping and Peaking in Foils Used in Thermal Disadvantage-Factor Measurements, *Trans. Am. Nucl. Soc.*, 9(1): 189 (June 1966).
23. H. Windsor, The Effect of Radial-Energy Transients on Experimental Material-Buckling Measurements, *Trans. Am. Nucl. Soc.*, 9(1): 130 (June 1966).
24. E. R. Cohen, Thermal Neutron Flux in a Square Lattice Cell, *Nucl. Sci. Eng.*, 1(4): 268 (August 1956).
25. W. W. Clendenin, Effects of Zero Gradient Boundary Conditions on Cell Calculations in Cylindrical Geometry, *Nucl. Sci. Eng.*, 14(1): 103 (September 1962).
26. A. Amouyal, P. Benoist, and J. Horowitz, Nouvelle Methode de Determination du Facteur d'Utilisation Thermique d'une Cellule, *J. Nucl. Energy*, 6(1/2): 79-98 (1957–1958).
27. R. E. Kay and R. E. Green, Atomic Energy of Canada Ltd., personal communication, October 1966.
28. R. C. Liikala, W. L. Purcell, and J. R. Worden, Sensitivity of Reactor Multiplication Values to Cross Section Uncertainties for Thermal Systems, in Conference on Neutron Cross Section Technology, March 22–24, 1966, Washington, USAEC Report CONF-660303, Book 1, pp. 75-87, 1966.

Nuclear Power To Explore the Ocean Deeps

By Edward J. Croke

Nuclear power is ideally suited to opening the undersea environment to man's use.[1] One of the most immediate and potentially significant applications of nuclear power in the conquest of the oceans involves the use of deep-diving submersibles for undersea exploration. Although a number of conventionally powered research and exploration submersibles have been and are being built, and numerous studies have been made of nuclear propulsion for such vehicles, the U. S. Navy's *NR-1* is the only nuclear-powered deep-diving submarine actually being built. Because the design features of deep-diving research submersibles are sure to influence the course of man's use of the sea, it is interesting to consider what performance and design features are desirable.

Depth Incentive

Although continental shelves are relatively accessible for exploration and exploitation, Fig. 1 graphically illustrates why it is desirable that exploration vehicles be capable of penetrating well beyond the (by definition) 600-ft limit of the continental shelves. Figure 1 shows that a vehicle that can reach 12,000 to 15,000 ft could explore more than half the total sea floor; a 20,000-ft-depth capability would put nearly 98% of the sea bottom within range. The manifest advantages of extreme deep-submergence capability in terms of exploration range are more strikingly evident in Fig. 2, in which the attainable areas of the ocean floor are superimposed on a Mercator projection of the land masses of the globe to a depth of 12,000 ft.

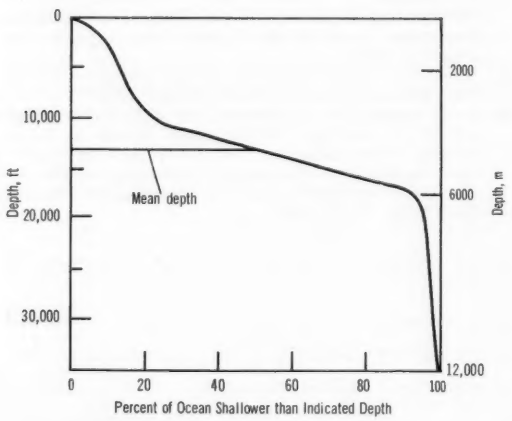

Fig. 1 Hypsographic curve of the oceans.[4]

Speed and Duration

Cruising speed need not be more than a few knots for an exploration vehicle (for fisheries research, speed might be somewhat greater); but if the submersible is to operate from a port, it would be desirable that speeds of tens of knots be maintained to minimize transit times between work sites. Submergence durations of several weeks at a time would be useful.

Configuration

For 12,000- to 20,000-ft depths, to minimize sealing problems associated with penetration of the hull by one or more rotating shafts, it would be appropriate to have a propulsion system whose electric propulsor motors are mounted in pods on the exterior of the hull. Hull construction might resemble a configuration proposed for the Deep Submergence Rescue Vehicle,[2] which consists of three interconnected pressure spheres surrounded by a hydrodynamic fairing. This arrangement lends itself to dividing the vehicle into separate dwelling, laboratory, and propulsion-system modules.

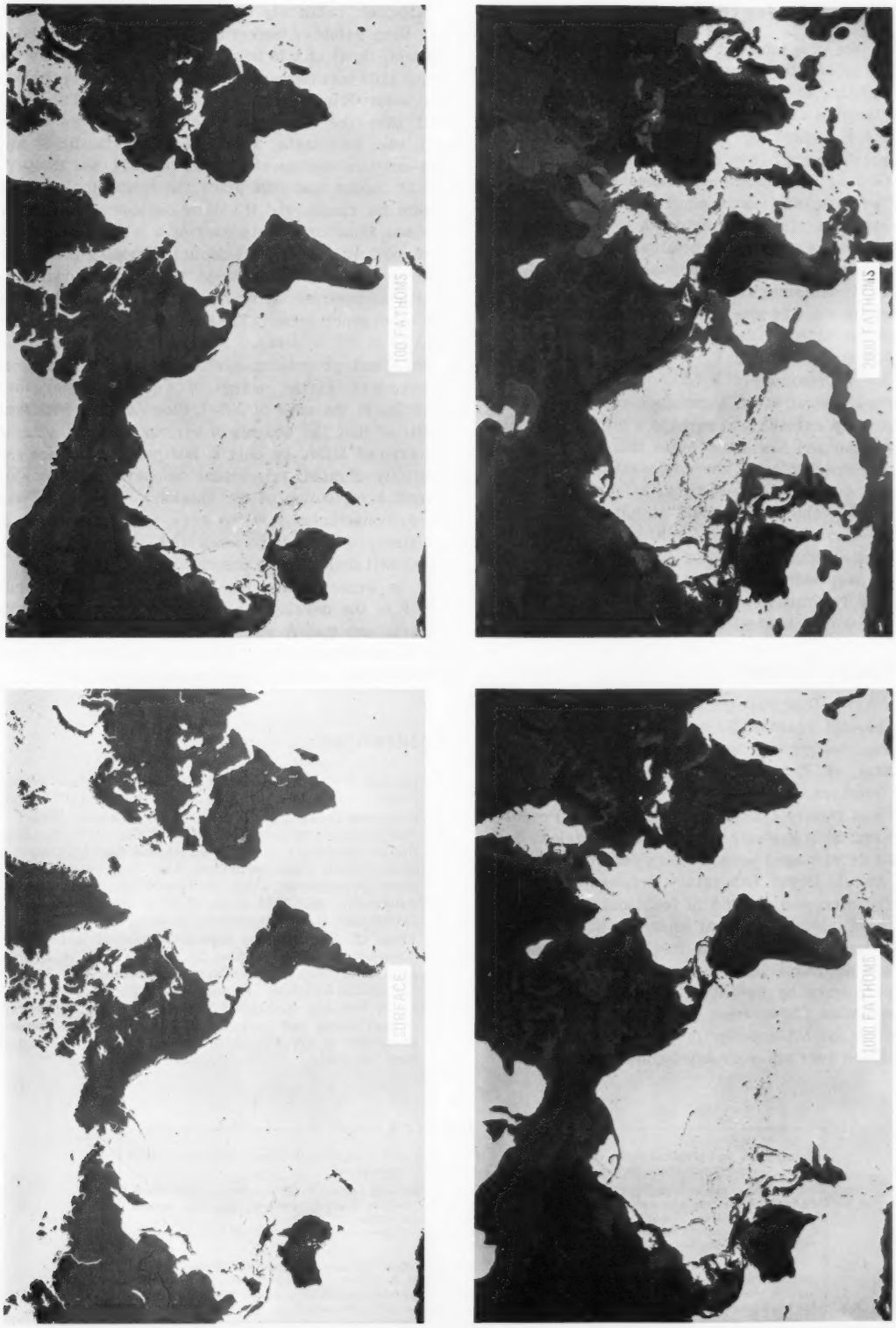

Fig. 2 The area of the sea floor that is attainable with vehicles capable of various operating depths.[5]

Conventional-Power Limitations

Except for the tethered *Kuroshio-II*, operated by Hokkaido University, Japan, the endurance of all 21 of the existing or projected "conventional" research and exploration submarines (see Table 2 of Ref. 1) is severely limited by the capacity of their electrochemical energy storage systems. *Kuroshio-II* achieves long operational endurance at the cost of limited performance range, since its umbilical power cable restricts its operating depth to about 600 ft. One of the best electrochemical-powered deep-submergence vessels, the *Aluminaut* (15,000 ft), is capable of cruising at 3 knots for only about 32 hr, whereas the famous *Trieste* bathyscaphe, which plumbed the ultimate deeps of the Philippine trench at 35,000 ft, is limited to a cruising speed of 1.5 knots for approximately 5 hr—or about 48 hr of submerged operation if significant maneuvering is avoided. It is evident, and perhaps a bit paradoxical, that man can and has spent more time and traveled farther in space than in the comparatively near and attainable ocean depths—primarily for want of a submersible vehicle that could simultaneously provide long-term life-support facilities and propulsive power. *NR-1*, with its reactor power supply, will be the first deep-submergence vehicle to overcome the power-supply limitation and open the ocean depth to long-term survey operations.

NR-1 Design Concept

The *NR-1* will be powered by a small, pressurized-water thermal reactor. Responsibility for the *NR-1* propulsion system has been assigned to the office of Vice Adm. H. G. Rickover, Director, Division of Naval Reactors, U. S. Atomic Energy Commission (AEC), and Deputy Commander for Nuclear Propulsion, Naval Ship Systems Command. The nuclear design and development work is being performed by the Knolls Atomic Power Laboratory, Schenectady, N. Y., under the direction of, and in technical cooperation with, the Division of Naval Reactors of AEC. The general design of the vehicle itself is the responsibility of the Naval Ship Systems Command and is being performed by the Electric Boat Division, General Dynamics Corporation, Groton, Conn. The AEC portion of the *NR-1* program was expected to cost $7.5 million over a 3-year development period.

Although relatively little unclassified information has been released concerning *NR-1* or its propulsion system, most of this information is derived from the April 1965 testimony of Vice Admiral Rickover before the Joint Committee on Atomic Energy.[3] The *NR-1* will have the capability of carrying a crew of five and two scientists, with laboratory facilities and life-support equipment. It will be designed to operate at depths that will place the continental shelves within its range, and it will be capable of settling on the sea floor or of maneuvering a few feet above the bottom. It will control its depth by flooding or blowing ballast tanks, as is the case with conventional submarines; however, it will be able to release weights for emergency ascent. The pressure hull will be fabricated of HY-80 steel.

Hull and propulsion-system weights are critical parameters in the design of a deep-submergence vehicle. In the case of *NR-1*, Vice Admiral Rickover testified that the weights of various reactor systems considered differ by only a few percent and are essentially of minor importance compared to the major weight contribution of the shielding. The vessel will be so constructed that the crew will have access, if required, to the reactor when it is shut down, and repairs will therefore be possible.

It is expected that the *NR-1* will be a major advance in the development of oceanographic research vessels and that it will provide the basic technology for the development of a generation of future nuclear-powered deep-submergence research vehicles.

References

1. Edward J. Croke, Ocean Technology and Nuclear Power, *Power Reactor Technol.*, 9(1): 1-18 (Winter 1965–1966).
2. *Undersea Technology*, 6(12): Cover (December 1965).
3. AEC Authorizing Legislation Fiscal Year 1966, Hearings Before the Joint Committee on Atomic Energy, Congress of the United States, 89th Congress, First Session on Reactor Development Program (Excluding Civilian Power Program), pp. 1038-1045, Part 2, Superintendent of Documents, U. S. Government Printing Office, 1965.
4. Allyn C. Vine, Depths Standardization of Instruments, *Oceanology*, 1(1): 12 (June 15, 1966). Also, H. H. Read and Janet Watson, *Introduction to Geology*, p. 11, The Macmillan Company of Canada Ltd., Toronto, 1962.
5. E. P. Wheaton (Lockheed Missiles and Space Division), Ocean Mining and Commercial Resources Development, presented at the Atomic Industrial Forum, Washington, Nov. 15, 1965.

LEGAL NOTICE

This journal was prepared under the sponsorship of the U. S. Atomic Energy Commission. Neither the United States, nor the Commission, nor any person acting on behalf of the Commission:

A. Makes any warranty or representation, expressed or implied, with respect to the accuracy, completeness, or usefulness of the information contained in this journal, or that the use of any information, apparatus, method, or process disclosed in this journal may not infringe privately owned rights; or

B. Assumes any liabilities with respect to the use of, or for damages resulting from the use of any information, apparatus, method, or process disclosed in this journal.

As used in the above, "person acting on behalf of the Commission" includes any employee or contractor of the Commission, or employee of such contractor, to the extent that such employee or contractor of the Commission, or employee of such contractor prepares, disseminates, or provides access to, any information pursuant to his employment or contract with the Commission, or his employment with such contractor.

NUCLEAR SCIENCE ABSTRACTS

The U. S. Atomic Energy Commission, Division of Technical Information, publishes *Nuclear Science Abstracts* (*NSA*), a semimonthly journal containing abstracts of the literature of nuclear science and engineering.

NSA covers (1) research reports of the U. S. Atomic Energy Commission and its contractors; (2) research reports of government agencies, universities, and industrial research organizations on a worldwide basis; and (3) translations, patents, books, and articles appearing in technical and scientific journals.

Complete indexes covering subject, author, source, and report number are included in each issue. These are cumulated quarterly, semiannually, and annually providing a detailed and convenient key to the literature.

Availability of *NSA*

SALE *NSA* is available on subscription from the Superintendent of Documents, U. S. Government Printing Office, Washington, D. C., 20402, at $30.00 per year for the semimonthly abstract issues and $22.00 per year for the four cumulated-index issues. Subscriptions are postpaid within the United States, Canada, Mexico, and all Central and South American countries, except Argentina, Brazil, Guyana, French Guiana, Surinam, and British Honduras. Subscribers in these Central and South American countries, and in all other countries throughout the world, should remit $37.00 per year for subscriptions to semimonthly abstract issues and $25.00 per year for the four cumulated-index issues.

EXCHANGE *NSA* is also available on an exchange basis to universities, research institutions, industrial firms, and publishers of scientific information. Inquiries should be directed to the Division of Technical Information Extension, U. S. Atomic Energy Commission, P. O. Box 62, Oak Ridge, Tennessee, 37830.

TECHNICAL PROGRESS REVIEWS may be purchased from Superintendent of Documents, U. S. Government Printing Office, Washington, D. C., 20402. *Nuclear Safety* at $3.00 per year for each subscription or $1.00 per issue; each of the other journals at $2.50 per year or $0.70 per issue. The use of the coupon below will facilitate the handling of your order.

POSTAGE AND REMITTANCE: Postpaid within the United States, Canada, Mexico, and all Central and South American countries except Argentina, Brazil, Guyana, French Guiana, Surinam, and British Honduras. For these Central and South American countries and all other countries, add $0.75 for each annual subscription or $0.20 for a single issue. Payment should be by check, money order, or document coupons, and MUST accompany order. Remittances from foreign countries should be made by international money order or draft on an American bank payable to the Superintendent of Documents or by UNESCO book coupons.

order form

SUPERINTENDENT OF DOCUMENTS
U. S. GOVERNMENT PRINTING OFFICE
WASHINGTON, D. C., 20402

Enclosed:
document coupons ☐ check ☐ money order ☐

Charge to Superintendent of Documents No._____

Please send a one-year subscription to

☐ ISOTOPES AND RADIATION TECHNOLOGY

☐ POWER REACTOR TECHNOLOGY

☐ REACTOR MATERIALS

(Each subscription $2.50 per year; $0.70 per issue.)

☐ NUCLEAR SAFETY

(Each subscription $3.00 per year; $1.00 per issue.)

SUPERINTENDENT OF DOCUMENTS
U. S. GOVERNMENT PRINTING OFFICE
WASHINGTON, D. C., 20402

(Print clearly)

_____
Name

_____
Street

_____
City, State, ZIP Code